TRAFFICKING OF *MYCOBACTERIUM TUBERCULOSIS* BACILLI IN TYPE II PNEUMOCYTES: A UNIQUE MODEL FOR HOST CELL INTERACTION.

by

KARI LEIGH FINE

(Under the Direction of Frederick D. Quinn)

ABSTRACT

One goal of infectious disease research is to determine points of intervention which will alter the scales of infection in favor of the host. To accomplish this goal, it is crucial to have a thorough understanding of the dynamic pathogen/host interplay which results in observed pathology. Until recently, studies of pathogenic *Mycobacterium* species responsible for pulmonary infections focused on the interaction of these bacteria with macrophages leaving the role for other host cell populations present in the lung unexplored. This body of work employs various techniques to examine trafficking of *Mycobacterium tuberculosis* (*Mtb*) bacilli in human alveolar type II pneumocytes from initial interactions at the host cell plasma membrane, internalization and passage through the fluid phagosomal/autophagosomal pathway. Data suggest that *Mtb* infection of epithelial cells is characterized by aggregation of large cholesterol-dense regions, or lipid rafts, which result in bacilli engulfment. Inhibition of raft formation significantly impacts early infection resulting in decreased numbers of internalized bacteria and diminished

survivability of those bacilli within 24 hours of infection. Once internalized the *Mtb* bacilli traffic through a phagosomal/autophagosomal pathway. Interference with the autophagosomal pathway results in decreased numbers of virulent *Mtb* bacteria and increased host cell survival. Taken together these data strongly suggest that *Mtb* has the ability to alter the epithelial cell autophagy pathway to support infection by the bacterium. The data presented here describe *Mtb*-induced changes in the host cell plasma membrane which facilitate infection success, as well as the trafficking route for virulent *Mtb* bacilli that differs from what has been previously described in macrophages. As with some other bacterial pathogens, it is evident that *M. tuberculosis* employs numerous strategies for survival and replication which are unique to the particular host cell infected.

INDEX WORDS: *Mycobacterium tuberculosis*, Autophagy, Lipid Rafts, Trafficking, Type II Pneumocytes

TRAFFICKING OF *MYCOBACTERIUM TUBERCULOSIS* BACILLI IN TYPE II PNEUMOCYTES: A UNIQUE MODEL FOR HOST CELL INTERACTION.

by

KARI LEIGH FINE

B.S. University of Vermont, 2000

A Dissertation Submitted to the Graduate Faculty of the University of Georgia in Partial Fulfillment of the Requirements for the Degree

DOCTOR OF PHILOSOPHY

ATHENS, GEORGIA

2012

TRAFFICKING OF *MYCOBACTERIUM TUBERCULOSIS* BACILLI IN TYPE II PNEUMOCYTES: A UNIQUE MODEL FOR HOST CELL INTERACTION.

by

KARI LEIGH FINE

Major Professor: Frederick D. Quinn

Committee: Russell Karls
Eric Lafontaine
Thomas Krunkosky
Kojo Mensa-Wilmot

Electronic Version Approved:

Maureen Grasso
Dean of the Graduate School
The University of Georgia
August 2012

DEDICATION

This work is dedicated to my parents and my sister who have always been supportive and challenged me to give my all in every endeavor. Thank you for learning how to dance with a child who heard the music in her head. I also dedicate this dissertation to my husband, Garry. Thank you for the encouragement during difficult days and celebrating the successes. I love you very much.

ACKNOWLEDGEMENTS

There are many people I would like to thank for their contributions to my work:

- First, I would like to thank my advisor, Dr. Frederick Quinn for his willingness to take on a dual degree student and giving me the freedom to shape my own research. Hopefully the lessons and experiences from the past five years will guide me to become the kind of scientist that will make you proud.
- I thank the members of my committee, Dr. Russell Karls, Dr. Eric Lafontaine, Dr. Kojo Mensa-Wilmot, and Dr. Thomas Krunkosky for their critical review of this work and support throughout the last five years. You have all pushed me to excel and I feel that your feedback has made me a better scientist.
- A special thanks to Barbara Reaves who has provided me with invaluable guidance and support. You have taught me a great deal about the world of science and I will be forever indebted to you for your mentorship.
- Lastly, I would like to thank the members of the Quinn-Karls lab who have provided helpful insight and support for this work. A special thank you to Shelly Helms not only for the extra set of hands whenever needed but also for being such a wonderful friend.

TABLE OF CONTENTS

Page

CHAPTER 1

INTRODUCTION

Mycobacterium tuberculosis (*Mtb*) is estimated to infect 1/3 of the world's population with approximately 8.9 million new cases each year. While significant research has been performed on this ancient pathogen, our inability to control and decrease the burden of infection in the human population reinforces the need for work towards a better understand of the host/pathogen relationship.

Much of what is known regarding *Mtb*/host cell interactions is specific to macrophages. The continued high prevalence of *Mtb* infections worldwide demonstrates that limiting research to this single cell type limits understanding of *Mtb*, and its complex relationship with the host. It is well known that the within the alveoli of the lung macrophages comprise only a very small percentage of the total cell population. Type I and type II pneumocyte epithelial cells form the bulk of the alveolar air interface, are the most numerous cells in the alveolus, are found to be the site of initial host cell interaction for other bacterial and viral lung pathogens examined to date, including *Legionella pneumophilia* and *Yersinia pestis* (228-229), yet have received limited attention regarding their role during the course of pulmonary *Mtb* infection. The aim of this study was to investigate aspects of internalization and intracellular trafficking of *Mtb* bacilli in human type II pneumocytes leading to a more complete understanding of the host/pathogen

interaction. This information will ultimately direct future research towards novel targets for modifying the outcome of *Mtb* infection.

CHAPTER 2

LITERATURE REVIEW

Mycobacterium tuberculosis, An Ancient Foe

Mycobacterium tuberculosis belongs to the family Mycobacteriaceae and is a genus and species within the Actinobacteria. Skeletal remains show prehistoric humans as early as 7000 B.C. having contracted tuberculosis (209), and as early as the fifth century B.C., Hippocrates described treating patients with phthisis or consumption. The earliest recorded epidemics of tuberculosis in Europe were in the 16th and 17th century A.D. It is believed that as humans congregated in greater numbers and trade increased, so did the incidence of tuberculosis (209). History shows that since the late 1800s, as knowledge of good public health practices and the development of appropriate therapeutics increased, the number of tuberculosis cases decreased. Unfortunately, a resurgence of disease has been observed in the past 20 years due to the rise of HIV co-infections and the rapid spread of antibiotic-resistant strains (21, 62).

Epidemiology

Approximately 1/3 of the world's population is infected with *Mtb* (86). While a peak of worldwide prevalence was noted in 2004, the number of new cases has continued to climb with 9.4 million in 2009, the largest single year increase in recorded history (117). The predominance of the cases are located in Asia and Africa with 22 countries

accounting for 80% of the global burden (251). Tuberculosis (TB) has been said to be a "disease of poverty" with high rates of infection among the undernourished in high population density zones (129). Another major contribution to the surge in TB has been the spread of Human Immunodeficiency Virus-1 (HIV-1). A reported 12% of the cases worldwide are coinfected with *Mtb* with most of these localized to sub-Saharan Africa (251).

The rise in multidrug resistant strains (MDR) of *Mtb* has also contributed to the increased global burden of TB. It was reported in 2006 that approximately 4.8% of confirmed cases of TB were considered MDR (116). The World Health Organization has reported MDR strains in 58 countries as of March, 2010 (252). MDR TB is defined as a strain of *Mtb* that is resistant to both isoniazid and rifampin while XDR TB (extremely drug resistant) is resistant to these as well as fluoroquinolones and at least one of the injectable medications (amikacin, kanamycin, capreomycin) (201). The genetic component to resistance is varied; 97% of rifampin-resistant strains have a mutation in gene *rpoB*, which encodes a mycobacterial RNA-polymerase subunit (116). The majority of isoniazid resistance can be linked to mutations in *katG* and *inhA*, two genes which decrease catalase and peroxidase production and thereby decrease activation of this drug *in vivo* (116, 209). Reports of *Mtb* resistant strains have become increasingly prevalent in the media creating an urgent public health need to develop better drugs and vaccines. To begin this process, an improved understanding of how this pathogen subverts the immune system is required (20, 152, 193, 198, 203, 208, 256).

Another potential factor contributing to the spread of TB is the infection of animals sharing space with humans. *Mycobacterium tuberculosis* positive cattle and

buffalo have been documented in areas of the world with high rates of human infection (5, 113, 213). Elephants are another species commonly infected with *Mtb*. These infections are not isolated to Asia and India but have also been documented among circus elephants in the United States (141, 191). Data suggest that cross infection occurs between humans and other animals, but the directionality of the infection is not always clear. It is understood, however, that *Mtb* is capable of infecting a range of mammalian hosts and this characteristic can contribute to global spread of the agent.

Clinical Disease

In 1948, using primarily animal models, Wallgren described four stages to the respiratory form of TB. The first stage included inhalation and internalization of the bacilli into the lower lung forming the primary Ghon complex. The Ghon complex is a lesion produced by the innate immune system consisting primarily of macrophages and bacteria. If the bacilli survive the macrophage onslaught, the second stage (active disease) is marked by bacterial replication and dissemination. Some individuals can go on to develop serious non-pulmonary miliary TB and TB meningitis. The third stage is marked by an increase in the host adaptive immune response. It is at this point that the granuloma becomes fully formed in the lung from the Ghon complex, walling off the infectious agent. The third stage can last years and depends primarily on the strength of the host adaptive immune system. The fourth stage of TB is often identified by the presence of caseous necrotic or liquefied tissue at the center of the granuloma. It is during this stage that secondary infection can occur if host immunity is ineffective at maintaining an intact granuloma and preventing bacterial release. HIV co-infection, immunosuppressive drugs and advancing

age, with the natural decline of the host immunological response, can all lead to breakdown of the granuloma.

Latent Infection

While the vast majority of healthy individuals that inhale *Mtb* bacilli ultimately clear the infection, latency is the most common form of infection among the minority population unable to clear the initial dose of inhaled bacilli. The case definition for latency is *Mtb* infection, controlled but not eliminated by an acquired immune response, resulting in no clinical signs (75). Some of these individuals will "reactivate" if the immune system becomes compromised, resulting in active infection. Historically, latent *Mtb* infections were thought to be dormant, but it is now recognized that a dynamic interaction is occurring between the host and bacteria during this time (15, 75, 258). An important component in our understanding of latency has been the use of animal models, such as mice, primates, rabbits and guinea pigs.

Animal Models of *Mtb* Infection

Mice have long been used as a model of human TB. The availability of inbred strains that establish rapid chronic infection by *Mtb* bacilli culminating in death of the host has allowed for low-cost, reproducible examination of disease progression. However, mice are not a natural host, which is evident by significant differences in observed disease phenotypes compared with human TB (236). The structures of murine granulomas are more diffuse, lack a hypoxic core, and fail to mineralize or progress to cavitary disease as observed during human TB. The immune cells associated with the granuloma in mice such as T cells, dendritic cells and neutrophils lack the organization seen in the human

lung (236). While some similarities are evident, such as the prominent B cell foci which appear 2-4 weeks post infection, the absence of necrosis within the mouse lung suggests that these structures have different roles in the two species. Nonetheless, the mouse has been deemed an acceptable model for proposed studies of mycobacterial pathogenesis but further testing in higher animals and primates is vital (100, 220).

Non-human primates, specifically macaques, are being used as models for primary and latent TB infection. Studies have shown that the lung pathology produced in primates during early infection is very similar to the Ghon complex described in humans (126-127). Importantly, these animals demonstrate latency in a manner not observed with other animal models (75). Cost and appropriate space make this model prohibitive for many laboratories yet the information they provide can be invaluable to our understanding of human infections.

The rabbit has been used as a surrogate model for human TB since the beginning of the 20th century. In the era before genomics and before differences in biochemical properties, such as protein expression, were elucidated, the rabbit infection model was used to effectively differentiate pathogenesis caused by *M. bovis* and *Mtb* (Smith 1898, Lurie 1922). Additionally, similarities to human cavitary disease seen in these animals have made them an excellent model for the study of long term infection (149). Also, as observed in most cases of human disease, the rabbit immune system is able to prevent dissemination and confine the bacteria to the lung. The liquefactive necrosis and granuloma structure present in human and rabbit pathology are noticeably absent in the mouse. Recently, a study by Manabe et al. tested the relative virulence of various *Mtb* laboratory strains via aerosol infection in the rabbit (133). Of the strains tested, the

laboratory strain Erdman was the most virulent, exhibiting pathology most similar to that seen in humans. While the rabbit may be more costly than murine lines, the similarities of rabbit to human tuberculosis in terms of progression, pathology, and clearance supports the rabbit as a relevant model system for examining all stages of *Mtb* infections. Moving forward, these models will help answer many of the questions that still exist today regarding the host/mycobacterial interaction.

Vaccination

The only licensed *Mtb* vaccine on the market today is *Mycobacterium bovis* bacille Calmette-Guerin (BCG). The original vaccine strain of *M. bovis* was attenuated via thirty nine serial passages in ox bile medium (30, 40). Several decades later genetic comparative analysis of *M. bovis* BCG and its parent strain, revealed three Regions of Difference: RD1, RD2 and RD3 (130). RD1 was determined to be present in both *M. bovis* and *Mtb* suggesting that the genes found there could encode for virulence factors important to *Mtb* (18). Greater than 90% of children in the world today have been vaccinated with BCG which has been shown to be protective against tuberculous meningitis in individuals less than 10 years of age (235). Unfortunately, the vaccine has proven to be of limited or no efficacy in the prevention of pulmonary TB in adolescents and adults (233). In addition to providing questionable levels of protection, vaccination confounds some diagnostic procedures. The need for an effective *Mtb* vaccine is a critical component for global control of this pathogen.

Diagnostics

While *Mtb* bacilli have circulated in human an animal populations for thousands of years, the diagnostic tools available are still insufficient and often impractical in developing countries where TB infection is most prevalent. Sputum smears and culturing are two widely used tests in countries lacking resources. While culturing remains the gold standard for diagnosis, *Mtb* replication rates (15-24 hour doubling) makes this method lengthy and delays identification of index and drug-resistant cases (117). The WHO approved line probe assays (LPAs) for sputum samples in 2008. This technique allows for a more rapid molecular detection of *Mtb* bacilli in samples. Nucleic acid amplification tests (NAAT) are also being used to analyze sputum samples in areas where technology and expertise are available. The tuberculin skin test (TST), detecting type IV hypersensitivity reactions to purified protein derivatives of *Mtb*, is still used commonly as a general screen for clinical and non-clinical infection. It should be noted that this test does not differentiate *Mtb*-infected from BCG-vaccinated individuals, and can produce false positive results in individuals exposed to other closely related *Mycobacterium* species. Confirmation is often performed by chest radiograph detecting granuloma formation.

These tests are often useful for diagnosing well-established cases of active TB infection but there is still a lack of effective methods for identifying latently-infected individuals. T-SPOT TB test and QuantiFERON-TB Gold are two new tests that were developed to fit this market (117). Results have shown the tests are as accurate as TB skin tests but most latently-infected individuals are still not detected. It is therefore

crucial that efforts be made to develop highly sensitive and specific diagnostics for this sector of the *Mtb* infected populus.

The Tuberculosis Complex

Historically, it was believed that upon domestication of cattle, which occurred approximately 10,000 to 25,000 years ago, that the etiological agent of cattle TB, *M. bovis*, adapted to human hosts eventually becoming the progenitor of *Mtb* (218). However, upon completion of the *Mtb* genome sequencing project, work by Brosch et al. proposed a common tubercle bacilli ancestor from which all members of the Tuberculosis Complex are derived (35).

The Tuberculosis Complex is composed of all *Mycobacterium* species that cause tuberculosis in humans or animals: *M. tuberculosis*, *M. bovis*, *M. africanum*, *M. microti*, *M. canettii* and *M. pinnipedii*. With the exception of *M. canettii*, nucleotide sequencing demonstrates approximately 99.95% homology between complex members (211). Regions of difference (RD) within the bacterial genome, have been used in various studies to differentiate animal-adapted subspecies, such as *M. bovis*, from *Mtb* and other human-adapted mycobacteria. Interestingly, RD9 which is absent in *M. bovis* and other animal adapted species, is also deleted in *M. africanum* which also primarily infects humans. It has been hypothesized that this commonality indicates the reverse zoonosis of tubercule mycobacteria from humans to cattle promoting the evolution of this species. While region and gene variation have been used to differentiate *Mtb* complex members, there is also a great deal of variety found within the species *Mtb*.

New molecular typing methodologies of TB isolates have demonstrated a number of species-, lineage- and strain-specific variations (37-39). These differences have provided unprecedented opportunities for linking particular variants to geographic and host preferences, specific virulence traits, antimicrobial resistance patterns, enhanced transmissibility and immune evasion. For example, spoligotype patterns have helped provide for the identification of major global *Mtb* clades including Beijing, Haarlem, S, T-Uganda, T, X, East African-Indian and Latin American-Mediterranean (LAM) (37-39, 231). Clinical data associated with infections with some of these strains demonstrate unique or enhanced virulence traits including modifications to granuloma formation, enhanced inflammatory cytokine production, and others (69-70). Thus, studies of these clades and sub-groupings within the clades are beginning to help identify strains possessing unique virulence patterns and antimicrobial resistances in humans. An example of this is the RD^{Rio} strain recently identified as a Latin American-Mediterranean sublineage of the *Mtb* complex (118-119). This particular strain has been categorized as a hyper-virulent strain by the morbidity associated with infection. Patients infected with this strain were more likely to present with enhanced hemoptysis (coughing of blood), weight loss, higher bacterial numbers in sputum and more advanced cavitary disease compared to typical isolates from this clade.

Passaged laboratory strains, descended from different *Mtb* lineages, are used in research to evaluate virulence factors and pathology resulting from *Mtb* infection. Strain H37Rv is a human isolate originally cultured in 1905 by the Trudeau Sanitorium. At that time Kubica et al. established 71 criteria to verify virulence of *Mtb* H37Rv and other isolates which included susceptibility to various antibiotics, bacterial growth *in vitro* at

various temperatures and colony morphology (109). Today, H37Rv is maintained as a virulent laboratory strain of *Mtb*. Likewise, *Mtb* Erdman, another strain from the Trudeau Mycobacterial collection isolated from a patient in 1962, is also used as a virulent laboratory strain. Both H37Rv and Erdman share phylogeny within the European/American lineage of the *Mtb* complex.

Several clinical isolates obtained during the last 20 years have been investigated regarding pathology, disease outcome *in vivo* and immunological response of the host (13, 154). Strain CDC1551 was isolated from an outbreak of *Mtb* on the Kentucky-Tennessee border between 1994 and 1996. It was originally believed that this isolate was hypervirulent compared to laboratory strains based on the significant delayed-type hypersensitivity response (DTH) to the PPD tuberculin skin test in affected patients (239). However, *in vivo* studies revealed this isolate to be less virulent as defined by time to death studies in mice and rabbit models (13). Comparatively, isolate HN878, which was obtained from Texas during a 1995-1998 outbreak was shown to be hyper-virulent *in vivo* while eliciting a modified Th1 immune response from the host (154). It is interesting to note that the HN878 strain is related to the hypervirulent W. Beijing lineage while CDC1551 is phylogentically related to the European/American grouping with the *Mtb* complex.

Physical and Genetic Characteristics of *Mtb* Bacilli

While tuberculosis has been documented in human populations for thousands of years the causative agent, *Mtb*, was first cultured by Robert Koch in 1882. *Mycobacterium tuberculosis* bacilli are gram positive, aerobic obligate intracellular rods. One of the most

unique physical characteristics is the thick lipid-rich cell wall, which stains "acid fast" and is a defining marker for this genus.

Over 200 genes in the *Mtb* genome are dedicated to the metabolism of fatty acids. The products from these reactions are used to synthesize the cell wall, indicating its crucial role in bacterial survival. Collectively, the plasma membrane, cell wall core and outermost layer are referred to as the cell envelope. The core is comprised of peptidoglycan linked with arabinoglycan and mycolic acids, which are long carbon chain fatty acids. An assortment of lipids, polysaccharides, lipoglycans and proteins form the outermost layer of the envelope, which conveys hydrophilic qualities to the bacterial surface. Notably some of the outer layer is shed into the milieu or broth medium during *Mtb* growth, which could have important functions *in vivo* (156).

Phosphatidylinositol mannosides also form a large portion of the cell wall. Phosphatidyl-myo-inositol mannosides, lipomannan and lipoarabinomannan (LAM) have been reported to be important for bacterial entry into host cells (32). Mutant *Mtb* strains lacking Mannose-capped LAM (ManLAM), a molecule associated with virulent mycobacteria, displayed defects in phagocytosis and increased lysosomal fusion with bacteria-containing compartments in macrophages (233, 243). It has also been suggested that the use of fatty acids allows *Mtb* to have broad tissue tropism in the human host (209). Differences in host cell responses to clinical isolates of *Mtb* have been attributed to variability in the molecule comprising the cell wall (154). While advancing technology has allowed for more rapid and precise characterization of *Mtb* cell wall chemistry, more questions have arisen as to composition and role of mycobacterial lipids during infection.

The genome of *Mtb* is approximately 4.4 $x10^6$ base pairs, which consists of approximately 4,000 genes (48). Large families of proteins containing repeat Pro-Glu (PE) or Pro-Pro-Glu (PPE) motifs comprise a significant portion of the genome. While PE and PPE proteins are not exclusive to *Mtb*, it has been proposed that they may be responsible for antigenic variation (12). Other virulence factors that have been identified include KatG (catalase-peroxidase), SodA (superoxide dismutase) and Acr (α-crystalline protein) which is a potential indicator of latent infection (262).

Another component of the *Mtb* genome that is crucial for virulence is the previously mentioned region of difference 1 (RD1). Notably, the nine genes encoded in this region are missing from the attenuated vaccine strain *M. bovis* BCG. Reintroduction of RD1 into BCG or deletion from *Mtb* has been shown to increase or diminish pathogenicity in these strains, respectively (124, 175). Several RD1 genes encode a unique mycobacterial secretion system, ESX-1, which has been shown to facilitate the release of virulence factors ESAT-6 (early secretory antigenic target of *Mycobacterium tuberculosis*) and CFP-10 (culture filtrate protein 10), also encoded in this section of genome (124, 130). During macrophage infection, ESAT-6 and CFP-10 have been shown to be secreted as a complex and dissociate within the acidic phagolysosomal compartment (34, 54). Further, ESAT-6 was shown to bind to cholesterol and phosphytidycholine in the endosomal membrane facilitating disruption and release of mycobacterial bacilli (54, 210). These data support the assertion that RD1 and its encoded proteins are essential for host cell modification during the infection.

Distal Lung Histology

To identify and understand the function of factors required to produce a successful infection in a respiratory pathogen such as *Mtb*, we must first acquire sufficient knowledge of the anatomical environment where the bacilli and host interact. The airway can be divided into conducting and respiratory portions. *Mycobacterium tuberculosis* bacilli in aerolized droplets, < 5μm in size, are believed to pass through the conducting to the respiratory sections of the airway. The respiratory region of the lung is comprised of the respiratory bronchioles, alveolar ducts and sacs, which collectively form the alveolus as well as connective tissue, which provide structure (84, 157). A range of cell types can be found in the respiratory airway, such as macrophages, mast cells, dendritic cells, lymphocytes and epithelial cells (33, 91, 212).

Three of the important epithelial cell types that comprise the lower respiratory bronchiole and alveolar surface are the Clara cells, and the type I and II pneumocytes (163, 183). Clara cells, found in the bronchioles, are dome-shaped cuboidal cells which secrete components that contribute to the surfactant layer (163). They are also progenitor cells and have been shown to divide and migrate to areas of damage in the lower lung (10).

The cells that line the alveoli, type I and II pneumocytes, are the primary components in gas exchange and surfactant production, respectively. Type I pneumocytes are squamous cells that cover over 90-95% of the surface area of the alveoli but only contribute approximately 10% of the total alveolar cell count (50, 163). Typically found adjacent to endothelial cells, type I pneumocytes are responsible for gas exchange. Given the constant bombardment of molecules and particulate matter that enter the terminal

alveoli and interact with these cells, these terminally differentiated and delicate cells have a very short lifespan. Type II cells are the progenitors of type I cells and are found tightly adhered to type I cells. While they contribute minimally to the respiratory surface, they comprise the majority of the alveolar epithelial cell number (84). By electron microscopy, these cells are characterized by numerous multivesicular and lamellar bodies. These structures indicate another important function of type II pneumocytes, the production and release of surfactant components.

Surfactant is an amalgamation of protein and lipid molecules that reduce surface tension at the air/lung interface via its amphiphilic nature (10, 17, 163, 226). As surfactants adsorb to the surface of the respiratory epithelium the lung can then expand during inspiration (17, 84). The major components are dipalmitoyl phosphatidylcholine and surfactant proteins (SP) SP-A, SP-B, SP-C and SP-D (87, 214). SP-A is the most abundant surfactant protein, which assembles into a "bouquet" configuration (17). SP-D is the largest surfactant molecule, and combined with SP-A, have been shown to contribute greatly to the lung immune response (3, 17, 107, 226, 233). SP-A and SP-D are both collectin family members (3). The carbohydrate regions of these molecules bind mannose and glucose while the collagen domain binds to the SP-A receptor on epithelial cells to facilitate entry of various respiratory pathogens into the host cell (3, 17). SP-A has also been shown to up-regulate mannose receptors on macrophages, contributing to clearance of mycobacteria during infection (17, 233). An interesting contradiction to the host immunological role of SP-D is that is has been shown to occlude the mannosyl oligosaccharides on the surface of mycobacteria preventing interaction with mannose receptors and subsequent phagocytosis by alveolar macrophages (209).

Alveolar macrophages (AM) and dendritic cells (DC) are two additional cell types associated with the respiratory epithelium and are very important for innate and acquired immune responses. AM cells are the most numerous immune cell found in the distal lung comprising 95% of cells in human BAL fluid (84). They are found in the alveolar space as sentinels scavenging for pathogens and particulate matter. These macrophages exhibit an alternative activated profile (42, 76). The AM are induced by IL-4 and inhibited by IFNγ while the converse is true for classically-activated macrophages (76). Innate immune receptors such as mannose receptors, scavenger receptor type I and β-glucan-receptors are commonly found on AM while the important T-cell co-stimulatory molecule B7 is not (42, 76, 219). Considering the daily bombardment by innocuous environmental particles, it is reasonable that these cells would be programmed to limit inflammation and, thus, are less efficient at stimulating T-cell responses and releasing chemotactic cytokines than their classically-activated counterparts (42). This has important implications for the overall immune response to respiratory pathogens.

Dendritic cells found in the lung are believed to be modulated by the AM (115). These cells are maintained in an immature state lacking the co-stimulatory molecules necessary for activating T-cells. Certain populations of DC have been shown to routinely cycle to the draining lymph node as a means of continually sampling the lung environment while others are more long-lived in the tissue. One surface molecule, dendritic cell–specific intercellular adhesion molecule-3-grabbing nonintegrin (DC-SIGN) was initially thought to bind bacterial pathogens, such as *Mtb;* this interaction blocks maturation of DC to result in the production of anti-inflammatory cytokines.

However, work by Schaefer et al. demonstrated that this surface molecule may limit pathology associated with chronic *Mtb* infection (192, 233)

Phagosomal Maturation

Studies have defined the typical process of phagosomal maturation, and identified which molecules are involved. Rab proteins, small GTPases, have been shown to control the transport and fusion of endosomal vesicles (103). Rab5 is recruited to early phagosomes by phosphatidylinositol 3-kinase class III (PI3KC3) soon after initial phagocytosis (102, 184, 243, 246). Guanosine diphosphate is bound Rab5 on the surface of an endosome and must be exchanged for guanosine triphosphate for phagosome maturation to proceed (238). Rab5 recruits phosphatidylinositol-3-phosphate (PI3P) to the phagosomal surface which in turn ensures the accumulation of early endosomal antigen- 1 (EEA-1) and later Rab7 (103).

Time-lapse studies have demonstrated that the presence of Rab7 on phagosomal compartments occurs during late stage maturation of the vesicle (261). Further, it has been shown that Rab5 is exchanged for Rab7 (Rab7 conversion) rather than present simultaneously on the phagosomal membrane (182). Studies with bacterial pathogens such as *Brucella* spp. and *M. bovis*, have shown that Rab7 interacting lysosomal protein (RILP) is next recruited to the phagosome and plays an important role in lysosomal fusion (217, 222). Fusion with the lysosome has been characterized by an acidified compartment paired with the presence of glycoproteins lysosomal associated membrane protein -1 and-2 (LAMP-1 & LAMP-2) (64). Pathogens, such as *Mtb* have been shown to manipulate the process of phagosomal maturation to prevent fusion with lysosome.

Entry of *Mtb* Bacilli Into Mammalian Host Cells

Over the past few decades, much effort has focused on identifying the cell receptors and mycobacterial components involved in the entry of *Mtb* bacilli into host cells. Adherence of *Mtb* bacilli to macrophages has been shown to proceed not only through specific receptor binding but also facilitated by opsonization of bacilli with SP-A, SP-D and fibronectin (83). Work by Larry Schlesinger's group has demonstrated that complement receptors (CR) 1, 3 and 4 on macrophages are essential for induction of phagocytosis of *Mtb* bacilli (195). Blocking of these receptors resulted in a 75% reduction of adherence and internalization of bacteria during early time points of infection. Further studies have demonstrated that mannose receptors (MR) are also crucial for adherence and entry of *Mtb* bacilli through binding to the mannose-capped lipoarabinomannan (99). Further, this interaction has been shown to be crucial for limiting phagosomal-lysosomal fusion (see below). Phagocytosis of *Mtb* bacilli by CR3 and MR has been linked to a dampening or absence of an immune response during infection. Collectively, these data indicate that specific receptor entry of *Mtb* in macrophages is important for bacterial survival and modulation of the host cell response.

While limited work has focused on entry of *Mtb* bacilli in nonphagocytic cells, work by several investigators has demonstrated that the lectin-like factor of *Mtb*, heparin-binding hemmaglutinnin (HBHA), is important for binding and entry of bacilli in epithelial cells (139). HBHA is an adhesin found on the surface of *Mtb* bacilli, which has been shown to selectively facilitate adherence and entry into nonphagocytic cells. Disruption of the responsible gene, *hbhA*, decreases bacterial survival and

extrapulmonary dissemination (106, 164). Further, vaccination of mice with purified native HBHA conveyed protection against aerosolized infection with *Mtb* Erdman (158).

Trafficking of *Mtb* Bacilli in the Macrophage

The infection of macrophages by *Mtb* and other pathogenic *Mycobacterium* species has been well characterized. Armstrong and Hart (1971) were the first to demonstrate that phagosomes containing *Mtb* bacilli do not mature into phagolysosomes (9). This work led others to examine the process now termed phagosomal maturation arrest (PMA). Following phagocytosis, facilitated by MR and CR 1, 3, and 4, pathogenic mycobacteria are maintained in an early phagosome (63, 99, 195). It has long been held that *Mtb* bacilli remain in the phagosomal compartment to undergo bacterial replication (242-243). However, some recent work indicates that *Mtb* and *Mycobacterium marinum* bacilli may escape from their compartment and enter the cytoplasm (205, 215-216, 240). Clemens and Horwitz (1995) utilized antibodies to Rab proteins to characterize Mycobacteria-Containing Phagosomes (MCPs) (44). They showed that late endosomal markers, such as CD63, Lamp-1 and -2, Rab7 as well as EEA-1 were absent from MCPs. Work by Via, et al. (1997) determined that PMA occurs between Rab5 and Rab7 endosomal maturation stages (45, 101, 244).

To better understand how this occurs, a series of experiments by Fratti et al. (2001), Malik *et al.* (2000, 2001) and Vergne et al. (2005) examined the recruitment of Rab5 and 7 effector proteins to the mycobacteria-containing phagosome (67, 131-132, 242). These studies demonstrated that ManLAM, found on the surface of pathogenic mycobacteria, prevent a rise in intracellular calcium levels (41, 79). This decreases

calmodulin kinase II activity and the cell is then unable to recruit PI3KC3, which reduces the amount of PI3P found on the phagosomal surface. *Mycobacterium tuberculosis* bacilli further ensure inhibition of lysosomal fusion by producing a lipid-phosphatase, SapM, which dephosphorylates the PI3P that might be delivered to the phagosome (242). PI3P ensures the binding of the important effector molecule EEA-1 which then tethers vesicles needed to deliver lysosomal hydrolases to the phagosome (243). By blocking the initiator of this cascade, pathogenic mycobacteria prevent the acidification of the phagosomal compartment. These findings were supported by Ferguson and colleagues, who demonstrated that coating *Mtb* bacilli with SP-D blocks the mannose cap and increases phagocytosis and phagosomal/lysosomal fusion (66).

Alternative explanations for PMA have been proposed. Findings by Welin et al. indicate that LAM does not block phagosomal maturation through PI3P blockage (249). Instead, it is suggested that LAM molecules insert into the MCP and physically prevent the tethering and delivery of Rab7 and hence block fusion with lysosomes.

The nature of PMA might bring into question how sequestered bacilli acquire the necessary nutrients, such as iron, needed to survive if the delivery of vesicles is blocked by ManLAM. Another complex lipid, phosphatidylinositol mannoside (PIM), found on the surface of the bacilli facilitates early endosomal fusion (243). This process is not only independent of PI3P but is in fact enhanced by the blocking of PI3K, which illustrates how pathogenic mycobacteria subvert late vesicle trafficking (241).

Autophagy and Pathogens

Within the cell, PI3K has many other important roles, one of which is as an initiator of the autophagy pathway. While the process of autophagy (self-eating) has been known for some time, the pathway has come under closer scrutiny in the past decade. Investigators are attempting to tease out the nature of the stimuli responsible for initiation and repression of autophagy as well as identify the molecules that regulate these responses.

Autophagy is divided into three categories: microautophagy, chaperone-mediated autophagy (CMA) and macroautophagy (65). Microautophagy is characterized by the sequestering of cytosolic components into the lysosome by directly budding into the compartment. Chaperone-mediated autophagy is the only category of autophagy that is found exclusively in higher eukaryotes and involves a specific tag located within protein sequences that target them to heat shock cognate protein 70 (Hsc70). This chaperone then interacts with and delivers the protein to a lysosome via the LAMP-2. Macroautophagy, hence referred to as autophagy, is considered to be an ancient cellular response to starvation allowing for recycling of amino acids and breakdown of damaged organelles including mitochondria (80, 122, 144). Additionally, autophagy is thought to be one of the earliest protective responses against intracellular pathogens. Once the pathway is activated, large components of the cytosol are enveloped in a double membrane compartment, which then matures and fuses with a lysosome.

Much of what is known about the formation and structure of the autophagosome is derived from yeast experiments; however, most molecules involved have also been confirmed in mammalian cells (19, 105). The autophagosome originates from a pre-autophagosomal structure, termed the phagophore, which associates with autophagy-

related gene proteins (Atg) Atg12, Atg 16, Atg1, Atg9, Atg5, Atg6/Beclin 1 and Atg8/LC3 I (161). The source of these membranes was thought to be strictly Golgi- or endoplasmic reticulum (ER)-derived. However, Ravikumar et al. have recently shown that the plasma membrane can also be utilized to form autophagosomes, which suggests initiation of autophagy could occur from multiple locations and time points, including early in the internalization process (178). The LC3 I then becomes covalently linked to phosphatidylethanolamine (PE) in the autophagosomal membrane resulting in LC3 II. Upon completion/ maturation of the autophagosome, most Atg proteins are removed from the compartment except LC3 II, which remains on the inner membrane. Rab7 colocalizes with Lc3 II on the autophagosomal membrane facilitating fusion with the lysosome and resulting in the formation of the autophagolysosome (94).

Inhibition and activation of autophagy is predominately controlled by two major complexes, mTOR (mammalian Target of Rapamycin) and Beclin 1/PI3K (hVps34), respectively (161). Various intra- and extra-cellular signals can positively or negatively regulate the pathway. Glucagon, which alerts the cell to decreased insulin, can stimulate the association of Beclin1 and PI3K to activate autophagy (123). Kinase PI3K also associates with mTOR to inactivate the pathway, and assists cellular homeostasis. Deregulation of autophagy has been implicated in neurological diseases and cancer and thus the delicate balance of this process is crucial both on a cellular and organismal level.

It has become increasingly clear that autophagy can play an important role in the mammalian defense response to intracellular pathogens by facilitating increased lysosomal fusion (148). The special term, xenophagy, has been utilized to describe the selective involvement of autophagy for elimination or containment of intracellular

pathogens (97). Endosomes containing *Salmonella enterica* serovar Typhimurium have been shown to associate with autophagy markers such as Lc3 during early infection. Further, bacterial load increased in autophagy-defective host cells (97). Studies by Py et al. and Birmingham et al. showed that *Listeria monocytogenes* induced autophagy involvement early in the infection process through secretion of Listeriolysin-O (LLO) (26-28, 174). Strains deficient in this protein did not induce autophagy. Further, mice deficient in autophagy proteins (*atg5* $^{-/-}$) had improved bacterial replication, suggesting autophagy supports clearance of *L. monocytogenes* (174). Recent studies by Meyer-Morse et al. have challenged the results of the previous studies, reporting that infection of bone marrow derived macrophages (BMDM) lacking *atg5* resulted in slightly decreased bacterial viability suggesting that the bacteria can manipulate the autophagy pathway to promote survival (140).

The assertion that a pathogen could manipulate the autophagy pathway to its advantage is not novel. *Shigella flexneri* bacilli facilitate their release from the phagosome into the host cell cytosol and produce IcsB, which inhibits autophagy, thus preventing re-capture and killing (153). *Coxiella burnetii*, well characterized as a bacterial pathogen that survives in acidified vacuoles, has been shown to modulate the autophagy pathway to improve survival. In non-phagocytic cells various studies have shown *C. burnetii* bacilli traffic through late endosomes that become labeled early with autophagy markers and that inhibition of the autophagy pathway negatively impacts bacterial survival (23, 82, 187). Certain positive-sense RNA viruses such as human poliovirus and mouse hepatitis virus utilize elements of the autophagy pathway to

enhance replication (93, 162, 171, 194, 221). Further, inhibition of the autophagy pathway reduces viral load.

Toll-like receptors (TLRs) have been identified as activators of the autophagy pathway in macrophages. Stimulation of TLR4 by bacterial lipopolysaccharides has been found to activate the autophagy pathway (254). Gutierrez, et al. demonstrated that autophagy up-regulation, through TLR4 stimulation, increased colocalization of lysosomes with *M. bovis* BCG-containing compartments (80). Deretic et al. later demonstrated that autophagy induction provided a mechanism to override mycobacterial-induced PMA in macrophages (56-57). While these data provide interesting findings regarding the relationship of *Mtb* infection and autophagy, it should be noted that in these studies pharmacological induction of the autophagy pathway was implemented. No evidence was provided to demonstrate the occurrence of spontaneous autophagy up-regulation during a typical *in vitro* infection of macrophages with *Mtb* bacilli.

A common finding in these studies is the intersection of the endosomal pathway with autophagy. The previously mentioned studies involving *C. burnetii*, *S. enterica* and *L. monocytogenes* have all shown co-association of endosomal markers, such as Rab5 and Rab7, with Lc3. Interestingly, proteomic analysis has shown that autophagy-associated proteins can be found on phagosomal membranes (204). However, it should be noted that studies have documented autophagosomes lacking traditional double membranes, suggesting that autophagosomal structure is altered during the maturation process to resemble an endosomal compartment (199).

We next must consider what processes are responsible for targeting intracellular pathogens towards the autophagy pathway. Studies have shown that pathogens such as

Mtb can be targeted to autophagy within phagosomes while some pathogens such as *L. monocytogenes* target to autophagy once the bacilli escape into the cytosol (61, 80, 145). *Salmonella* spp. can target to autophagy from damaged bacteria-containing compartments (29). Innate immune receptors such as TLR2 and TLR4 as well as signaling lipids such as PI3P have been shown to recruit autophagy proteins early in the infection process (254, 257). Another important stimulus targeting pathogens to autophagy appears to be linked to the ubiquitin conjugation system. The ubiquitin protein (UB) is a small protein associated with tagging and targeting cytosolic proteins for degradation by the proteasome system. Ubiquitination has been linked to the autophagy pathway through three separate host cell adaptor proteins: p62/SQSTM1, NDP52 and NBR1 (199). The specific adaptor type recruited appears to be dependent on the nature of the pathogen itself.

Ubiquitin has previously been shown to play a unique role during *Mtb* infection in macrophages. Studies by Purdy and Alonso et al. have shown that ubiquitin proteins are delivered to the lysosome and subsequently become UB-derived fragments with mycobactericidal properties (4, 172-173). They hypothesize that increasing the killing properties of the lysosome could facilitate improved bacterial clearance. This process was contingent upon artificial upregulation of the autophagy pathway (i.e. pharmacological or starvation-induced) which suggests that while UB-killing mechanisms can be facilitated *in vitro*, this is not a natural process that occurs during *Mtb* infection. If xenography occurs during unperturbed *Mtb* infection, then the role ubiquitin might play in this process has yet to be described.

Lipid Rafts and Pathogens

Studies have documented that pathogens can begin to manipulate the host cell environment well before internalization. The plasma membrane of mammalian cells is a complex arrangement of lipids, proteins and carbohydrates that convey information about the extracellular milieu to the intracellular environment. Investigators have discovered that the organization of these macromolecules is not random and specific areas of the membrane can be organized to facilitate signaling, endocytosis and numerous other biological functions. These aggregates are known as lipid rafts. We define these rafts as small (10-700nm) cholesterol-dense regions containing glycosylphosphatidyinositol (GPI) - anchored proteins, sphingolipids as well as other protein receptors (36, 128, 245). It is well-accepted that lipid rafts themselves are heterogeneous structures that vary in their protein/lipid composition and ratio (166). Lipid rafts are also dynamic; in a fluid state of aggregation and separation. Early studies of lipid raft domains consisted of detergent extraction techniques which investigators later discovered induced artifact in the system and produced erroneous data (167). It has since been determined that special techniques, such as electron microscopy, are required to characterize lipid rafts in an unperturbed system (166).

Important components of lipid rafts are the caveolae. Composed of caveolin protein, this structure is an invagination in the plasma membrane 50-80nm in diameter and has been shown to function in endocytosis (114). Raft-dependent endocytosis also has been shown to be reliant upon dynamin, a GTPase involved in the scission of vesicles from the plasma membrane (114). This internalization pathway has proven to be important to the internalization of various pathogens and toxins. Simian virus 40 (SV40)

and cholera toxin b-subunit (CT-B) have been shown to localize and become internalized in a raft/caveolae-dependent manner (265). *Escherichia coli* and *Campylobacter jejuni* also were shown to utilize this pathway for entry into epithelial cells (60, 248). Thus, caveolae in lipid rafts can serve critical functions for pathogen internalization and subsequent trafficking.

As discussed, lipid rafts are defined as inherently ultramicroscopic structures. However, studies with various pathogens and bacterial toxins have shown that large aggregations of cholesterol-dense, raft-like areas can occur and be characterized by confocal microscopy. Rafts can be visualized by staining with CT-B or pharmacological agents such as Filipin, which identify cholesterol rich areas. Co-labeling with antibodies for proteins such as caveolin-1 is considered an appropriate means to collectively characterize super aggregates (78, 245). Large lipid raft-like aggregations were reported for *L. monocytogenes* in response to the bacterial protein Listeriolysin-O (LLO) (74). Functionally, these aggregates can serve as platforms for endocytosis as well as innate immune signaling.

The cholesterol found in the raft domains has been shown to be important for endocytosis, survival and exocytosis of several pathogens. Human immunodeficiency virus 1 (HIV-1) is dependent upon raft domains for budding (150). *Chlamydia* spp. and *Helicobacter pylori* bacilli have been shown to preferentially bind cholesterol dense regions of the plasma membrane and depletion of cholesterol in the membrane has been shown to decrease binding of *Shigella flexerni* to epithelial cells (90, 96, 111). Gatfield and Pieters have shown that depletion of cholesterol in the plasma membrane is also detrimental for entry of *M. bovis*, BCG in macrophages (73). Collectively, we can

hypothesize that various pathogens manipulate the lipid raft domains, facilitating aggregation, to ensure entry and perhaps influence trafficking once inside the host cell.

Another interesting observation has been the link between lipid-raft dependent entry of bacterial pathogens and the autophagy pathway. Amer et al. have shown that *Legionella pneumophila* bacilli attach to lipid raft aggregates and become internalized (6). Co-labeling with autophagy markers and CT-B showed that the bacteria were contained in autophagosomes with lipid-raft domains in the vacuole membrane. Further, internalization and trafficking to autophagosomes in a raft-dependent manner appeared to assist in lysosomal evasion for this pathogen. Treatment with 3-methyladenine (3MA), an inhibitor of PI3K important for progression of the autophagy pathway, decreased the number of viable bacteria. It is interesting to speculate that this lipid raft/autophagy relationship could be involved in the trafficking of other pathogens such as *Mtb*.

Epithelial Cells and Respiratory Pathogens

Over the past decade there has been an increased focus on alveolar epithelial cells and the role they play in respiratory infection. As mentioned, alveolar macrophages are poorly reactive cells and thus require additional support to stimulate an effective immune response. Work by Kannan, et al. demonstrated that type II pneumocytes release monocyte chemoattractant protein (MCP-1) which enhances alveolar macrophage response to *Pseudomonas aeruginosa* (16). Colonization of epithelial cells has also proven to be essential to successful infections by *Legionella pneumophila* and *Burkholderia cepacia* (135, 225, 230). Blocking carbohydrate moieties on the surface of type II pneumocytes can enhance bacterial clearance and is postulated to be a target for

drug intervention (223, 228, 230). It has also been demonstrated that alveolar epithelial cells are responsible for IL-8 production, a neutrophil chemoattractant, which is crucial for the lung immune response against *L. pneumophila* (227).

Viral infections also target lung epithelial cells. Type II pneumocytes produce surfactant proteins which are vital to lung protection. As previously described, SP-A has been shown to play an important role in the lung immune response by increasing phagocytosis of pathogens. Aside from being the primary site of replication, it has been demonstrated that Respiratory Syncytial Virus (RSV) invades alveolar epithelial cells and reduces SP-A production be interfering with translation and exocytosis, resulting in viral load increase (3, 43). As with bacterial infections, these cells also release cytokines such as IL-8 to recruit immune cells crucial for the clearance of RSV (250). Taken together, these data reinforce the important role epithelial cells play in lung immunity (3, 42, 55, 72, 188, 190, 227, 250, 253)

Successful *Mtb* infections require the bacilli to transit from the lung alveoli through the blood to other organs. How mycobacteria migrate through the alveolar epithelial and endothelial cells and into the blood and what role these cells play in pathogenesis have not been examined in great detail. Previous *in vitro* studies focusing on epithelial and endothelial cells demonstrated that *Mtb* bacilli enter and replicate in type II alveolar pneumocytes in both monolayer and bilayer systems (22, 24, 138). Non-pathogenic mycobacteria, such as *M. smegmatis*, have also been shown to invade alveolar epithelial cells by macropinocytosis before being killed by the host cell (72). This suggests that entry into epithelial cells is not exclusive to pathogenic mycobacteria.

As with other respiratory pathogens, cytokines released from type II pneumocytes during the course of pathogenic mycobacterial infections may play an important role in bacterial clearance. A study by Sato et al. showed that human alveolar A549 type II cells release tumor necrosis factor α (TNF-α) and granulocyte-macrophage colony stimulating factor (GM-CSF) after *Mtb* infection, which help activate alveolar macrophages (190). However, the trafficking pattern of the bacilli through these cells and how they respond to a mycobacterial infection is yet undetermined. Other studies have shown that the actual movement through this tissue layer can induce phenotypic changes in the bacteria potentially contributing to virulence (136). The alveolar epithelial layer, therefore, may play an important role in early steps of *Mtb* infection.

In vitro infection models have shown that alveolar epithelial cell death following *Mtb* infection is mainly due to necrosis while infected macrophages typically undergo apoptosis (51, 58). A recent study by Kinhikar et al. has shown that ESAT-6 could be responsible for bacilli binding to epithelial cells and is associated with host cell death (104). Collaborative work with Dr. C. Harold King of the Emory University School of Medicine resulted in isolation of a mutant of *Mtb* strain Erdman (ΔRv3351c), which has also been associated with reduced necrosis in alveolar epithelial cells. The mutation was localized to gene *Rv3351c*; its product is of unknown function. We can speculate that disruption of the epithelial cell layer caused by *Mtb* virulence proteins facilitates increased bacteria dissemination from the lung.

Other mycobacterial mutants have demonstrated reduced virulence attributed to success in alveolar epithelial cells (8, 106, 146, 158, 164). The heparin-binding hemagglutinin (ΔHBHA) mutant has been shown to demonstrate reduced attachment and

dissemination from the lung. This adhesion molecule is expressed on the surface of *Mtb* and is believed to be specific for entry into epithelial cells (158). Kohama et al. demonstrated that extrapulmonary dissemination of *M. bovis* BCG bacilli was decreased when mice were immunized with recombinant HBHA protein prior to infection (7). Additionally, an increased Th-1 immune response was noted against the pathogen. These data allude to an important role for alveolar epithelial cells in the course of *Mtb* infection.

Conclusion

While extensive efforts and resources have been dedicated to examining *Mtb* and its interactions with various mammalian hosts and macrophages, it is evident that there are still significant gaps in our knowledge. The goal of the research described in this dissertation was to characterize *Mtb* interactions and trafficking within alveolar epithelial cells. Our data suggest major differences exist in the mechanisms used by *Mtb* bacilli to attach to, enter and replicate within professional and non-professional phagocytic cells.. However, we find that similarities exist between *Mtb* and other bacterial pathogens regarding their interaction with epithelial cells. This work has important implications for our understanding of this ancient pathogen, its many mechanisms for virulence and identifying and exploiting novel targets for vaccines and therapeutics.

CHAPTER 3

INVOLVEMENT OF THE AUTOPHAGY PATHWAY IN TRAFFICKING OF *MYCOBACTERIUM TUBERCULOSIS* BACILLI THROUGH CULTURED HUMAN TYPE II EPITHELIAL CELLS

Fine K.L., M. Metcalfe, E. White, M. Virji, R. Karls, F.D. Quinn. Accepted by *Cellular Microbiology*. Reprinted here with permission of publisher.

Abstract

Interactions between *Mycobacterium tuberculosis* bacilli and alveolar macrophages have been characterized, while trafficking of *M. tuberculosis* bacilli in epithelial cells has not been examined. In this study, we microscopically analyze endosomal trafficking of *M. tuberculosis* strain Erdman in A549 cells, a human type II pneumocyte cell line. Immuno-electron microscopic (IEM) analyses suggest that *M. tuberculosis* bacilli are internalized to a compartment labeled first with Rab5 and then with Rab7 small GTPase proteins. This suggests that, unlike macrophages, *M. tuberculosis* bacilli traffic to late endosomes in epithelial cells. However, fusion of lysosomes with the bacteria-containing compartment appears to be inhibited, as illustrated by IEM studies employing LAMP-2 and Cathepsin-L antibodies. Examination by confocal microscopy, transmission electron microscopy and IEM found *M. tuberculosis*-containing compartments surrounded by double-membranes and associated with the autophagy markers ATG16 and Lc3, providing evidence for involvement and intersection of the autophagy and endosomal pathways. Interestingly, inhibition of the autophagy pathway using 3-methyladenine improved host cell viability and decreased numbers of viable intracellular bacteria recovered after 72 hours post infection. Collectively, these data suggest that trafficking patterns for *M. tuberculosis* bacilli in alveolar epithelial cells differ from macrophages, and that autophagy is crucial for this process.

Introduction

Mycobacterium tuberculosis, the causative agent of tuberculosis, infects an estimated 1/3 of the world population; thus studies regarding mycobacterial interactions with host cells are critical for developing intervention strategies (86). Much of what is known regarding intracellular trafficking of *M. tuberculosis* bacilli has been derived from studies in human and murine macrophages as this cell type was historically believed to control initial success or failure of *M. tuberculosis* infections (137, 209). A process referred to as phagosomal maturation arrest (PMA) has been described which is characterized by recruitment of early endosomal markers, such as EEA-1 and Rab5, but not late markers, such as Rab7, to endosomal compartments containing virulent mycobacteria (9, 44-45, 244). PMA is also characterized by the absence of lysosomal-associated markers indicating prevention of lysosomal fusion with the bacterial-containing endosomes (131-132). Notably, non-pathogenic mycobacteria, such as *Mycobacterium smegmatis*, do not induce PMA and are degraded following phagosome/lysosome fusion (81).

The alveolar epithelial cell has been shown to play a major role during infection with numerous respiratory pathogens. Infection with Respiratory Syncytial Virus (RSV) has been demonstrated to reduce surfactant protein-A (SP-A) in alveolar epithelial cells which can increase viral load (3). Colonization of alveolar epithelial cells has proven to be essential for successful infections by bacterial pathogens *Legionella pneumophila* and *Burkholderia cepacia* (135, 230). Further, Bauman *et al.* demonstrated that epithelial cell infection with *Pseudomonas aeruginosa* induced the release of monocyte chemoattractant protein which enhances alveolar macrophage response to the pathogen (16).

Increasingly, the alveolar epithelial cell has been scrutinized for its role during *M. tuberculosis* infection. Previous *in vitro* studies demonstrated that *M. tuberculosis* bacilli can enter and replicate to high numbers in type II alveolar pneumocytes in both monolayer and in epithelial/endothelial bilayer systems, although internalization of alveolar epithelial cells is much slower than that observed in macrophages (22, 24, 138). Sato *et al*. showed that human alveolar A549 type II cells release tumor necrosis factor α (TNF-α) after infection with *M. tuberculosis* bacilli, which helped activate alveolar macrophages (190). Other studies have shown that mycobacterial movement through epithelial cells of the alveolus can induce phenotypic changes in *M. tuberculosis* that contribute to virulence (136). The alveolar epithelial layer, therefore, may play an important role, particularly in early stages of *M. tuberculosis* infection.

Recently, the autophagy pathway has been examined for its role in the host cell response to the presence of intracellular pathogens. Autophagy is divided into three categories: microautophagy, chaperone-mediated autophagy, and macroautophagy (65). Macroautophagy, here after referred to as autophagy, is considered to be an ancient cellular response to starvation allowing for recycling of amino acids and breakdown of organelles such as mitochondria (80). Additionally, autophagy is thought to be one of the most primitive mammalian cell responses against intracellular pathogens by providing secondary support when these organisms escape the typical phagosome/lysosome fusion mechanism (148, 196). A role for autophagy has been proposed for killing of *M. tuberculosis* bacilli (80). Studies report that stimulation of the autophagy pathway can increase lysosomal killing of *M. tuberculosis* bacilli in phagocytic cells (4, 172). This increased mycobactericidal capacity of lysosomes could explain why the autophagy

pathway is associated with improved clearance of *M. tuberculosis* bacilli in phagocytic cells. It is possible that autophagy could play a significant role in *M. tuberculosis* infections of nonphagocytic cells which have more limited means of controlling intracellular bacteria.

This study examined the internalization and trafficking of *M. tuberculosis* bacilli in the alveolar epithelial cells. Findings demonstrated previously undiscovered mycobacterial manipulation of host cell trafficking machinery, which promotes intracellular survivability of the bacteria.

Results

Replication *of Mycobacterium tuberculosis* Erdman bacilli in Type II Pneumocytes is verified by viable counts and TEM.

To verify *M. tuberculosis* bacilli replicate in A549 cells, amikacin-protection viability count experiments were conducted at an MOI of 100 with *M. tuberculosis* Erdman (fig. 1, panel A) A significant increase in intracellular bacteria was observed between T0, after a 6 hr uptake, and 72 hours post infection (hpi). To further examine relative levels of intracellular bacteria over this early time course, TEM analysis was conducted (fig. 1 panels B-D). As infections progressed, the percentage of intracellular bacteria observed increased from 23% at 18 hpi to approximately 75% by 96 hpi supporting the data obtained by viability count assay (fig. 1, panel E).

Mycobacterium tuberculosis-containing compartments co-localize with Rab7 with limited association of LAMP-2 and Cathepsin-L

Studies investigating intracellular trafficking of *M. tuberculosis* bacilli in macrophages have shown that virulent strains are capable of inducing phagosomal maturation arrest (PMA) (44-45, 244). Immuno-electron microscopy (IEM) and confocal studies demonstrated this with Rab5, an early endosomal marker present on *M. tuberculosis* containing compartments, and Rab7, a late endosomal marker which was absent (244). To determine if *M. tuberculosis* Erdman can initiate PMA in alveolar epithelial cells, A549 cells were infected and bacterial co-localization with Rab5 and Rab7 was examined. As a control, similar studies were conducted in J774 macrophages.

IEM experiments were conducted to quantify the association of early and late endosomal markers with bacilli-containing compartments. At 12 hpi, Erdman-infected A549 cells showed 42% of mycobacteria-containing endosomes (MCE) were labeled with both Rab5 and Rab7 and 20% were labeled with Rab5 alone (fig. 2, panels A & E). In contrast, only 25% of J774 macrophage MCE were double-labeled while 45% labeled with Rab5 alone (fig. 2, panels C & E). At 72 hpi, double labeling of A549 *M. tuberculosis* Erdman-containing endosomes at 72 hpi decreased to 24% (fig. 2, panels B & F). The majority of A549 bacteria-containing endosomes at this time point (72%) were labeled with Rab7 alone indicating that most of these compartments do acquire late endosomal markers (fig. 2, panel F). In J774 cells, 78% of the *M. tuberculosis* Erdman-containing compartments were labeled with Rab5 alone at 72 hpi, supporting previous observations of PMA (fig.2, panels D & F) (9, 44-45, 244).

Trafficking of *M. tuberculosis* bacilli to late endosomes in A549 cells was further investigated to evaluate fusion of lysosomes with the bacteria-containing compartment. IEM studies were performed using antibodies to lysosomal targets such as lysosomal associated-membrane protein 2 (LAMP-2) and cathepsin-L (fig. 3, panels A-D). At 12 hpi, 50% of bacilli-containing compartments were labeled with cathepsin-L (fig. 3, panel A & E). This number decreased to 24% by 72 hpi (fig. 4 panel B & E). IEM analysis of LAMP-2 colocalization at 12 and 72 hpi was also performed (fig. 3, panels C & D). Quantification demonstrated < 25% MCE associated with LAMP-2 antibodies at 72 hpi, supporting the trend observed with Cathepsin-L (fig. 4 panel F). These data indicate that lysosomal delivery to late endosomes containing *M. tuberculosis* Erdman is inhibited allowing for bacterial survival and replication in type II pneumocytes.

3-methyladenine treatment alters trafficking of *Mycobacterium tuberculosis* bacilli

TEM studies of infected human type II pneumocytes revealed double-membrane compartments containing *M. tuberculosis* Erdman bacilli (fig. 4, panel A). This observation suggests that autophagy plays a role in mycobacterial trafficking in alveolar epithelial cells. To address this hypothesis, A549 cells infected with *M. tuberculosis* Erdman bacilli were analyzed by IEM and confocal microscopy using an anti-Lc3A/B antibody; Lc3A/B is a common marker for autophagosomes (fig. 4, panels B-D). Confocal images showed Lc3 labeling of bacteria-containing compartments at 72 hpi (fig. 4, panel B). Results of the IEM experiments showed Lc3 labeling of 75% and 90% of Erdman-compartments at 12 and 72 hpi, respectively (fig. 4, panels C-E). These findings

suggest that trafficking of *M. tuberculosis* through A549 cells involves the autophagy pathway during early infection.

To determine the timing of autophagy involvement in the trafficking of *M. tuberculosis* bacilli, A549 cells were transfected with a plasmid coding for an ATG16-GFP fusion protein. ATG16 is a protein associated with early autophagophore nucleation and recruitment of autophagic membranes. Infection of the A549 cells with *M. tuberculosis* Erdman bacilli was analyzed by obtaining confocal z-stack microscopic images at 3 hpi. Images demonstrate association of ATG16 with bacilli during this early time point (fig 5, panels A). Three-dimensional construction of the z-stack slices demonstrates this association occurs at or close to the surface of the host cell suggesting that the autophagy pathway becomes involved in trafficking of *M. tuberculosis* bacilli immediately upon entry.

To further explore the role of autophagy in trafficking of *M. tuberculosis* bacilli in type II pneumocytes, A549 cells were pretreated with the autophagy inhibitor 3-methyladenine (3MA) prior to infection. TEM images at 12 hpi showed that bacilli attached and internalized in similar numbers in 3MA-treated and -untreated cells, but that the mycobacteria-containing compartments appeared disorganized in drug-treated cells (fig. 6, panels A, B). At the same time point, IEM experiments showed >10% of Lc3-labeling of these endosomes (fig. 6, panel E & G). Interestingly, autophagy inhibition by 3MA appears to wane over time; IEM images at 72 hpi showed that 85% of Erdman-containing compartments acquired Lc3 (fig. 6, panels F & G). TEM images at 72 hpi also showed reorganization of double membranes around mycobacteria-containing compartments (fig. 6, panels C & D).

Inhibition of autophagy impacts survivability of *Mycobacterium tuberculosis* bacilli and infected host cells

To further evaluate microscopic changes from 3MA infections with *M. tuberculosis* bacilli, A549 cells were either untreated or pretreated with 3MA, infected with Erdman and processed for bacterial viability count studies (fig. 7, panel A). Significant reductions in viable bacteria were observed in host cells pretreated with 3MA at 72 hpi ($p < 0.001$). Lactate dehydrogenase (LDH) release experiments were conducted to determine how bacterial viability correlated to host cell survivability. Cells treated with 3MA and infected with *M. tuberculosis* Erdman released 25% less LDH at 84 hpi compared to untreated cells (fig. 7, panel B). These results suggest that disrupting the autophagy pathway provides an advantage to the host cells infected with *M. tuberculosis* Erdman.

Discussion

Although much research has been devoted to examining *M. tuberculosis* interaction with phagocytic cells, some recent efforts have focused on the type II pneumocytes and how they might contribute to the pathogenesis associated with *M. tuberculosis* respiratory infections (24-25, 55, 136, 253). Several investigators have shown that internalization of mycobacteria in both A549 cells as well as murine primary lung epithelial cells is mediated by actin-dependent mechanisms (22, 110). In a transwell system, it has also been demonstrated that *M. tuberculosis* bacilli can transverse A549 cells to endothelial cells which would support a mechanism for hematogenous dissemination of mycobacteria *in vivo* (24). Studies have also demonstrated that infection of type II pneumocytes cell lines with *M. tuberculosis* resulted in host cell death by necrosis (51, 58). The

characterization of the fate of *M. tuberculosis* bacilli once inside the lung epithelial cell has yet to be described. The aim of this study was to document vacuolar trafficking patterns observed for *M. tuberculosis* bacilli in type II pneumocytes during early time points of infection.

In macrophages, Armstrong and Hart (1971) were the first to demonstrate that phagosomes containing *M. tuberculosis* bacilli may not mature into phagolysosomes [2]. Following phagocytosis, facilitated by mannose and complement receptors 1, 3 and 4, virulent strains of *M. tuberculosis* are believed to be maintained in an early phagosome (63, 99, 195). Though recent studies suggest that *M. tuberculosis* and *M. marinum* bacilli may escape from their compartment and enter the cytoplasm, others report that the bacilli remain within vesicles (205, 215-216, 240). Clemens and Horwitz (1995) characterized the Mycobacteria-Containing Phagosomes (MCPs) in terms of protein markers found on their surfaces. They showed that late endosomal markers, such as CD63, Lamp-1 and Lamp-2, Rab 7 as well as a marker for early endosomes, Early Endosomal Antigen (EEA-1) were largely absent from MCPs (44-45). Work by Via *et al*. (1997) determined that phagosomal maturation arrest (PMA) occurs between Rab5 and Rab7 endosomal maturation stages (244). Both Rab5 and Rab7 are known to direct trafficking of endosomes (243). More recently, Seto *et al.* have shown that differential recruitment of Rabs 14, 22a, 32, 38 and 39 could also be important markers for PMA in macrophages (197) .

Though still an area of ongoing research, the process by which pathogenic mycobacteria interfere with normal intracellular trafficking appears to be closely linked to the mannose-capped lipoarabinomannan (ManLAM) found on the surface virulent

Mycobacterium species. This complex lipid appears to inhibit the late endosomal fusion processes thereby decreasing the tethering of lysomsomes and subsequent acidification of the phagosomal compartment. It has been suggested that ManLAM activates p38 mitogen- activated protein kinase (MAPK) which then phosphorylates the guanine nucleotide dissociation inhibitor (GDI). This phosphorylation leaves Rab5 in its inactivated GDP-bound form thus interfering with the protein's ability to facilitate fusion with late endosomal vesicles (41, 79). These findings were supported by Ferguson and colleagues who demonstrated that coating *M. tuberculosis* bacilli with surfactant protein-D blocks the mannose cap and increases phagocytosis and phagosomal/lysosomal fusion (66). However, findings by Welin *et al.* indicated that LAM does not block phagosomal maturation through p38 MAPK interactions (249). Instead, it is suggested that LAM molecules insert into the *M. tuberculosis*-containing compartment and physically prevent the tethering and delivery of Rab7 and hence block fusion with lysosomes.

It has been demonstrated in this study, that unlike macrophages, the majority of *M. tuberculosis*-containing compartments in type II pneumocytes mature into late endosomes, thus by-passing classic PMA. By 72 hpi, over 90% of *M. tuberculosis* Erdman-containing vacuoles were either double-labeled with Rab5 and Rab7 or labeled with Rab7 alone, which can be characterized as late endosomes. It is believed that the double-labeled compartments reflect a transition period between early to late endosomes as described by other investigators (182). Our bacterial-viability count and TEM studies, however, do demonstrate survivability of *M. tuberculosis* bacilli in type II pneumocytes, thus it was important to further examine delivery of lysosomes to the mycobacteria-containing compartments. At 12 hpi, total labeling of *M. tuberculosis* endosomes with

LAMP-2 or cathepsin-L antibodies was ≤ 52%. This number dropped dramatically to 17-24% labeling by 72 hr pi. These data suggest that mechanisms of lysosomal inhibition require time to be up-regulated and once initiated are successful at preventing lysosomal fusion in type II pneumocytes. Further studies examining the mechanism for diminished lysosomal fusion with MCE are currently underway.

One possible explanation for the differences observed between trafficking of *M. tuberculosis* bacilli in macrophages and type II pneumocytes could be the role of the autophagy pathway. The data presented here demonstrated that *M. tuberculosis* Erdman bacilli can be found within double-membrane compartments in A549 cells, suggestive of autophagy. In addition, 90% of endosomes containing *M. tuberculosis* Erdman were associated with the autophagosomal marker Lc3 as early as 12hpi. Further, at 3 hpi, the autophagy protein ATG16 was found to be associated with *M. tuberculosis* bacilli around the surface of the host cell. These observations led to a hypothesis that the autophagy pathway is involved in early trafficking of virulent mycobacteria in type II pneumocytes and perhaps provides a general means for the bacteria to evade host cell defenses. Alternatively, autophagy may serve as a default mechanism for the epithelial cell as it attempts to remove intracellular mycobacteria. Other investigators have hypothesized that this pathway can provide defensive support for infected macrophages when intracellular pathogens escape the typical phagosome/lysosome pathway (80, 196). *Listeria monocytogenes*, which escapes the phagosome to reside in the host cell cytosol, has been shown to be recaptured by an autophorous vacuole and delivered to a lysosome (148). While some pathogens are ultimately killed in the autophagy pathway, select viruses and bacteria apparently have evolved intracellular survival strategies. *Shigella flexneri*, for

example, produces IcsB which inhibits autophagy once the bacteria facilitate their release into the cytosol (153). Certain positive-sense RNA viruses such as human poliovirus and mouse hepatitis virus utilize elements of the autophagy pathway to enhance replication (93, 171, 194). In fact, inhibition of the autophagy pathway has been observed to reduce viral load.

The role of autophagy during infection with *M. tuberculosis* is still under investigation. Studies in macrophages have shown that in up-regulation of autophagy under starvation conditions can overcome PMA to eliminate mycobacteria (80). Recently, Zullo *et al.* demonstrated that mycobacteria are capable of inducing the autophagy pathway in non-manipulated macrophages (80, 268). However, the impact this pathway might have on trafficking and bacterial survival has yet to be described. To date, no investigation has characterized the role of autophagy during *M. tuberculosis* infection in type II epithelial cells.

In this study, the PI3K inhibitor 3MA, which has been shown to block the autophagy pathway, was used to determine if inactivation of this pathway had an impact on the survival of mycobacteria in type II pneumocytes (168). While the effects of 3MA inhibition of the autophagy pathway appear to wane over a 72 hour period, the impact of early inhibition appears to have significant long term implications for *M. tuberculosis* survival in type II pneumocytes. Bacterial viable counts were monitored in 3MA-treated and untreated A549 cells infected with *M. tuberculosis* Erdman bacilli. Significantly fewer viable bacteria were detected from monolayers treated with 3MA compared with untreated controls at 72 hpi. These data correlated with host cell viability measurements demonstrating that at 72 and 84 hpi, host cells pretreated with 3MA and infected with *M.*

tuberculosis Erdman showed a 15-25% reduction in LDH release compared to infected non-treated controls. Reduced host cell necrosis of 3MA-treated cells infected with virulent *M. tuberculosis* strains suggests that blocking autophagy is advantageous to the host cell, and trafficking through the autophagy pathway are a means for mycobacterial survival.

It should be noted that TEM images of 3MA studies showed disorganized endosomes which begin to reform by 72 hpi. An alternative possibility that 3MA is inhibiting the Class III PI3-kinase, hVPS34, important for bacterial trafficking to late endosomes, must be examined to further evaluate these findings (165, 179). More studies specifically targeting the autophagy pathway are underway and will help determine if and where virulent mycobacteria manipulate this pathway and how mycobacterial mutants are impaired in this process.

Concluding Remarks

Collectively, this study suggests that *M. tuberculosis* has developed a multifaceted cell-specific approach to infection and colonization of the lung. The PMA that occurs in macrophages is not utilized in type II pneumocytes; however, lysosomal delivery remains impaired. The observation that the autophagy pathway could be utilized to the advantage of mycobacteria has been seen with other pathogens (153). How and where *M. tuberculosis* commandeers the pathway is under investigation.

Methods

Bacterial Culture

The *Mycobacterium tuberculosis* strain Erdman was obtained from the Tuberculosis/Mycobacteriology Branch of the Centers for Disease Control and Prevention and grown in Middlebrook 7H9 broth supplemented with 0.5% glycerol, 0.05% Tween 80, 0.5% bovine serum albumin (fraction V, Boehringer-Mannheim) and 0.085% NaCl. For confocal microscopy, *M. tuberculosis* Erdman was transformed with plasmid pFJS8gfpmut2 expressing green fluorescent protein (GFP) (247) or plasmid pGCRED2 expressing DsRed2 and maintained by inclusion of kanamycin at 50 µg/ml or hygromycin at 50 µg/ml, respectively. Plasmid pCGRed2 was a generous gift from Drs. Garry Coulson and Mary Hondalus, Department of Infectious Diseases, University of Georgia. Bacterial plating studies utilized Middlebrook 7H11 agar supplemented with 0.5% glycerol, 0.05% Tween 80 and 1 x ADS (31).

Cell Culture

A549 (CCL-185) human type II alveolar epithelial cells were obtained from the American Type Culture Collection (ATCC) and maintained in EMEM supplemented with 5% FBS or RPMI 1640 supplemented with 15% FBS, respectively. J774 murine macrophages were obtained from ATCC (TIB-67) and maintained in DMEM with 10% FBS.

Epithelial Cell Infection

Epithelial cell monolayers were infected at an MOI of 100 (100 bacteria per host cell) with *M. tuberculosis* bacilli. To disperse the inocula, bacteria were vortexed for 5 min then passed through an insulin syringe into the appropriate tissue culture wells. This method of bacterial dispersion was confirmed by microscopy to produce single bacilli for infection (data not shown). Cold synchronization was performed to coordinate bacterial internalization. This procedure included incubation of host monolayers at 4°C for 2 hr; 1 hr preceding infection and 1 hr after addition of the bacteria. After uptake, infected cells were incubated at 37°C with EMEM and amikacin [50µg/ml]; this was considered time point zero. Infections were maintained for 96 hr with samples taken at various hours post infection (hpi). For autophagy-inhibition studies, A549 cells were pretreated for 24 hr with 4 mM 3-methyladenine (Sigma) at 37°C.

Transfection With ATG16-GFP Plasmid

Plasmid pEGFP-ATG16L1 used in these studies was a generous gift from Dr. Tomatsu Yoshimori, Osaka University. To begin the transfection process, $1.0x10^5$ A549 cells were plated onto coverslips in 6 well Costar® dishes. The plates were incubated overnight at 37°C with 5% CO_2. Next the transfection mixture was prepared by combining 100 µl Opti-MEM media, 3µl of GeneJuice® (Novagen) and 1µg of the ATG16-GFP plasmid (per well). The solution was mixed by pipetting and incubating at room temperature for 10 min. The transfection mixture was added, drop wise, to each well of A549 cells and plates were returned to 37°C to incubate for 48 hr. Sample wells were imaged by confocal microscopy to verify transfection success. Transfection medium was removed

from each well after 48 hr, cells were washed with PBS, and EMEM with 5% FBS was added prior to infection. Infection proceeded at MOI=100 as described. At 3 hpi, infected medium was removed and cells were fixed with 3.7% paraformaldehyde. After staining with DAPI, coverslips were mounted with Prolong Gold® (Invitrogen) and imaged with a Nikon A1R confocal laser microscope system.

Immunofluorescence

For confocal microscopy, A549 cells were grown as monolayers to confluence, harvested after trypsin-treatment for 3 min at 37°C, seeded onto sterile cover slips and placed within 6-well Costar® dishes at 5 x 10^5 cells per well. The cells were allowed to adhere for 12 hr at 37°C and were infected as described previously. Specimens were fixed at indicated time points with 3.7% paraformaldehyde for 1 hr and washed 3 times with 1xPBS. The cells were then permeabilized for 10 min with 0.1% Triton X-100 and blocked for 30 min with PBS containing 3% BSA. Rabbit polyclonal anti-Lc3 (Novus Biologicals, Littleton, CO) antibodies, which detect Lc3A and B, were added to appropriate wells at a dilution of 1:200 and incubated at room temperature for 1 hr. Anti-Lc3 antibodies were detected with Alexa Fluor® 555 goat-anti-rabbit IgG (Invitrogen). Secondary antibody was added at a dilution of 1:500 and incubated for 1 hr at room temperature. Phalloidin Alexa Fluor®647 (Invitrogen) was added to select slides and incubated at room temperature for 35 min. Images were obtained using a Zeiss LSM 510 confocal microscope. Infections were performed in duplicate and experiments were repeated three times.

Transmission Electron Microscopy (TEM)

Cells were harvested and seeded into T25 flasks at a density of 5.0 x 10^6 cells/ml. Monolayers were cold synchronized and infections conducted as described previously. Specimens were fixed with 2.5% glutaraldehyde for 1 hr and then placed in phosphate buffer. Samples were then treated with 1% osmium tetroxide for 45 min and an ethanol series was used to dehydrate the specimens. Thorough infiltration was completed with three ratios of propylene oxide: resin (Epon-araldite). Resin recipes were based on protocols by Mollenhauer (143). Specimens were incubated 1 hr in resin followed by resin exchange and overnight incubation at room temperature. After an additional resin exchange, samples were embedded and polymerized overnight at 60°C. Ultrathin sections were mounted onto copper grids and stained with 4% uranyl acetate and lead citrate. Imaging was performed using a Tecnai BioTwin (FEI Company, Hillsboro, OR) electron microscope operating at 80 or 120 kV. Digital images were captured using a 2K x 2K camera (AMT, Danvers, MA). Images were sized for publication using Microsoft® Picture Manager and Adobe® Photoshop 7.0.

Immuno-Electron Microscopy (IEM)

Cells were seeded onto coverslips and infections performed as described for TEM. At the indicated time points, specimens were harvested and placed in 1.5% paraformaldehyde/0.025% glutaraldehyde solution for 1 hr, and then in phosphate buffer. The fixed specimens were dehydrated using a graded ethanol series; cells were incubated in different ratios of 85% ethanol: LR White embedding media as outlined by Goldsmith *et al.* (77). Samples were then allowed to incubate 1 hr in 100% LR White followed by a

fresh exchange and overnight incubation at 4°C. The following day, specimens were incubated in fresh LR White for 1 hr, placed in gelatin capsules, centrifuged (1500 x g, 5 min) and the blocks polymerized by incubation for 20-24 hr at 58°C. Ultrathin sections were mounted onto nickel grids and blocked with normal goat serum diluted 1:100. Each grid was incubated with a 1:500 dilution of anti-Lc3 (Novus Biologicals), anti-cathepsin-L (Abcam), anti-LAMP-2 (Invitrogen), anti-Rab5 (Abcam) or anti-Rab7 (Santa Cruz Biotechnology) antibody for 75 min. Gold-conjugated secondary antibodies, 12-nm goat-anti-rabbit IgG or 20-nm goat-anti-mouse (Jackson ImmunoResearch), were used at a 1:20 dilution with 1 hr incubation. Samples were imaged using a Tecnai BioTwin (FEI Company, Hillsboro, OR) electron microscope operating at 80 or 120 kV. Digital images were captured using a 2K x 2K camera (AMT, Danvers, MA). Images were cropped using Adobe® Photoshop 7.0.

For gold-label enumeration, control grids of uninfected cells with primary and secondary antibodies or with secondary antibody alone and infections with killed *M. tuberculosis* Erdman were incubated and background levels of labeling quantified. Compartments with greater than background levels of antibody binding were scored as positive. Accordingly, each grid of infected cells was scored for positive labeling. A minimum of one to two 20nm particle for Rab5, three 12nm particles for Rab7, two 12 nm particles for LAMP-2 and Cathepsin-L and a minimum of four 12nm particles for Lc3 were scored as positive in the respective experiments. A total of three grids were examined from three different block faces within a single sample to ensure data obtained was representative of each infected well. Quantification was conducted on three fields per grid. Percentages were calculated as positive-scored compartments among the total

number of compartments counted. Infections were performed in duplicate and experiments were repeated three times.

Intracellular Viability Counts

Epithelial cell monolayers (3MA-treated and untreated) were infected in parallel (MOI = 100) with *M. tuberculosis* strain Erdman. Monolayers were washed 3 times with PBS and incubated for 2 hr in EMEM with amikacin [200 μg/ml] and 5% FBS. Monolayers were washed with PBS and EMEM with amikacin [50μg/ml] was applied to the monolayers; this was defined as time point zero. At 24 and 72 hpi, the cells were washed with Hanks Balanced Salt Solution and lysed with 0.1% Triton X-100. Viable bacilli were enumerated by serial dilution of lysates in 1 x PBS + 0.05% Tween 80 and plating on 7H11 agar supplemented with 10% ADS, O.5% glycerol and 0.05% Tween 80. All infections were performed in triplicate and experiments were repeated three times.

Lactate Dehydrogenase (LDH) Release Assay

Host cells were seeded onto 6-well Costar® dishes at 1.0 x 10^6 cells per well 24 hr prior to infection. 3MA-treated cells were prepared as described previously. Prior to infection, each well was washed 3 times with Hanks Balanced Salt Solution and fresh medium was added. Cells were infected with *M. tuberculosis* strain Erdman at an MOI of 100 for up to 84 hr. All infections were performed in triplicate. Supernatants were sampled at various times and filtered through PVDF membranes (0.22-μm pore size). Immediately following collection, supernatants were assayed for LDH activity using the Cytotoxicity Detection Kit (Roche, Indianapolis, IN) (58). Percent LDH release was calculated using the

following formula: [(Release from strain - Background)/(Max release – Background)] x 100. Infections were performed in triplicate and experiments were repeated three times.

Quantification of TEM

Measures were taken to ensure that TEM quantification of each infected well of type II pneumocytes was representative of the heterogeneous population of infected cells in every sample. Each infected well was embedded and a total of three faces per block were cut to produce three grids per face, for a total of 9 grids per sample. This measure ensured that varying depths of a single sample were thoroughly analyzed. Ultrathin sections applied to copper grids were subdivided based on the transversing support wires which cross the surface of the grid. Twenty grid fields containing 10-15 infected pneumocytes per field were quantified for each of the nine grids per sample. The number of bacteria inside the cells was divided by the total number of bacteria within the defined grid fields to determine the percent internalization. Infections were performed in duplicate and experiments repeated three times.

Statistical Analysis

Statistical significance of bacterial counts, IEM gold labeling and LDH release data was examined by ANOVA and Tukey's HSD post-hoc comparison ($\alpha = 0.05$) using SPSS 17.0® statistical software.

Acknowledgements

We thank Barbara Reaves, Cynthia Goldsmith, Charles Humphrey and Sharif Zaki for their critical reviews of the manuscript and technical assistance in several parts of this project. This work was supported in part by research grants from the American Lung Association (R.K.) and the University of Georgia Faculty of Infectious Diseases (F.Q.).

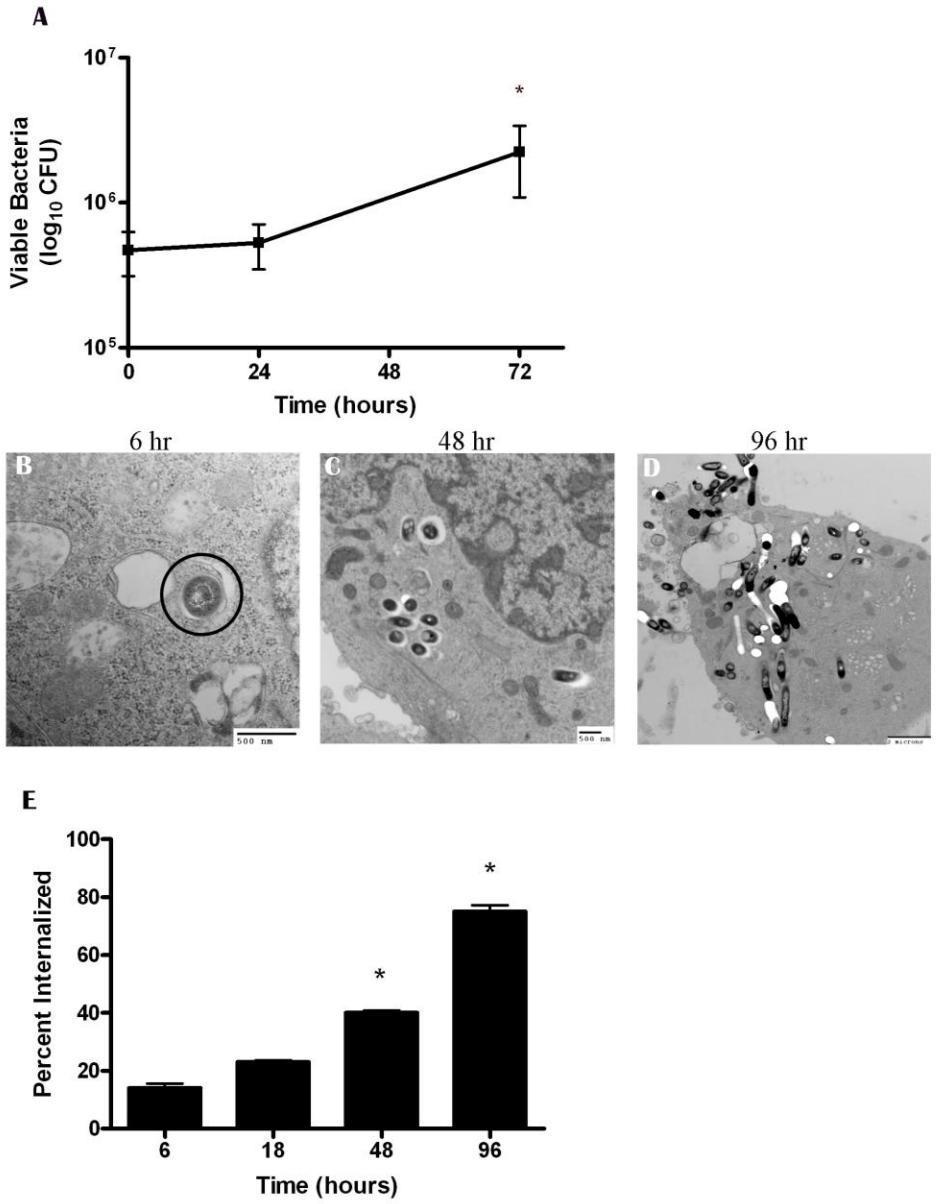

Figure 1. Bacterial viability counts and transmission electron microscopy demonstrate increasing numbers of intracellular *M. tuberculosis* bacilli in human type II epithelial cells. Internalized bacterial viability counts (by antibiotic protection assays) from A549 cells infected with *M. tuberculosis* Erdman at 0, 24 and 72 hpi demonstrate a significant increase in numbers of intracellular bacteria in an infected population of host cells over a 72 hr window (*p-value < 0.001) (A). Infected samples were embedded for TEM analysis as described in the methods. For the nine grids that represented each infected well of A549 cells, an average of 10-15 infected pneumocytes per grid field were analyzed. Representative images of infected A549 cells from this study at 6, 24, and 96 hpi demonstrate an increasing intracellular bacilli (electron dense rods) burden over time (B-D). Bacilli are circled in panel B only. Enumeration from TEM

images (E) demonstrate a significant increase in intracellular bacteria over time (*p-value < 0.001). Viable count assays were performed in triplicate and TEM infections in duplicate with all experiments repeated three times. Data is reported for one experiment of triplicate infections which are representative of the findings for three experiments. Quantification of TEM data is an average for the three experiments.

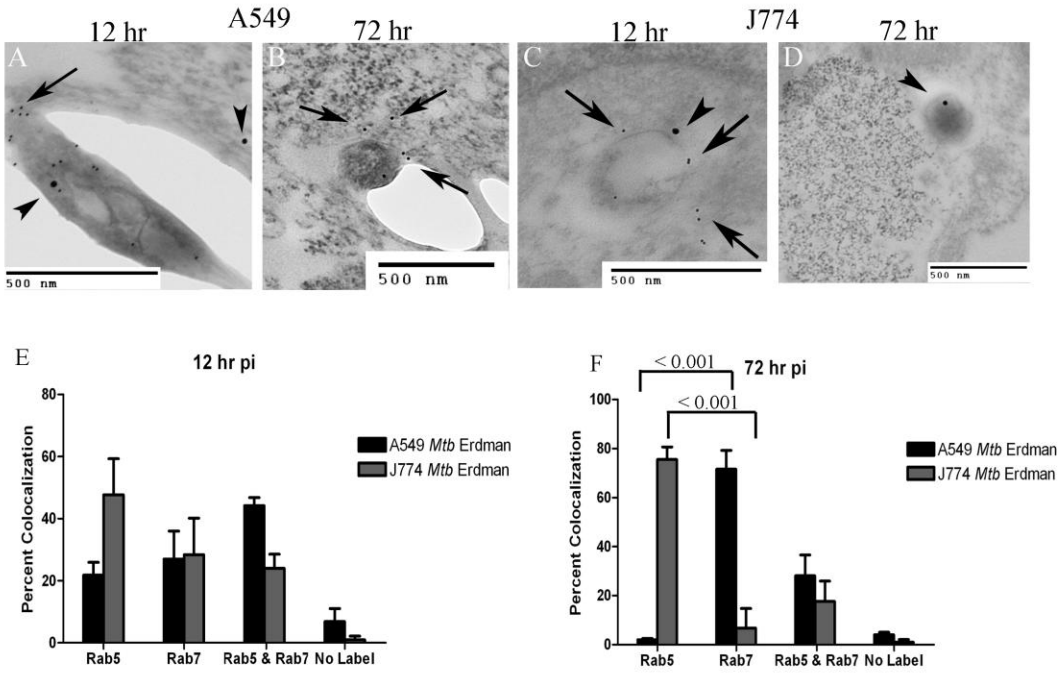

Figure 2. Microscopic examination of Rab5 and Rab7 co-localization with endosomes containing *M. tuberculosis* bacilli in human type II pneumocytes and murine macrophages. A549 (A and B) and J774.A1 (C and D) infections with *M. tuberculosis* bacilli were examined by IEM with anti-Rab5 and anti-Rab7 antibodies labeled with 20-nm (arrow heads) and 12-nm (arrows) gold particles, respectively. Co-localization of bacilli with Rab5 and Rab7 by IEM was quantified at 12 hpi and 72 hpi (E and F). A minimum of one or three gold particles was required to score Rab5 or Rab7 positive, respectively. In A549 cells, significantly more bacilli-containing compartments were associated with Rab7 compared to Rab5 at 72 hpi (p-value < 0.001). Conversely, in macrophages the majority of bacilli-containing compartments were labeled with Rab5 at the same time point (p-value < 0.001). A total of 27 grid fields from nine grids were analyzed from three block faces within each sample. An average of 10-15 pneumocytes per grid were assessed. Infections were performed in duplicate and experiments repeated three times. Quantification is the average for all three experiments.

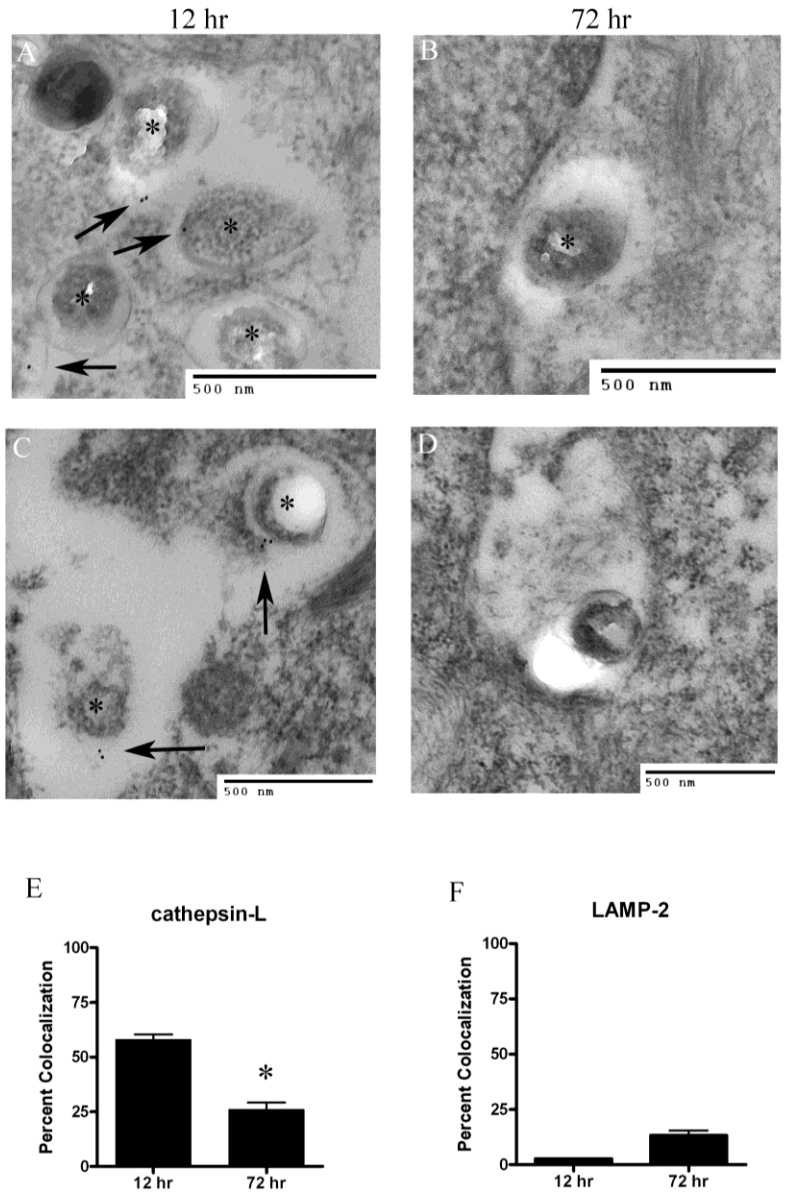

Figure 3. LAMP-2 and cathepsin-L co-localization with *M. tuberculosis*-containing endosomes in A549 cells indicates limited lysosomal delivery. Following infection with *M. tuberculosis* bacilli for the indicated times, specimens were prepared for IEM as described with cathepsin-L labeled with 12-nm gold particles (A, B). Experiments were repeated with gold-labeling of LAMP-2 (C, D). * Denotes bacilli. A minimum of two gold particles per compartment were required to score lysosomal positive. Arrows identify gold particles in each panel. Co-localization of bacilli with cathepsin-L and LAMP-2 by IEM was quantified (E, F). Significantly fewer Cathepsin-L markers were associated with mycobacteria-containing compartments at 72 hpi compared to 12 hpi (* p-value < 0.05). Quantification was performed as described in the methods and figure 2. Infections were performed in duplicate and experiments repeated three times. Quantification is the average for the three experiments.

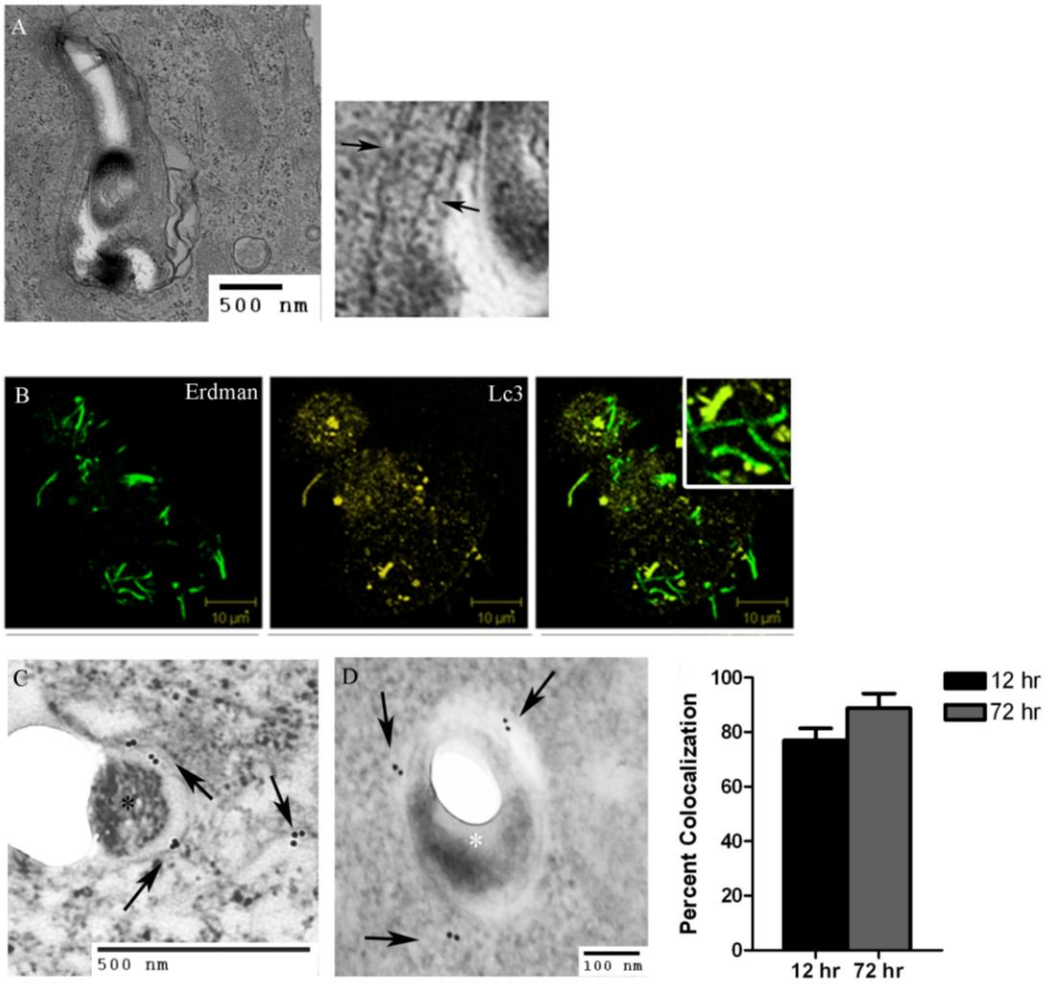

Figure 4. Detection of autophagosomal compartments surrounding *M. tuberculosis* bacilli in A549 cells. A549 cells were infected with *M. tuberculosis* Erdman bacilli at an MOI = 100 and examined by TEM. Double-membrane vacuoles containing bacilli (*) of strain Erdman (A) were detected at 48 hpi. Inset to the right shows magnified region highlighting membrane segments (arrows). Confocal microscopy at the same time point demonstrates co-labeling of GFP-expressing *M. tuberculosis* bacilli (green) with Lc3 (yellow) (B). Punctate Lc3 staining is observed around some bacilli (inset). IEM was used to measure co-localization of Lc3 with *M. tuberculosis*-containing compartments at 12 (C) and 72 hpi (D). Infected and control specimens were incubated with anti-Lc3 antibodies then labeled with 12-nm gold particles (arrows). Enumeration of Lc3 labeling from 27 grid fields per sample is presented (E). Arrows identify Lc3 markers associated with bacteria-containing compartments. Infections were performed in duplicate and experiments were repeated three times. Quantification is the average for the three experiments.

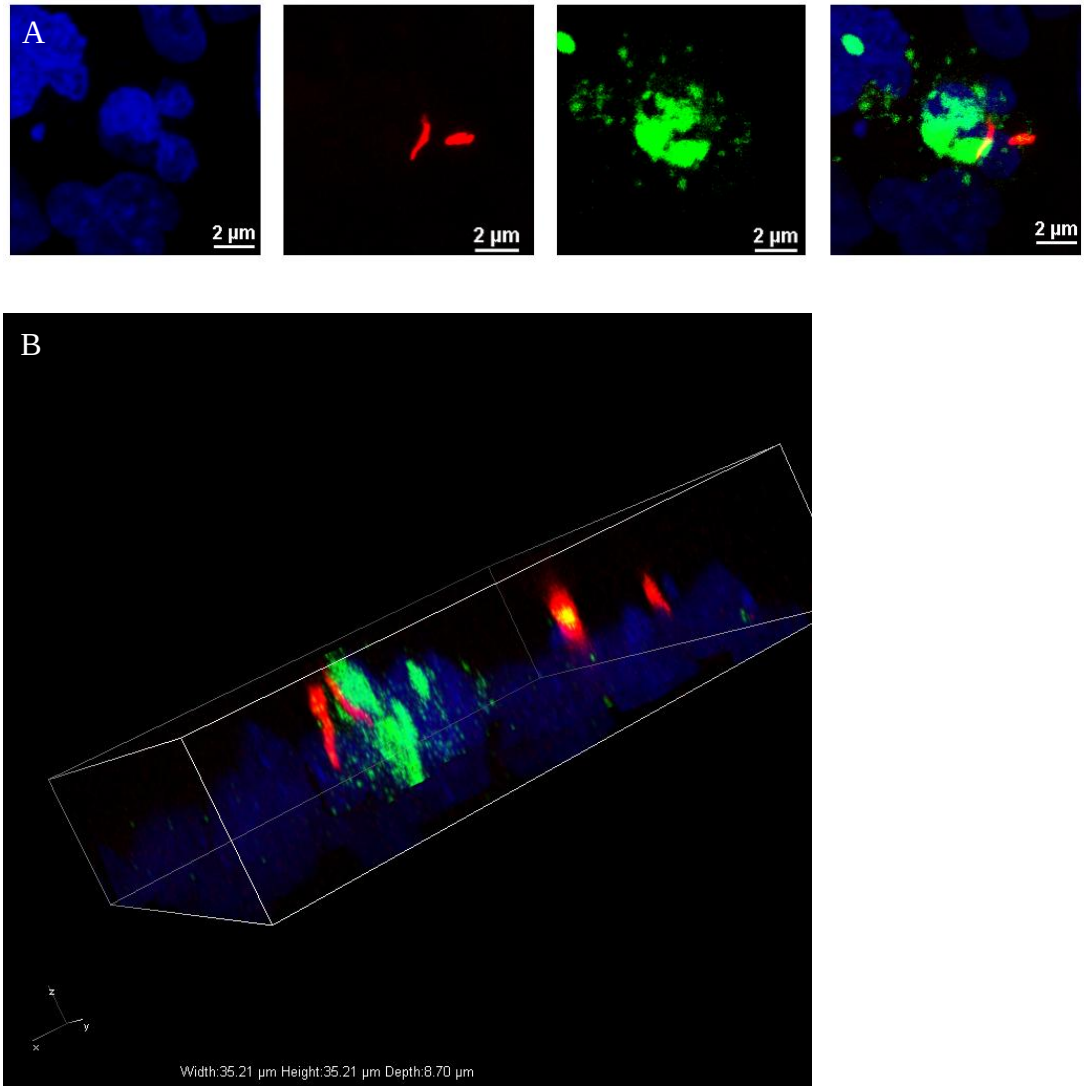

Figure 5. *M. tuberculosis* bacilli colocalized with ATG16 at 3 hours post infection. A549 cells were seeded onto coverslips in 6 well dishes and transfected with the EGFP-ATG16L1 plasmid for 48 hr. The cells were infected with *M. tuberculosis* Erdman transformed with pGCRed2. After 3 hpi, coverslips were fixed, stained with DAPI and mounted for confocal microscopy. A merge of confocal z-stack slices show colocalization of ATG16 (green) with *M. tuberculosis* bacilli (red) (A). A 3D reconstruction of confocal slices demonstrates association of ATG16 with the bacilli toward the surface of the host cell suggesting early association of the autophagy pathway (B). Infections were performed in triplicate and images were obtained with a Nikon A1R confocal laser microscope system

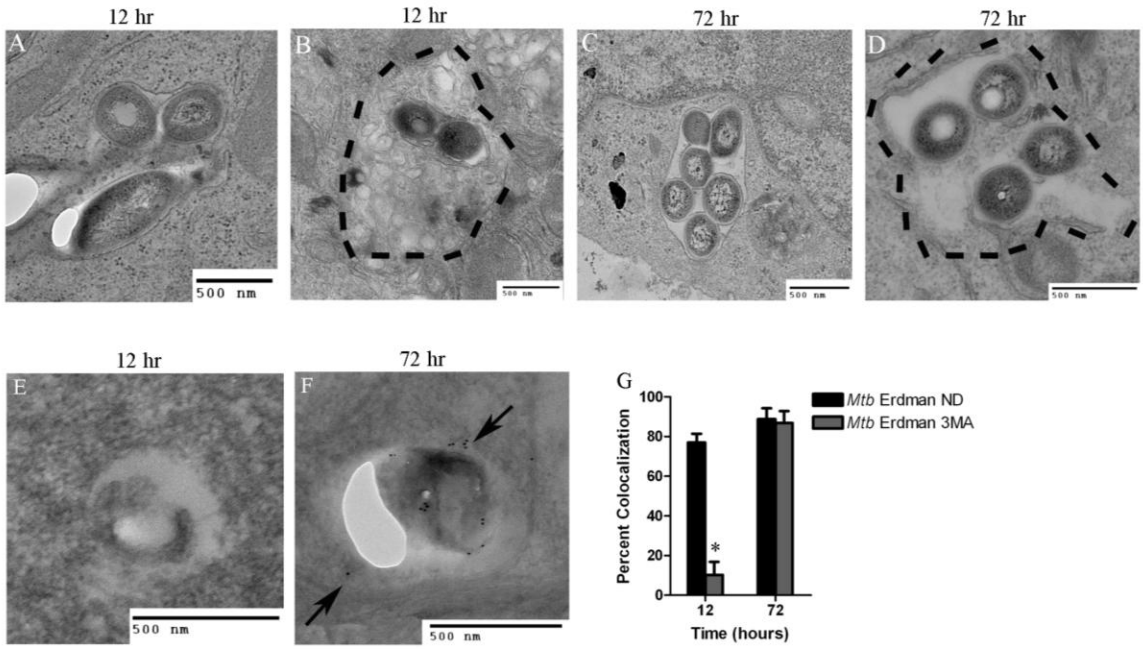

Figure 6. TEM and IEM analysis of 3MA treatment on autophagosomal trafficking of *Mycobacterium tuberculosis* bacilli in A549 cells. Untreated (A,C,E) or 3MA-treated (B,D,F) A549 cells infected with *M. tuberculosis* Erdman bacilli and examined by TEM (A-D) or IEM using anti-Lc3 labeled with 12-nm gold particles (E,F) as described. Loose vacuoles containing *M. tuberculosis* bacilli from cells pretreated with 3MA at 12 and 72 hpi have been outlined (B, D respectively) compared to the untreated cells (A, C, respectively). Reorganization of autophagosomes begins to occur at 72 hpi. Little co-localization of Lc3 with endosomes containing *M. tuberculosis* bacilli is detected at 12 hpi (E), but co-localization is evident at 72 hpi (arrows) (F). Microscopic quantification of Lc3 co-localization with bacterial-containing endosomes from 27 grid fields per sample is presented (G). Pretreatment with 3MA produced significantly fewer Lc3-labeled compartments compared to non-drug treated infections at 12 hpi (*p-value < 0.001). Infections were performed in duplicate and experiments were repeated three times. Quantification presented is an average of all three experiments. Images are representative of overall findings and quantification is the average for the three experiments.

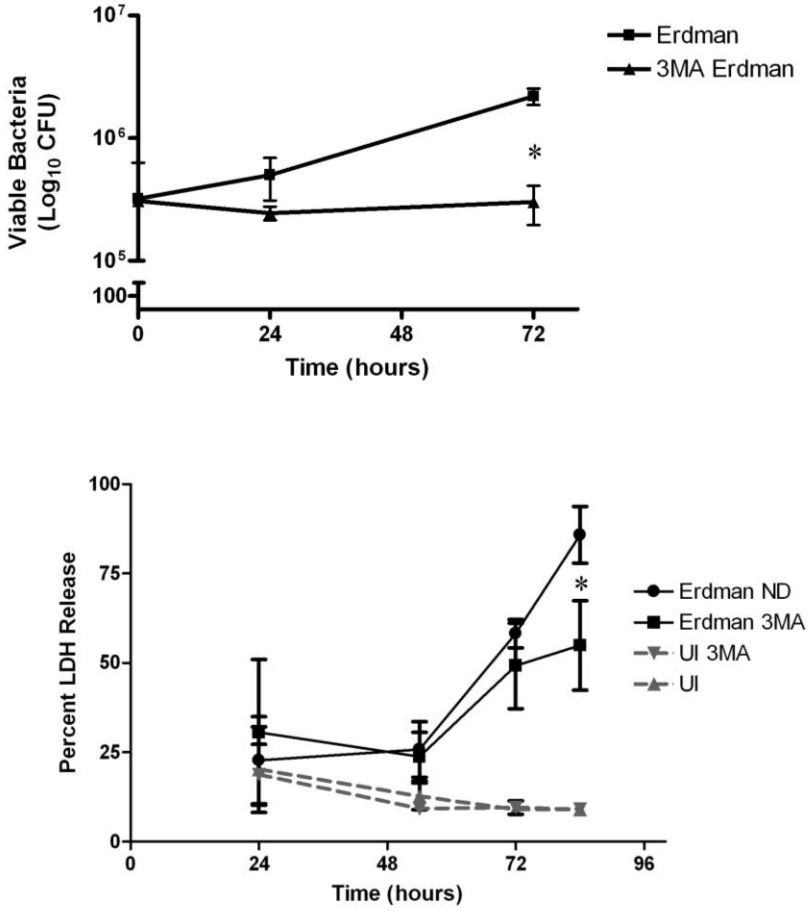

Figure 7. Effects of 3MA treatment on bacterial and host cell survival. Untreated or 3MA-treated A549 cells were infected with *M. tuberculosis* Erdman bacilli as described in Methods. Samples were analyzed for bacterial viability (A). Significant differences were noted in viable counts between 3MA-treated and non-treated cells at 72 hpi (*p-value<0.001). Untreated or 3MA –treated A549 cells were also monitored for LDH release over time uninfected (UI) or following infection with *M. tuberculosis* Erdman (B). Significant differences in LDH release are observed between 3MA-treated and untreated A549 infections at 84 hpi (*p-value < 0.001). Infections were performed in triplicate and experiments repeated three times. Viability count data is reported for one experiment with is representative of trends observed in three experiments. LDH data is the average from three experiments.

CHAPTER 4

THE ROLE OF LIPID RAFT AGGREGATION IN THE INFECTION OF TYPE II PNEUMOCYTES BY *MYCOBACTERIUM TUBERCULOSIS* BACILLI

Fine K.L., B.J. Reaves, R.K. Karls, F.D. Quinn. Submitted to *PLoS One*, 05/31/2012.

Abstract

Dynamic, cholesterol-dense regions of the plasma membrane, known as lipid rafts (LR), have been observed to develop during and may be directly involved in infection of host cells by various pathogens. This study focuses on LR aggregation induced in alveolar epithelial cells during infection with *Mycobacterium tuberculosis* bacilli. We report dose- and time-dependent increases in LR aggregation after infection with three different strains at multiplicities of infection of 1, 10 and 100 from 6-24 hr post infection (hpi). Specific strain-dependent variations were noted among H37Rv, HN878 and CDC1551 with H37Rv producing the most significant increase from 15 aggregates per cell (APC) to 27 APC at MOI 100 during the 24 hour infection period. Treatment of epithelial cells with Culture Filtrate Protein, Total Lipids and Gamma-Irradiated whole cells from each strain failed to induce the level of LR aggregation observed during infection with any of the live strains. Filtered supernatants from infected epithelial cells did produce comparable LR aggregation, suggesting a secreted mycobacterial protein produced during infection of host cells is responsible for LR aggregation. Disruption of lipid raft formation prior to infection indicates that *M. tuberculosis* bacilli utilize LR aggregates for internalization and survival in epithelial cells. Treatment of host cells with the LR-disruption agent Filipin III produced a nearly 22% reduction in viable bacteria for strains H37Rv and HN878, and a 7% reduction for strain CDC1551 after 6 hpi. This study provides evidence for significant mycobacterial-induced changes in the plasma membrane of alveolar epithelial cells and that *M. tuberculosis* strains vary in their ability to facilitate aggregation and utilization of LR.

Introduction

Mycobacterium tuberculosis (*M. tuberculosis*), the causative agent of tuberculosis (TB), has infected an estimated one-third of the world's population with potentially 60-90% of these individuals harboring the latent form of the disease (86). While significant research has been focused on *M. tuberculosis*/host interactions, there remains a paucity of data defining attachment and internalization of bacilli with the epithelial cells that line the alveolus.

Over the last 15-20 years our understanding of eukaryotic cell membrane organization has changed dramatically. Areas of the plasma membrane, known as lipid rafts (LR), have been described as dynamic regions within the membrane enriched in cholesterol, glycosphingolipids, sphingomyelin, phospholipids with acyl chains, glycosylphosphatidylinositol (GPI)- linked proteins as well as other membrane proteins such as innate immune receptors (128, 151, 234). Studies utilizing phototonic force microscopy and fluorescent resonance energy transfer have established the size of rafts in an unperturbed cell system to be approximately 5nm-50nm in diameter which would be undetectable by light microscopy (128, 170, 200). However, other studies have demonstrated that stimuli applied to the plasma membrane, such as bacteria and/or the toxins they produce, can induce aggregation of LR to a size observable by confocal microscopy (71, 74, 108, 169, 186, 255).

Lipid raft aggregation on target host cells in response to interactions with infectious agents has yielded interesting results for viruses and bacteria alike. Influenza virus has been shown to associate with LR via hemagglutinin and neuraminidase, and examination of enveloped virions post-budding shows a significant number of raft

domains within the viral envelope (14). Further, it has been demonstrated that LR are important for HIV-1 viral budding (92). During bacterial infections, LR have been shown to induce important changes in lipid raft formation. Some bacterial proteins, produced during infection, help facilitate hijacking of the host cell. Binding of cholera toxin subunit B to ganglioside (GM1) found in LR; is required for uptake of the toxin (121). Further, various bacterial proteins have been shown to induce LR aggregation to promote host cell responses to the pathogen. For example, treatment of macrophages with Listeriolysin-O (LLO) has been shown to induce large "super" aggregates of LR which facilitate signaling through receptor tyrosine kinase domains, suggesting LR aggregation may facilitate an innate immune response during infections with *Listeria monocytogenes* (74).

LR have also been shown to promote internalization of various bacterial pathogens. This function appears to be linked to caveolin proteins found within the microdomains. Caveolin proteins associate intimately with LR forming invaginations known as caveolae. These invaginations have been shown to facilitate the uptake and colonization of pathogenic strains of *Escherichia coli*, *Salmonella typhimurium* and *Pseudomonas aeruginosa* (60, 85, 125). Caveolin-1-deficient mice have been shown to be more resistant to pulmonary *P. aeruginosa* infection; this correlates with LR/caveolae-dependent endocytosis of the bacteria in type I alveolar epithelial cells (263-264, 266). These studies also found a signaling function for LR platforms in the same host cells in response to *P. aeruginosa* attachment. Collectively, this work demonstrates that LR serve important functions during bacterial invasion.

Previous studies have also investigated the role of LR and cholesterol aggregation during *M. tuberculosis* infection of macrophages and mast cells. Shin *et al*. demonstrated translocation of Toll-like Receptor-2 (TLR2) to LR in macrophages treated with the *M. tuberculosis* 19kDa lipoprotein LpqH (202). Gatfield and Pieters (2000) performed staining with the LR-disruption agent Filipin to demonstrate cholesterol clustering around *Mycobacterium bovis* BCG during infection and that subsequent depletion of cholesterol inhibited uptake of the bacilli in macrophages (73). Interestingly, *M. tuberculosis* entry into mast cells has also been shown to be LR dependent (147). Other studies have demonstrated that mycobacterial cell wall lipids such as lipoarabinomannan can become incorporated into membrane rafts found in phagosomes to inhibit phagosome/lysosome fusion in macrophages (88, 249).

To date, no investigation has been conducted to characterize variations in LR aggregation in non-phagocytic cells during infection. Further, no studies have compared the variance in plasma membrane response to multiple strains of *M. tuberculosis* and the subsequent role of the aggregates produced. To evaluate the role of LR aggregation in *M. tuberculosis* pathogenesis within alveolar epithelial cells, type II pneumocytes were infected with virulent laboratory strain H37Rv as well as more recent clinical isolates, CDC1551 and HN878 (13, 134, 237). The objective of this study was to examine dose- and time-dependent LR aggregation in response to different *M. tuberculosis* strains in the alveolar type II epithelial cell.

Results

Live *Mycobacterium tuberculosis* strains induce dose and time-dependent Lipid Raft aggregation in A549 cells

To investigate lipid raft (LR) aggregation, monolayers of A549 human type II pneumocytes were infected with *M. tuberculosis* strains HN878, CDC1551 and H37Rv. Bacterial multiplicities of infection (MOI) of 1, 10 and 100 were used to assess LR aggregation based on strain and bacterial load differences. Listerolysin-O (LLO), produced by *L. monocytogenes*, has been shown to induce LR "super" aggregation and was thus applied to uninfected cells as positive control for these studies (74). Aggregation was assessed by quantifying the colocalization of Cholera Toxin-B (CT-B)-stained puncta and caveolin-1 antibody labeling. This is shown for the control, LLO treatment in Figure 1 A. At a MOI of 10, confocal images demonstrated an increase in LR aggregation compared to uninfected controls at 6 hr post infection (hpi) (data not shown). By 24 hpi, LR aggregation was notably increased for each strain compared to uninfected controls (Fig. 1 panel B). Strain-related differences were observed at 24 hpi with HN878 and H37Rv producing higher levels of LR aggregation compared to CDC1551 (Fig. 1 panel B). Similar observations were made for MOI 1 and 100 at both time points (supplemental data Fig. 1 & 2 panels A- B).

LR aggregates produced on A549 cell membranes after infection with H37Rv, HN878 and CDC1551 were quantified from confocal images for each MOI at 6 and 24 hpi using colocalization of CT-B and caveolin-1 as the marker for LR aggregation. A time-dependent increase in LR aggregation was noted for all three strains (Fig. 2 panels A, B & C). Significant dose-dependent increases were also observed for H37Rv and

HN878 at 6 and 24 hpi. The level of aggregation observed at 24 hpi was comparable to LLO positive controls. These data suggest that *M. tuberculosis* bacilli induce LR aggregation in a dose and time dependent manner and that individual isolates vary in their ability to induce LR aggregation.

Mycobacterium tuberculosis-derived Total Lipids and Culture Filtrate Proteins induce limited Lipid Raft aggregation

The novel observation of LR aggregation in response to infection with *M. tuberculosis* bacilli was further examined to determine if acellular mycobacterial components were capable of inducing the LR aggregation observed during infection with live bacteria. To answer this question, total lipid extracts (TL) and culture filtrate proteins (CFP), secreted by the bacteria when grown in broth culture, from each strain were obtained and applied to alveolar epithelial cells. After treatment and labeling for LR, images were quantified for induction of aggregates as described (see above and supplemental figure 3). Significantly fewer LR aggregates were observed for all three strains with TL treatment compared to live bacterial infections at 6 and 24 hpi (Fig. 3). Total lipid extracts from all three strains induced < 4 aggregates per cell at both time points. Interestingly, at 6 hpi, HN878 TL produced increased numbers of aggregates (2.8) compared to H37Rv (1.8) and CDC15551 (1.1), similar to the trend observed with live infections at the same time point. This pattern was repeated at 24 hpi though no significant differences were noted among strains. However, the number of LR aggregates produced by TL treatment was significantly decreased compared to aggregation induced by live bacterial infection with each strain (p-value <0.001).

Epithelial cell monolayers treated with CFP from each strain were processed for confocal microscopy and LR aggregates quantified. The number of aggregates observed for H37Rv and HN878 CFP was significantly increased compared to controls (Fig. 4). There was no significant difference noted in the number of LR aggregates between 6 and 24 hr post treatment. Overall, CFP treatments produced significantly fewer aggregates compared to infections with live bacteria for all three strains at 6 and 24 hpi (p-value < 0.001).

Collectively these data suggest that the mycobacterial components, TL or CFP from broth-grown cultures, do not demonstrate the degree of LR aggregation observed during infection with live *M. tuberculosis* strains.

Gamma-Irradiated bacteria induce limited Lipid Raft aggregation

To determine if the binding of inactivated but intact *M. tuberculosis* bacilli to the A549 cell membrane was sufficient to induce the level of LR aggregation observed during infection with live mycobacterial strains, aliquots of gamma-irradiated bacilli were obtained for all three strains and applied to epithelial cell monolayers as described. All Gamma-Irradiated strains yielded statistically significant increases in LR aggregation compared to uninfected controls (p-value < 0.001). Differences in LR aggregation between strains at both time points was not significant, however, addition of irradiated HN878 bacilli did produce a slight increase in LR aggregate number compared to the other two strains which might be attributed to differences in cell wall components observed in previous studies (Fig. 5) (49). Strain CDC1551 induced aggregation similar to H37Rv at 6 and 24 hpi (Fig. 5). An increase in total LR aggregates was noted from 6 to

24 hpi for each strain in a manner similar to infection with live strains. However, the number of LR aggregates observed overall was significantly decreased compared to live infections.

To test whether accumulated input from gamma-irradiated bacilli and CFP would result in the same induction of LR observed with live strains, summation of these experiments was performed for comparison. The number of LR aggregates induced by gamma-irradiated bacilli and CFP is indicative of some basal level of aggregation induced at 6 and 24 hpi. However, these components only account for 40-55% of the LR aggregation seen at 24 hpi with live H37Rv, HN878 and CDC1551 (p-value < 0.001, 0.01 and 0.05 respectively) (Fig. 6). These data suggest that products secreted by live bacteria during an infection are responsible for the level of LR aggregation observed.

Mycobacterial-proteins produced during infection induce Lipid Raft aggregation

To determine if the LR-inducing product(s) from live bacilli is a secreted protein expressed during infection of host cells, monolayers of epithelial cells were infected with *M. tuberculosis* strains that were pre-treated with amikacin to inhibit active bacterial protein synthesis, or infected with non-treated bacilli. After 24 hpi, supernatants from the infected cells and controls were collected then filtered to remove bacteria. The filtered supernatants were then applied to a fresh monolayer of A549 cells and incubated for 24 hr. Cells were fixed and prepared for confocal analysis as described. No significant difference in the number of LR aggregates was noted between control supernatants, uninfected and uninfected with amikacin, or supernatants from A549 cells infected with amikacin-treated bacteria (p value > 0.05) (Fig. 7). However, A549 cells treated with filtered supernatants from infections with strains not treated with antibiotic produced a

significant increase in LR aggregates compared to amikacin-treated controls (p-value < 0.001). Supernatants from H37Rv and HN878 infections produced ~37 and 38 aggregates per cell, respectively, compared to ~5 and ~4 aggregates per cell induced by supernatants from the same mycobacterial strains pretreated with amikacin. A similar trend was observed with supernatants from CDC1551 infections (~30 aggregates per cell) compared to supernatants from amikacin-treated bacteria (~7 aggregates per cell). In these experiments, a slight increase in total LR aggregate numbers was observed compared to live bacteria experiments although not statistically significant (p-value > 0.05). These data confirm that mycobacteria-induced LR aggregation results from proteins secreted by live *M. tuberculosis* strains during infection of epithelial cells

Toll-Like Receptors do not co-localize with mycobacteria-induced Lipid Raft aggregates

It was previously demonstrated during infection with various pathogens that aggregation of LR serves to protect monocytes and epithelial cells through increased innate immune receptor signaling (206, 234). To determine if the *M. tuberculosis*-induced LR aggregation served as platforms for host receptors, Toll-Like Receptor (TLR) 2 and 4, both important cellular receptors which initiate innate responses to mycobacteria, were examined for colocalization with CT-B stained puncta (59, 89, 202). Positive controls PamCSK4 and LPS were used for TLR2 and TLR4 translocation to LR, respectively. Epithelial cells infected with live *M. tuberculosis* strains produced <6% colocalization of TLR2 antibodies with CT-B stained aggregates compared to 32% with positive controls (Fig. 8, A). Likewise, live infections produced <7% colocalization compared to 15% with LPS (Fig. 8, A). In both experiments TLR colocalization with LR aggregates was

significantly lower than colocalization with positive controls (p-value < 0.001). These data suggest that LR aggregates are not functioning as platforms for TLR2 or TLR4 in response to live *M. tuberculosis* infection.

To determine if basal LR aggregation observed on A549 cells after addition of CFP, TL and gamma-irradiated-whole bacteria may serve to produce the low level of TLR colocalization demonstrated with live bacteria, epithelial cells were treated with these components as described and evaluated for colocalization. Treatment with TL, CFP and gamma-irradiated bacteria from all three *M. tuberculosis* strains produced <10% colocalization with TLR2 and <12% colocalization with TLR4 compared to approximately 30% colocalization with positive controls (Fig. 8, B-D). Collectively, these data suggest that constitutively-expressed components may be responsible for low level TLR colocalization with LR aggregates and subsequently some signaling functions. However, the degree of aggregation observed with live *M. tuberculosis* strains compared to TLR2 and TLR4 colocalization suggests alternative functions for these platforms.

Mycobacterium tuberculosis bacilli colocalize with and utilize Lipid Raft aggregates for internalization

Previous studies demonstrated the important association of plasma membrane cholesterol with the entry of *M. tuberculosis* bacilli in macrophages (73). To determine if the observed LR aggregation serves to pool plasma membrane cholesterol and facilitate mycobacterial entry into epithelial cells, bacilli colocalizing with CT-B/caveolin-1 puncta were visually quantified. At 24 hpi, 40-52% of H37Rv, HN878 and CDC1551 bacilli viewed per field colocalized with CT-B puncta (Fig. 9). These data suggest that live

bacilli associate with approximately half of the LR aggregation observed and that these areas may help facilitate bacterial entry into the host cell.

Disruption of the LR entity using this sterol binding agent has been shown to eliminate caveolae-dependent endocytosis (155). To evaluate if LR aggregate formation induced by *M. tuberculosis* bacilli was crucial for internalization, epithelial cells were treated with the LR/cholesterol-disrupting agent Filipin III and viable numbers of intracellular bacteria were quantified. Confocal images verified disruption of LR aggregates at 6 hpi (data not shown) and 24 hpi with controls and all three strains of *M. tuberculosis* (Fig. 10, panel A & B). To confirm that Filipin treatment did not disrupt overall internalization mechanisms control experiments were conducted with fluorescent dextran. A549 cells treated with Filipin for 6 hr showed no significant decrease in endocytosis of dextran (data not shown).

In parallel, Filipin- and non-Filipin-treated host cells were infected with all three *M. tuberculosis* strains, and viable count experiments conducted as described. After 6 hr of bacterial uptake (T0), infections with HN878 and H37Rv in Filipin-treated A549 cells saw a significant reduction in intracellular bacteria compared to non-drug treated host cells (p-value < 0.001; <0.01 respectively) (Fig. 11, panel A). While not statistically significant, a 7.5% reduction in intracellular bacterial numbers was observed for CDC1551 between non-treated and Filipin-treated A549 cells at the same time point (Fig. 11, panel A). These data do suggest that disruption of LR aggregation negatively impacts internalization of *M. tuberculosis* bacilli in epithelial cells and that the kinetics and mechanism of internalization appear to vary for different *M. tuberculosis* strains.

Comparison of numbers of viable bacteria from T0 to T24 was also performed to determine if lack of LR-mediated internalization impacted survivability of *M. tuberculosis* bacilli once inside the host cell. Filipin-treated cells infected with H37Rv produced a 12–fold reduction in numbers of viable bacteria from T0 to T24 (Fig. 11, panel B). Further, a 5-fold and 25-fold reduction was observed with CDC1551 and HN878 Filipin-treated infections, respectively (Fig. 11, panel B). These data suggest that inhibiting LR-mediated internalization of *M. tuberculosis* bacilli in epithelial cells does impact intracellular numbers of those bacteria.

Discussion

Cell biologists have studied the dynamic changes that can occur in the plasma membrane of various mammalian cell types allowing for aggregation of lipid rafts (LR). These structures are thicker than adjoining regions of the membrane and rich in cholesterol, sphingolipids as well as transmembrane proteins. In an unperturbed environment, line tension, or boundary energy, prevents significant aggregation of the 10-200nm-sized LR (166). Various LR markers were employed in this study to characterize the presence, density and quantity of these structures in response to infection with *M. tuberculosis* bacilli. Cholera toxin- B (CT-B), which binds to ganglioside (GM1) found in lipid rafts (LR), has been utilized in numerous microscopy studies to examine the presence of LR on mammalian cell plasma membranes (6, 68, 74, 232, 234). Caveolin proteins, which bind to cholesterol in LR, have also been used as a set of markers to identify these structures (60). Caveolin-1 is one example which has been shown to coalesce to form flask-like invaginations called caveolae (47, 189, 260). Caveolae LR are considered to be

a subset of the LR population and thus it should be noted that quantification using caveolin-1/CT-B colocalization might under represent the total LR population present on the host cell plasma membrane (120, 160). However other studies have utilized these markers to demonstrate LR involvement in normal cell functions and disease processes (159, 176-177, 224, 267).

Aggregation of LR has been shown to occur in response to various stimuli. Cross-linking of transmembrane proteins found in LR has been shown to induce aggregation of these cholesterol-dense areas (95, 259). Studies employing bacterial proteins, such as listeriolysin O (LLO) have been shown to induce sizable LR clusters that can be viewed microscopically (71, 74, 142). To determine if *M. tuberculosis* bacilli were capable of inducing lipid raft aggregation, A549 human type II alveolar epithelial cells were infected with three strains of live *M. tuberculosis* bacilli at three different MOI. Time and dose-dependent increases in LR aggregation were observed from 6-24 hours post infection (hpi). It was also shown that total lipids (TL) and culture filtrate protein (CFP) components purified from broth-grown cultures, and gamma-irradiated bacilli did not produce the same degree of LR aggregation observed during infection with the actively growing strains.

Subsequent studies were performed to examine LR aggregation facilitated by mycobacterial-proteins expressed and secreted specifically during infection with viable bacilli. Filtered supernatants from infected type II pneumocytes were able to induce a similar level of LR aggregation observed when live bacteria were present. Thus, in a manner similar to secreted LLO, *M. tuberculosis* proteins produced and secreted during infection with live bacilli are capable of inducing aggregation of cholesterol-dense LR.

This unknown mycobacterial soluble product could induce LR aggregation through binding of protein receptors found within the rafts, analogous to GM1 and cholera toxin. Future work will focus on identifying this product(s) as well as the mechanism of LR aggregation.

Some significant differences in the number of LR aggregates were also noted among infections with live *M. tuberculosis* strains at each time point. Using the same number of infecting bacteria, strain CDC1551 induced fewer aggregates per cell (APC) than H37Rv and HN878 at 6 and 24 hpi. Previously published observations of CDC1551 infection in animal models supports a phenotype of decreased virulence compared to HN878 (13, 237). This virulence phenotype could be correlated with the diminished LR aggregation observed in this study. CDC1551 has been shown to stimulate a robust Th1 immune response in aerosol-infected mice and guinea pigs and less host death compared to H37Rv infections (13). Conversely, strain HN878 has been shown to stimulate a relatively lower Th1 response and faster time-to-death in these same animal models (13, 154, 180, 237). The observed increased virulence associated with strain HN878, as quantified by the rapid time-to-death of infected animals, has been attributed, in part, to unique phenolic glycolipids (PGL-tb) found in the cell wall of this strain (49, 207). HN878 is a member of the *M. tuberculosis* Beijing/W genotype known to have an intact polyketide synthase operon (*pks1-15*) required for PGL-tb synthesis. These data could correlate with the increased level of LR aggregation noted after addition of the HN878 TL fraction. However, PGL-tb is likely not solely responsible for the enhanced virulence of HN878 since studies by Sinsimer *et al.* (2008) have shown that other factors produced by this strain can contribute to the development of this phenotype (207). Our future

studies will examine purified PGL-tb from strain HN878 to determine if this factor alone can significantly contribute to the increased LR aggregation observed.

Lipid rafts and toll-like receptors (TLR) have been shown to have important signaling functions during *M. tuberculosis* infection of macrophage cell lines (202). To evaluate this in epithelial cells, A549 monolayers were treated with CFP and TL mycobacterial components, gamma-irradiated cells or infected with live bacilli from three *M. tuberculosis* strains; TLR2 and TLR4 colocalization with LR aggregates was evaluated. The data presented here indicated that unlike macrophages, LR aggregation does not function as a platform for TLR2 and TLR4 accumulation during *M. tuberculosis* infection of epithelial cells. It is possible that human carcinoma cell lines do not produce innate immune responses in a manner analogous to healthy human type II pneumocytes. However, studies with A549 cells have demonstrated the presence and up-regulation of TLR2 and TLR4 responses to infection with *Klebsiella pneumoniae* (181). Additionally, positive controls from this study demonstrated a significant increase in TLR colocalization with LR aggregates supporting the assertion that LR aggregates do not predominately serve as platforms for innate immune receptors during *M. tuberculosis* infection of epithelial cells.

Chlamydia trachomatis, uropathogenic *Escherichia coli*, *Listeria monocytogenes, Pseudomonas aeruginosa* and *Salmonella* spp. have been shown to utilize LR as a means of internalization in various cell types (6, 78, 112, 266). To determine if the LR aggregates induced in our studies function as a means for internalization of *M. tuberculosis* bacilli in epithelial cells, colocalization of aggregates and bacteria was examined. For each *M. tuberculosis* strain, approximately half of the bacteria viewed in

each microscopic field colocalized with LR puncta and caveolin-1 antibody. Invaginations formed in LR, caveolae, have been shown to internalize viruses as well as bacteria and their toxins in epithelial cells (92, 206). We have demonstrated that disruption of LR aggregation using the cholesterol-binding agent Filipin III significantly diminished the number of intracellular viable bacteria for all three strains by 6 hpi. The sterol-binding agent Filipin prevents aggregation of cholesterol which has been shown to be crucial for the stability of caveolae and thus use of this agent selectively inhibits caveolae-dependent endocytosis (155). Other studies have shown that entry of *M. tuberculosis* bacilli into type II pneumocytes is dependent upon actin polymerization (22, 110). Because actin polymerization contributes significantly to caveolae-mediated endocytosis, we hypothesize that LR/caveolae-dependent endocytosis may play an important role for entry of *M. tuberculosis* bacilli in non-phagocytic cells (98).

Studies examining *M. tuberculosis* and *Mycobacterium avium* infections in the macrophage have demonstrated that cholesterol aggregation in the plasma membrane is crucial for uptake and later recruitment of host proteins to the phagosomal membrane and prevention of lysosomal fusion (53, 73, 249). Thus, the impact of Filipin pre-treatment on intracellular survival of *M. tuberculosis* bacilli was examined. A significant negative-fold change in the number of viable intracellular bacteria was seen for all three mycobacterial strains examined from T0 to T24 hpi in Filipin-treated host cells. This finding indicates that, similar to macrophages, *M. tuberculosis* bacilli require cholesterol aggregation for internalization and survival during infection of the epithelial cell. Cholesterol-dependent inhibition of lysosomal fusion may explain previous observations demonstrating the absence of lysosomal-associated markers with *M. tuberculosis*-containing endosomes in

epithelial cells (Fine *et al*., in press). Future work will focus on investigating the contribution of cholesterol in the membrane of the bacteria-containing compartment to bacterial survival.

Aggregation of LR facilitated by *M. tuberculosis* infection contributes to bacterial internalization and survival in the alveolar epithelial cell. It will be important to identify and understand the function of the specific mycobacterial factor/s responsible for LR stimulation and if these may be related to virulence of different mycobacterial strains. It is also evident that *M. tuberculosis* bacilli interact with alveolar epithelial cells using mechanisms different from those observed with macrophages. Thus, these interactions between *M. tuberculosis* bacilli and epithelial cells deserve closer scrutiny in order to uncover the role these cells play in pulmonary disease.

Methods

Bacterial Culture

The following cultures were obtained through the NIH Biodefense and Emerging Infection Research Resources Repository, NIAID, NIH: *Mycobacterium tuberculosis*, strains H37Rv (NR-13648), CDC1551 (NR-14825) and HN878 (NR-13647). *Mycobacterium tuberculosis* strains were grown in Middlebrook 7H9 broth supplemented with 0.5% glycerol, 0.05% Tween 80 and 10% ADC (strain CDC1551) or 10% OADC (strains HN878; H37Rv). For confocal microscopy, strains were transformed with plasmid pGCRED2 expressing DsRed2 and maintained by inclusion of hygromycin at 50 µg/ml. Plasmid pCGRed2 was a generous gift from Drs. Garry Coulson and Mary Hondalus, Department of Infectious Diseases, University of Georgia. Gamma-irradiated

bacteria also were obtained through NIH Biodefense and Emerging Infections Research Resources Repository, NIAID, NIH: *M. tuberculosis*, strains H37Rv (NR-14819), HN878 (NR-14821) and CDC1551 (NR-14820).

Cell Culture

A549 human type II alveolar epithelial cells were obtained from ATCC (CCL-185) and maintained at 37°C, 5% CO_2 in EMEM supplemented with 5% FBS. A549 cells were grown as monolayers to confluency, harvested with trypsin-treatment for 3min at 37°C, and $5.0x10^5$ cells seeded onto sterile coverslips placed within 6-well Costar® dishes. The cells were allowed to adhere for 12 hr at 37°C in 5% CO_2 and then infected with *M. tuberculosis* bacilli.

Epithelial Cell Infection

Epithelial cell monolayers were infected in 6-well dishes, as described, at the indicated MOI (1, 10, or 100) with the indicated *M. tuberculosis* strains. Bacteria were grown in 7H9 broth with gentle shaking to an OD_{600} 1.0 then centrifuged to remove broth media. The pellet was resuspended in EMEM supplemented with 5% FBS. To disperse innocula, bacteria vortexed for 5 min then passed through an insulin syringe and deposited directly into the appropriate tissue culture wells. This method of bacterial dispersion was confirmed by microscopy to produce single bacilli for infection (data not shown). Cold synchronization was performed to coordinate bacterial attachment. This procedure included incubation of the monolayer at 4°C for 2 hr; 1 hr preceding infection and 1 hr after addition of the bacteria. Subsequently, infected cells were incubated at 37°C in 5%

CO_2; this was considered time point 0. Experiments involving gamma-irradiated bacteria were conducted in the same manner using inocula of 100 bacilli per host cell. Control experiments were conducted with Listeriolysin-O (LLO). Cells were treated with 2µg/ml LLO (Diatheva s.r.l.) for 15 or 30 min at room temperature (74). For Filipin studies, cells were pretreated and maintained throughout the infection with a final concentration of 5µg/ml (11). Filipin III was obtained from Sigma (F-4767) and reconstituted with DMSO. Control experiments with DMSO alone at the concentration applied in Filipin studies produced no cytotoxic effects (data not shown). Infections were performed in triplicate and experiments repeated three times.

For consistency, cold synchronization of A549 cells was employed prior to the addition of live or gamma-irradiated bacteria and culture filtrate protein (CFP) or total lipid (TL) reagents (see below). A549 cells were incubated for 1 hr at 4°C before and after addition of cells, proteins or extracts. The host cells were then returned to 37°C (Time = 0 hr).

Bacterial Culture Filtrate Protein and Total lipid Treatment of Epithelial Cells

The following reagents were obtained through NIH Biodefense and Emerging Infection Research Resources Repository, NIAID, NIH: *M. tuberculosis* Culture Filtrate Proteins (CFP), strains H37Rv (NR-14825); HN878 (NR-14827); CDC1551 (NR-14826), and Total Lipids (TL), strains H37Rv (NR-14837); HN878 (NR-14839) and CDC1551 (NR-14838). For CFP experiments, monolayers of A549 cells were treated with 4µg/ml of proteins based on previously published work (58, 154). Control monolayers were treated with 0.01M ammonium bicarbonate, the solution in which the culture filtrate proteins

were dialyzed. Treatments were performed in triplicate and experiments repeated three times.

Total lipids were reconstituted in DMSO and monolayers of A549 cells treated with a final concentration of 2 μg/ml. Concentrations of TL used were based on previously published work and titrations performed prior to experimentation which microscopically assessed DMSO treatment and subsequent impact on host cell viability (data not shown) (52, 134, 185). At the concentration applied, control monolayers of A549 cells treated with DMSO alone produced no adverse effects noted by microscopic examination (data not shown).

Confocal and Immunofluorescence Microscopy

For confocal microscopy, A549 cells were grown as monolayers to confluence, harvested with trypsin-treatment for 3 min at 37°C, and 5.0 x 10^5 cells seeded onto sterile coverslips placed within 6-well Costar® dishes. The cells were allowed to adhere for 12 hr at 37°C in 5% CO_2 and then infected with *M. tuberculosis* bacilli or treated with gamma-irradiated bacilli, CFP or TL as described. Specimens were fixed at indicated time points with 3.7% paraformaldehyde for 1 hr at 4°C. The specimens were washed 3 times with 1x PBS, and cells permeabilized for 10 min with 0.1% Triton X-100. The samples were then blocked for 30 min with PBS containing 3% BSA. For lipid raft (LR) aggregation studies, cells were incubated with rabbit polyclonal anti-caveolin-1 (Abcam) at a 1:200 dilution for 1 hr at room temperature (RT). The antibodies were detected using a 1:500 dilution goat-anti-rabbit 633 (Invitrogen) antibodies incubated for 1 hr at RT. Concurrent staining of detergent-resistant aggregates was performed using Cholera toxin B (CT-B)

488 (Invitrogen) at a dilution of 1:200. Filipin-treatment experiments were conducted and labeled with CT-B and caveolin-1 as described. Images were obtained with either the Zeiss Axiovert 200M and Apotome or a Nikon A1R confocal laser microscope system.

For Toll-like receptor experiments, A549 cells were seeded onto coverslips as described. Positive controls for TLR-2 stimulation were conducted using 1µg/ml of Pam3CSK4 (InvivoGen) for 6 hr at 37°C. TLR4 stimulation was performed using *E. coli* 0111:B4 strain LPS (InvivoGen) at 10µg/ml for 6 hr at 37°C. Experimental wells of A549 cells were infected with *M. tuberculosis* strains CDC1551, HN878 and H37Rv at an MOI of 100. At 6 and 24 hpi, specimens were fixed and prepared for labeling as described. Cells were incubated with either mouse monoclonal anti-TLR4 (Santa Cruz) or mouse monoclonal anti-TLR2 (Abcam) antibodies at a 1:200 dilution for 1 hr at RT. Both primary antibodies were detected using goat-anti-mouse 633 antibodies (Invitrogen) at a 1:500 dilution for 1 hr at RT. Separate experiments were conducted using mouse monoclonal transferrin receptor antibody (Zymed) at a 1:200 dilution as a negative control for colocalization with LR. The antibody was detected using donkey-anti-mouse 633 (Invitrogen) at a dilution of 1:500. CT-B 488 staining was also performed as described for each well during the secondary antibody incubation period. Images were obtained with a Nikon Eclipse TiE confocal microscope. All cells in each experiment were also stained with Dapi at a 1:500 dilution for 1 hr at RT. All infections were performed in duplicate and experiments repeated three times.

Supernatant Treatment

A549 cells were seeded onto 6-well plates as described and infected with *M. tuberculosis* strains CDC1551, HN878 and H37Rv. *Mycobacterium tuberculosis* strains were preincubated at 37°C for 1 hr in EMEM 5% FBS and 50µg/ml amikacin to inhibit protein synthesis. Pretreated bacterial cells were applied to epithelial cell monolayers in a manner previously described in parallel with non-drug treated bacteria. Amikacin (50µg/ml) was maintained on infected and control cells for the duration of the time course. Supernatants were pipetted into a 3ml syringe and passed through Millex-GV 0.22µm PVDF filters (Millipore) to remove bacteria. The filtered supernatants were applied to a new monolayer of A549 cells seeded onto coverslips and incubated at 37°C for 24 hr. Aliquots of filtered supernatants were applied to 7H11 agar plates supplemented with 0.5% glycerol, 0.05% T80, 10% ADC (CDC1551) or OADC (HN878; H37Rv) and 50 µg/ml hygromycin to verify removal of bacteria. Specimens were processed for confocal microscopy as described and imaged with a Zeiss Axiovert 200M and Apotome. Infections were performed in duplicate and experiments repeated twice.

Intracellular Bacterial Viability

Epithelial cell monolayers were seeded onto 24-well plates at 2.5 x10^4 cells per well and allowed to adhere for 12 hr prior to infection. Filipin- or non-Filipin-treated A549 cells were infected with *M. tuberculosis* strains at an MOI of 100 as described. After 6 hr at 37°C, medium was removed from each well, monolayers washed 3 times with 1x PBS and incubated for 2 hr in EMEM with amikacin (200 µg/ml), +/- Filipin and 5% FBS. The medium again was removed, and monolayers washed with PBS and EMEM with

amikacin, +/- Filipin and 5% FBS was applied; this was defined at time point 0 (T0). At T0 and T24, the cells were washed and lysed with 0.1% Triton X-100. To verify that Filipin treatment did not significantly impact general endocytosis mechanisms, A549 cells were seeded onto coverslips in 6-well Costar® dishes. After 6 hr incubation with or without Filipin, 100µg of 10,000MW dextran-Texas Red (Invitrogen) was added to each well. Uptake proceeded at 37°C, 5% CO_2 for 30 min after which cells were washed and fixed as described previously. Coverslips were processed for confocal microscopy and imaged with the Zeiss Axiovert 200M as described (supplemental Fig. 4). Infections were performed in triplicate and experiments repeated three times.

Assessment of Colocalization

Confocal images were obtained as described and imported into ImageJ 1.451/Java 1.60_20 software and analyzed using the JACoP plugin. LR aggregates were first quantified using ImageJ as described. Colocalization of TLR labeling with LR aggregates was evaluated in JACoP using Pearson and Manders coefficient. Bacteria colocalization with LR aggregates and/or caveolin-1 antibodies alone were analyzed in a similar manner.

Quantification of LR Aggregates

Images of specimens were obtained as described and a total of 15 fields were imaged per coverslip for each experiment. Three coverslips were obtained for all three *M. tuberculosis* isolates, at each timepoint for all three experimental replicates (total = 54 coverslips per experiment). Once colocalization of CT-B and caveolin-1 was verified

using Image J, JACoP plugin, aggregates were quantified and analyzed for size and area using ImageJ 1.451/Java 1.60_20 (2). Numbers of aggregates were normalized to the number of host cells imaged per field to acquire an average number of aggregates per host cell/per field for each treatment condition.

Statistical Analysis

Statistical significance of aggregate numbers and viable bacterial counts was examined by ANOVA and Tukey's HSD post-hoc comparison ($\alpha = 0.05$) using SPSS 17.0® statistical software.

Acknowledgements

We thank Garry Coulson for critical reviews of the manuscript. We also thank Shelly Helms for technical assistance in several parts of this project. Confocal microscopy was conducted in and supported by the University of Georgia, College of Veterinary Medicine Cytometry Core Facility. This work was supported in part by research grants from the American Lung Association (R.K.) and the University of Georgia Faculty of Infectious Diseases (F.Q.).

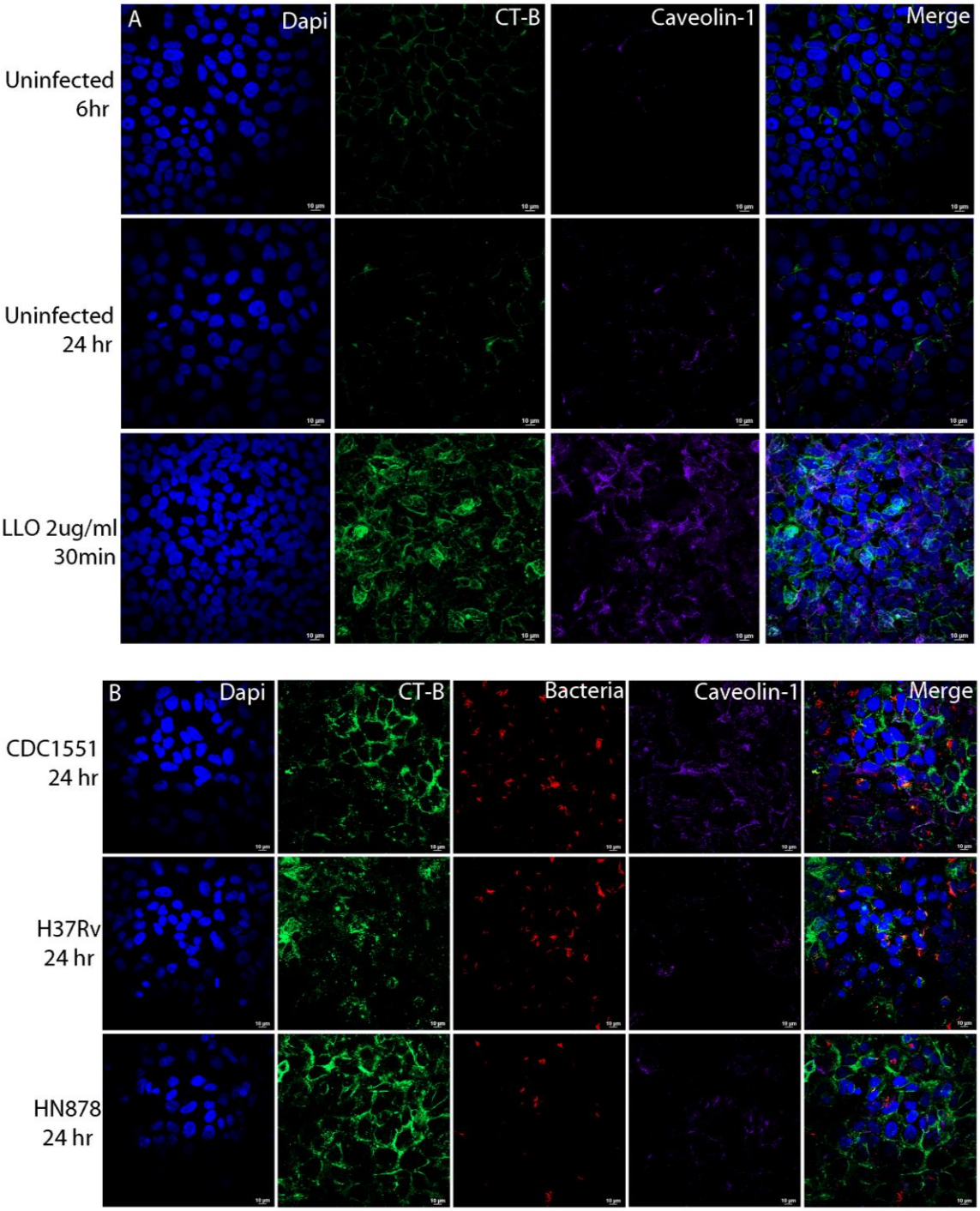

Figure 1. Infection with *Mtb* strains H37Rv, HN878 and CDC1551 induce dose--dependent LR aggregation at 6 hr and 24 hr post infection (hpi). A549 type II alveolar epithelial cells were infected at three MOI's, 1 (supplemental Fig. 1 A), 10 (B) and 100 (supplemental Fig. 1 B) and specimens prepared for confocal microscopy as described. Uninfected controls demonstrated low levels of LR present at 6 and 24 hpi (A). A549 cells treated with Listeriolysin-O (LLO) as positive controls were assessed 15 (data not shown) and 30 min post treatment (A). Infections with strain CDC1551, HN878

and H37Rv demonstrated a time-dependent increase in LR aggregation from 24 hpi (B). This was consistent with findings at 6 hpi (data not shown). Infections were performed in triplicate and experiments repeated three times. A total of 15 fields were imaged per coverslip, quantifying approximately 30-50 host cells per field. Images were captured at 63x magnification and LR aggregation quantified using ImageJ software.

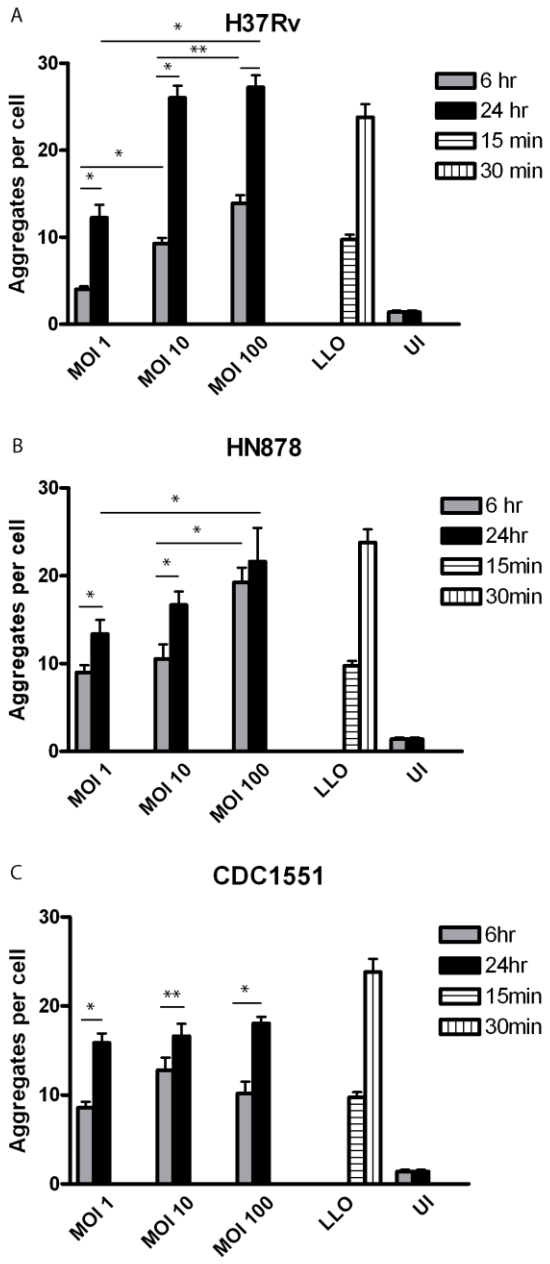

Figure 2. Quantification of confocal images demonstrate a time-, dose- and strain-dependent increase in LR aggregation for CDC1551, HN878 and H37Rv. Analysis by confocal microscopy at 6 and 24 hours post infection (hpi) demonstrated a time-dependent increase in LR aggregation for H37Rv (A), HN878 (B) and CDC1551 (C) (*p-value < 0.001 and ** <0.05). Dose-dependent increases in LR aggregation were also significant for H37Rv and HN878 at 6 and 24 hpi (*p-value <0.001 and ** p-value < 0.05). At MOI 100, strain HN878 and H37Rv consistently produced higher levels of LR aggregation compared to CDC1551. Infections were performed in triplicate and experiments repeated three times. A total of 15 fields were imaged per coverslip, quantifying approximately 30-50 host cells per field. Quantification represents the average of three experiments.

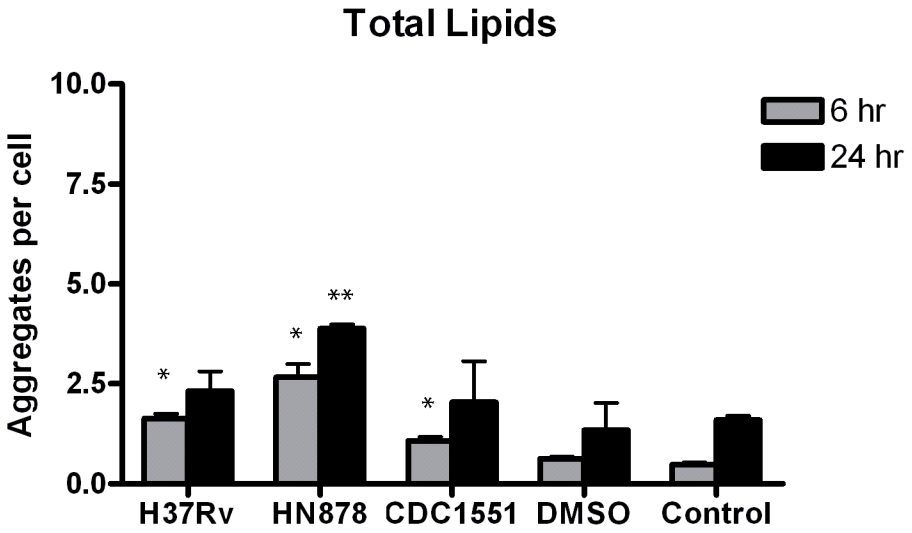

Figure 3. Treatment of A549 cells with total lipids (TL) from strain CDC1551, HN878 and H37Rv produces an increase in LR aggregates compared to uninfected controls. A549 cells treated with TL from the indicated *M. tuberculosis* strains were processed for confocal microscopy at 6 and 24 hr post-treatment as described. At 6 hr post-treatment, a significant increase in LR aggregation was observed in TL treated A549 cells compared to uninfected controls (* p-value < 0.05). At 24 hr post-treatment HN878 TL produced significantly higher aggregate numbers compared to uninfected controls (**p-value < 0.001). It should be noted that LR aggregation for CDC1551 and H37Rv at 24 hr post-treatment was not significantly different from uninfected and DMSO controls (p-value 0.977 and 0.737, respectively). Treatments were performed in triplicate and experiments repeated three times. A total of 15 fields were imaged per coverslip, quantifying approximately 30-50 host cells per field. Data presented is the average of three experiments. Images to obtain LR data were captured at 63x magnification.

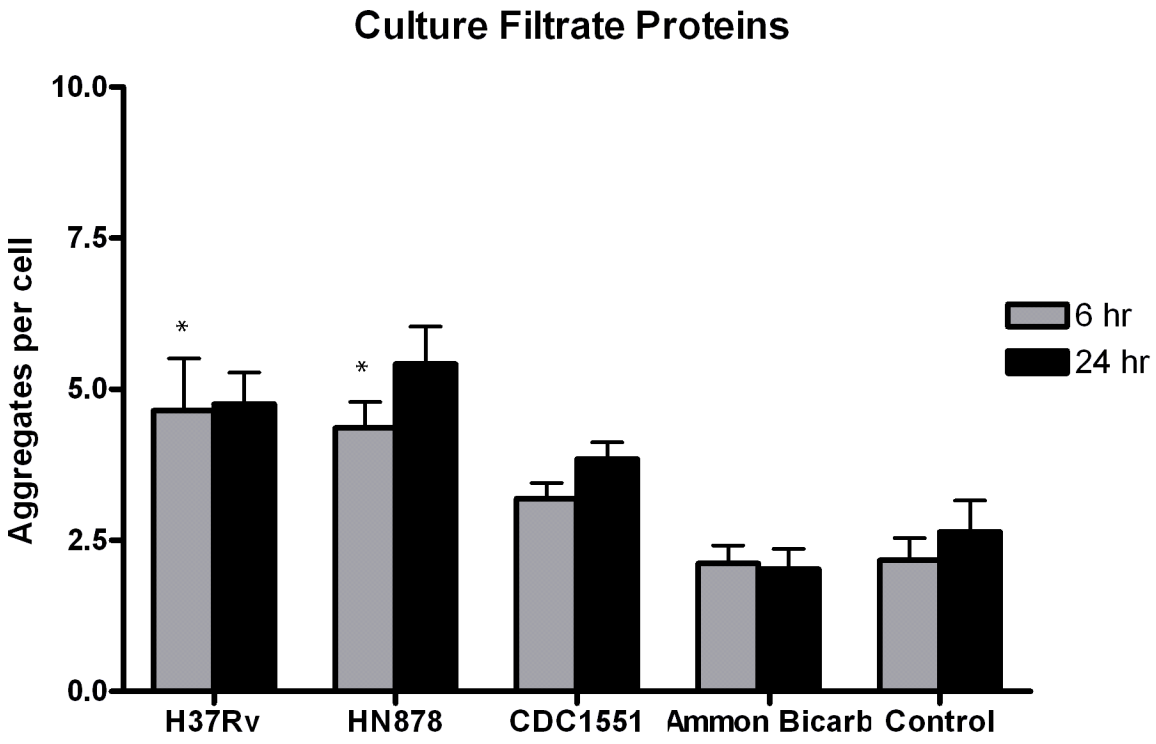

Figure 4. Treatment of A549 cells with Culture Filtrate Proteins (CFP) from each *Mtb* strain produce varying increases in the number of LR aggregates compared to uninfected controls. Following treatment with CFP from strain CDC1551, HN878 and H37Rv, specimens were prepared for and analyzed by confocal microscopy. Compared to controls, treatment with CFP from CDC1551 did not produce statistically different LR aggregation values at 6 and 24 hours post treatment (p-value = 0.598 and 0.379, respectively). LR aggregation for HN878 and H37Rv was significantly different from controls at 6 hpi (*p-value = 0.033 and 0.012, respectively). Treatments were performed in triplicate and experiments repeated three times. A total of 15 fields were imaged per coverslip, quantifying approximately 30-50 host cells per field. Data presented is the average of three experiments. Images were captured at 63x magnification and analyzed using ImageJ software.

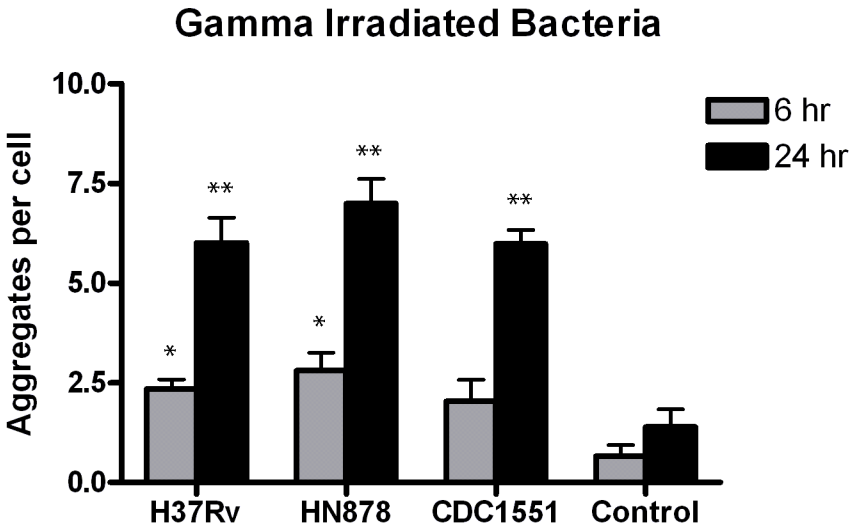

Figure 5. Addition of gamma-irradiated *Mtb* strains produces low level A549 cell LR aggregation. Gamma-irradiated CDC1551, HN878 and H37Rv bacilli were added to monolayers at an inoculum of 100 bacilli per host cell. The cells were then processed for confocal microscopy and LR aggregation defined by CT-B staining and quantified as described. Controls without bacilli produced LR aggregation at 6 and 24 hr post-treatment comparable to controls for other previous experiments. At 6 hr post-treatment a significant increase in LR aggregation was observed with strains H37Rv and HN878 compared to controls (* p-value < 0.001). LR aggregation with all three strains at 24 hr post-treatment was significantly increased compared to controls (**p-value < 0.001). Treatments were performed in triplicate and experiments repeated three times. A total of 15 fields were imaged per coverslip, quantifying approximately 30-50 host cells per field. Data presented is the average of three experiments. Images were captured at 63x magnification.

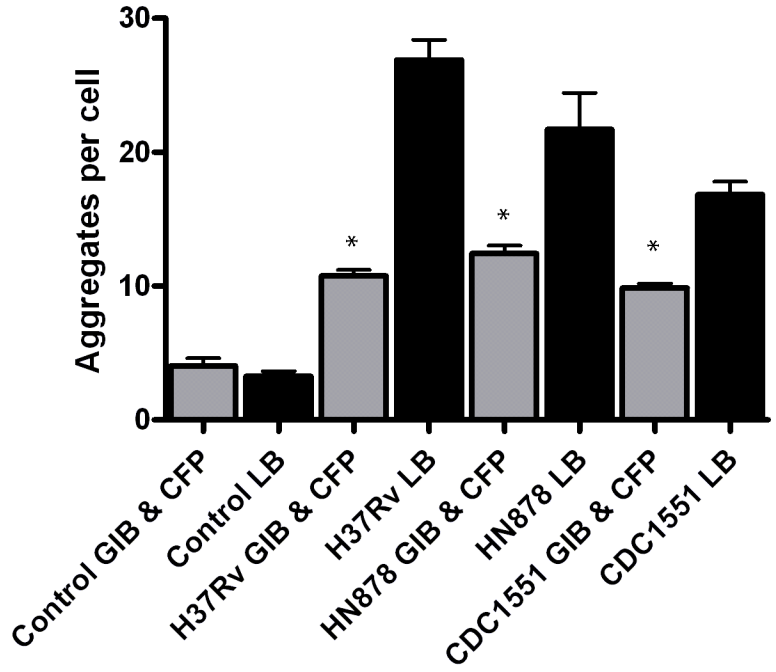

Figure 6. LR aggregation produced by gamma-irradiated bacteria and CFP does not equal aggregation observed with live bacteria. Data from figures 5 and 4 were combined for comparison with LR aggregation data from live bacteria experiments. Less than 55% of the aggregation observed with live *Mtb* infection can be explained by constitutively expressed components from H37Rv, HN878 and CDC1551 (*p-value < 0.001, 0.01 and 0.05, respectively). (GIB- gamma irradiated bacteria; LB- live bacteria; CFP- culture filtrate proteins)

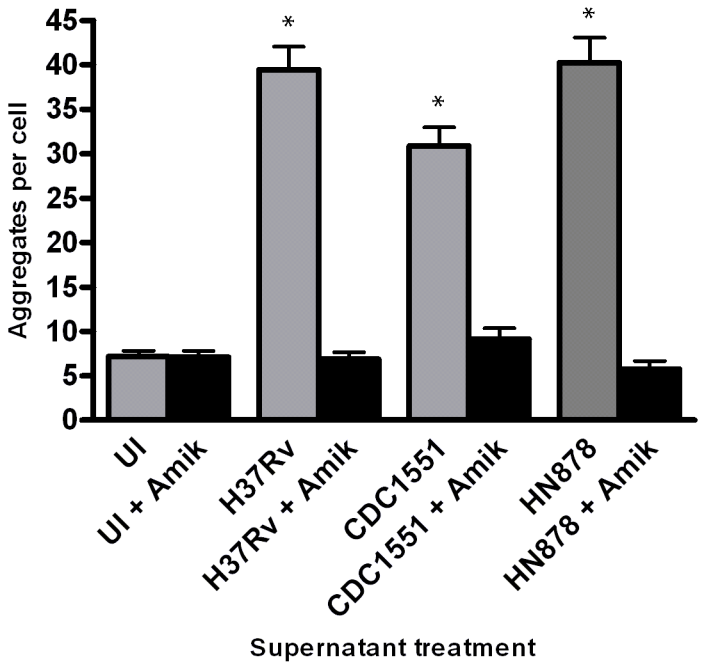

Figure 7. Supernatants from live *Mtb* bacilli induce LR aggregation in alveolar epithelial cells. A549 cells were infected with CDC1551, HN878 and H37Rv that were either pretreated with amikacin or untreated at MOI 100 for 24 hr. Supernatants were then micro-filtered and applied to fresh monolayers of A549 cells seeded onto coverslips and allowed to incubate for 24 hr. Coverslips were prepared for confocal microscopy as described. Supernatants from infections with untreated bacteria produced significantly more LR aggregation compared to supernatants from infections with amikacin-treated bacteria (*p-value <0.001). Infections and subsequent supernatant treatments were performed in duplicate and experiments repeated twice. A total of 15 fields were imaged per coverslip, quantifying approximately 30-50 host cells per field. Data presented is the average of two experiments. Images to quantify LR aggregation were captured at 63x magnification. (UI = uninfected cells; Amik = supernatants from bacteria pretreated with Amikacin)

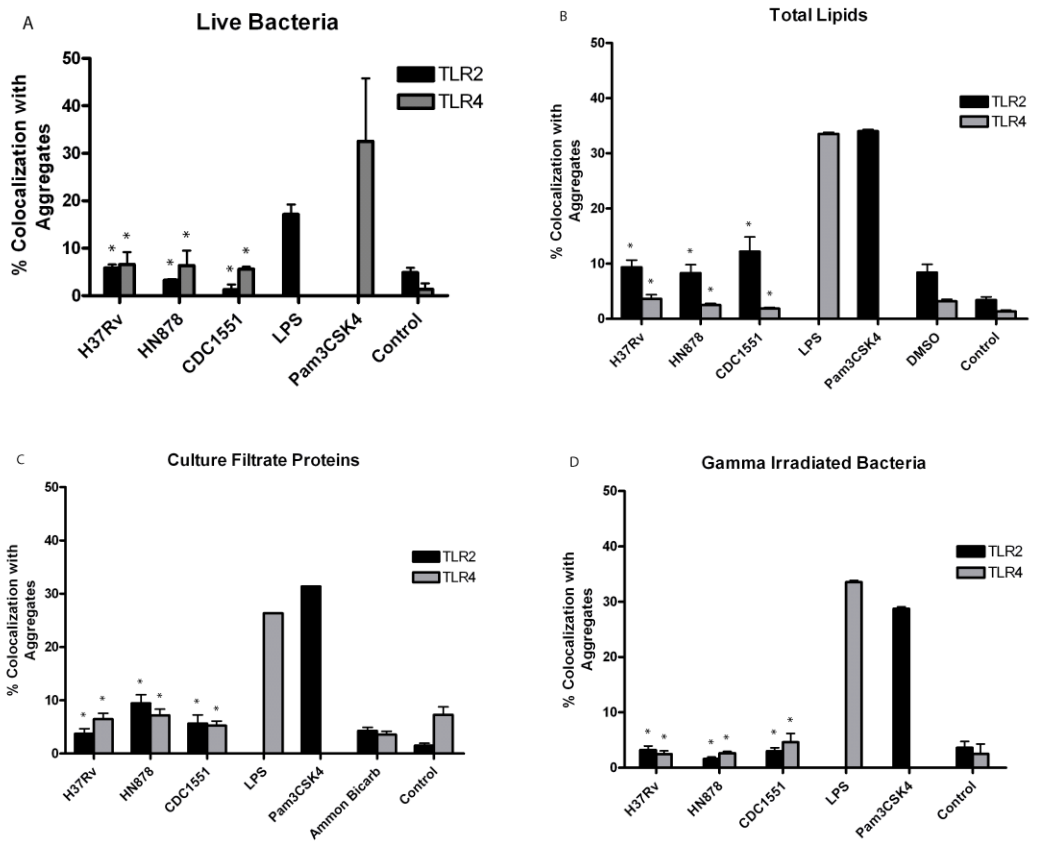

Figure 8. Toll-Like Receptor 2 and TLR4 do not colocalize with LR aggregates after infection with live *Mtb* strains or treatment with cell fractions or gamma-irradiated bacilli. A549 cells were infected with live *Mtb* strains CDC1551, HN878 or H37Rv at MOI 100 or treated with total lipids (TL), culture filtrate proteins (CFP) and gamma-irradiated cells for 24 hr, as described. Colocalization of anti-TLR2 and anti-TLR4 antibodies with LR aggregates was analyzed from confocal images using Manders coefficient values. Infections with CDC1551, HN878 and H37Rv produced significantly less TLR2 and TLR4 colocalization compared to positive controls (*p-value <0.001) (A). There were no significant differences between TL-treated cells and DMSO controls at this time point (B) (TLR4, p-value= 0.532 to 0.983; TLR2, p-value= 0.775 to 1.0). TLR2 and TLR4 colocalization for controls and CFP-treated cells was comparable (C). At 24 hr post-TL (B) and –CFP (C) treatment colocalization of receptors was significantly decreased compared to positive controls (*p-value < 0.001). These findings also held true for epithelial cells infected with gamma-irradiated bacteria from all three strains (*p-value < 0.001) (D). Images were collected at 63x magnification and analyzed using ImageJ JACoP plugin. Infections were performed in duplicate and experiments repeated three times. Data represents the average of three experiments.

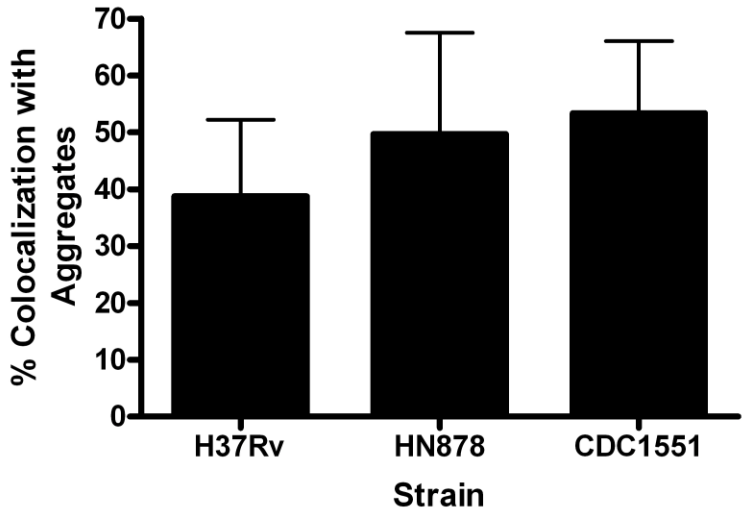

Figure 9. CDC1551, HN878 and H37Rv bacilli colocalize with LR aggregates at 24 hr post infection (hpi). A549 cells were infected with live *Mtb* strains CDC1551, HN878 and H37Rv; colocalization of fluorescent bacteria with LR aggregates was quantified as described. No statistical difference was noted for LR colocalization between strains at 24 hpi. Infections were performed in triplicate and experiments repeated three times. Analysis was performed on 15 fields per coverslip using ImageJ JACoP plugin. Images were captured at 63x magnification. Data represents the average of three experiments.

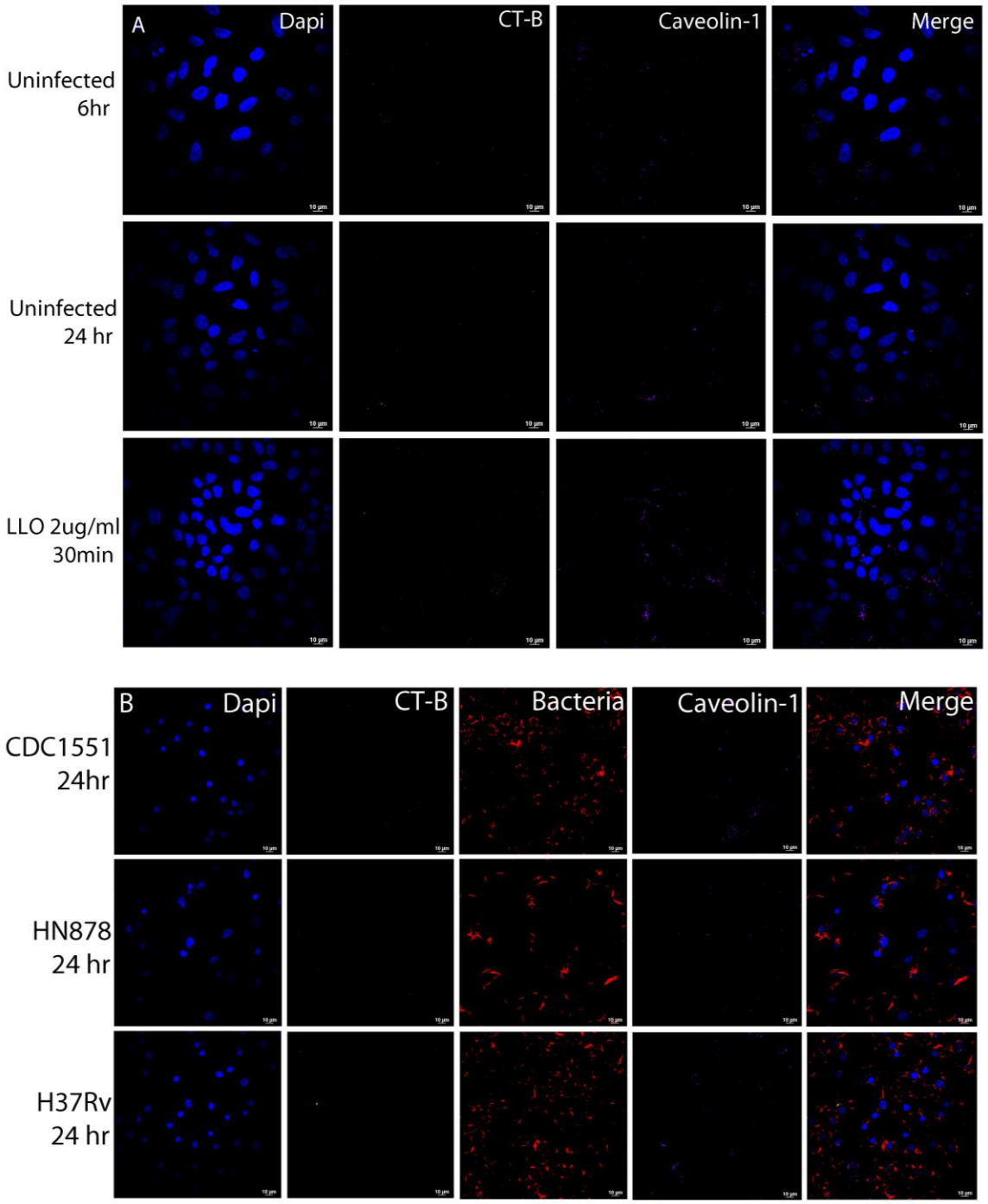

Figure 10. Treatment of epithelial cells with Filipin disrupts mycobacterial-induced LR aggregation. A549 cells were treated with cholesterol-binding, LR-disruption agent Filipin III and LR aggregation observed for controls and infections with all three live *Mtb* strains. Confocal microscopy demonstrated an absence of CT-B puncta at 6 and 24 hours post infection for controls (A) and live *Mtb* strains (B). Images were collected at 63x magnification. Infections were performed in triplicate and experiments repeated three times.

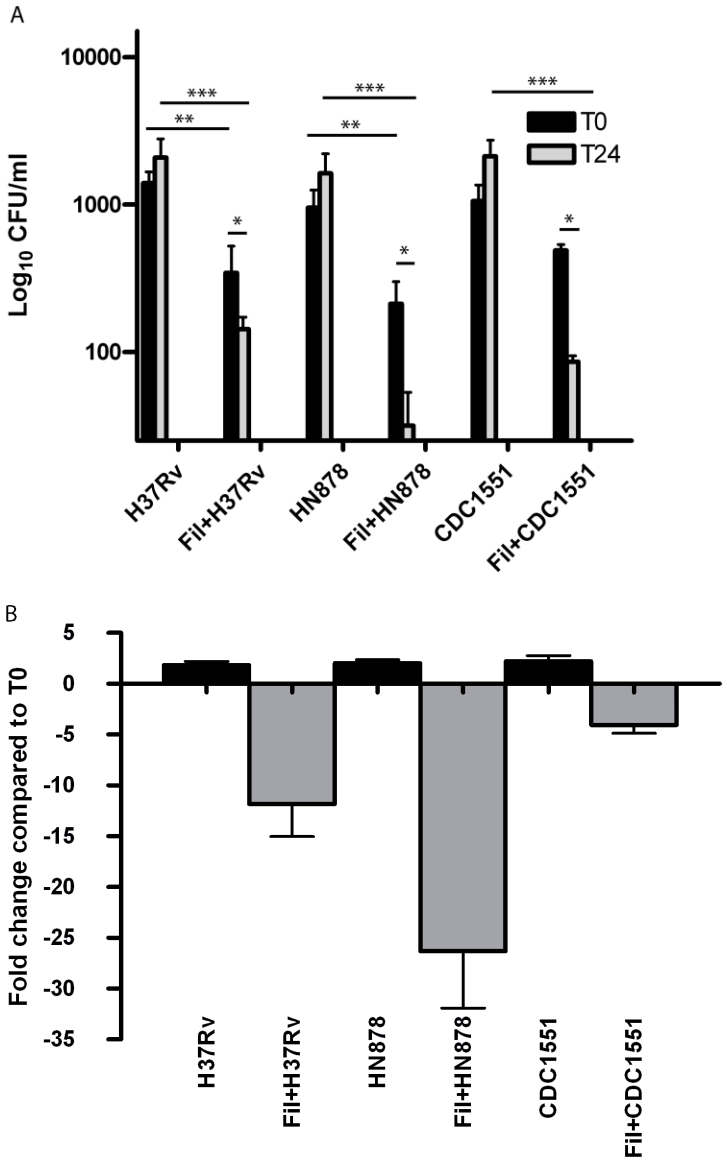

Figure 11. Filipin-treated A549 cells have significantly fewer viable intracellular bacteria after uptake and 24 hours post infection. Filipin- and non-Filipin treated epithelial cells were infected with CDC1551, HN878 and H37Rv at MOI 100. Viable bacilli were quantified at T0, after bacterial uptake, and T24 (A). Numbers of viable intracellular bacteria were significantly decreased in Filipin-treated compared to non-treated host cells infected with HN878 and H37Rv at T0 (**p-value <0.001; <0.01, respectively) and T24 (***p-value < 0.001 (A). No significant difference was found between drug-treated and non-drug treated host cells infected with CDC1551 at T0 (p-value >0.05). A significant difference was found between treatments for CDC1551 infections at T24 (***p-value <0.01). The calculated fold change from T0 to T24 indicates a significant decrease in the number of viable intracellular bacteria over time (B) (* p-value < 0.001). Infections were performed in triplicate and experiments repeated three times. Raw data represents the results from one experiment that illustrates trends observed in three experiments.

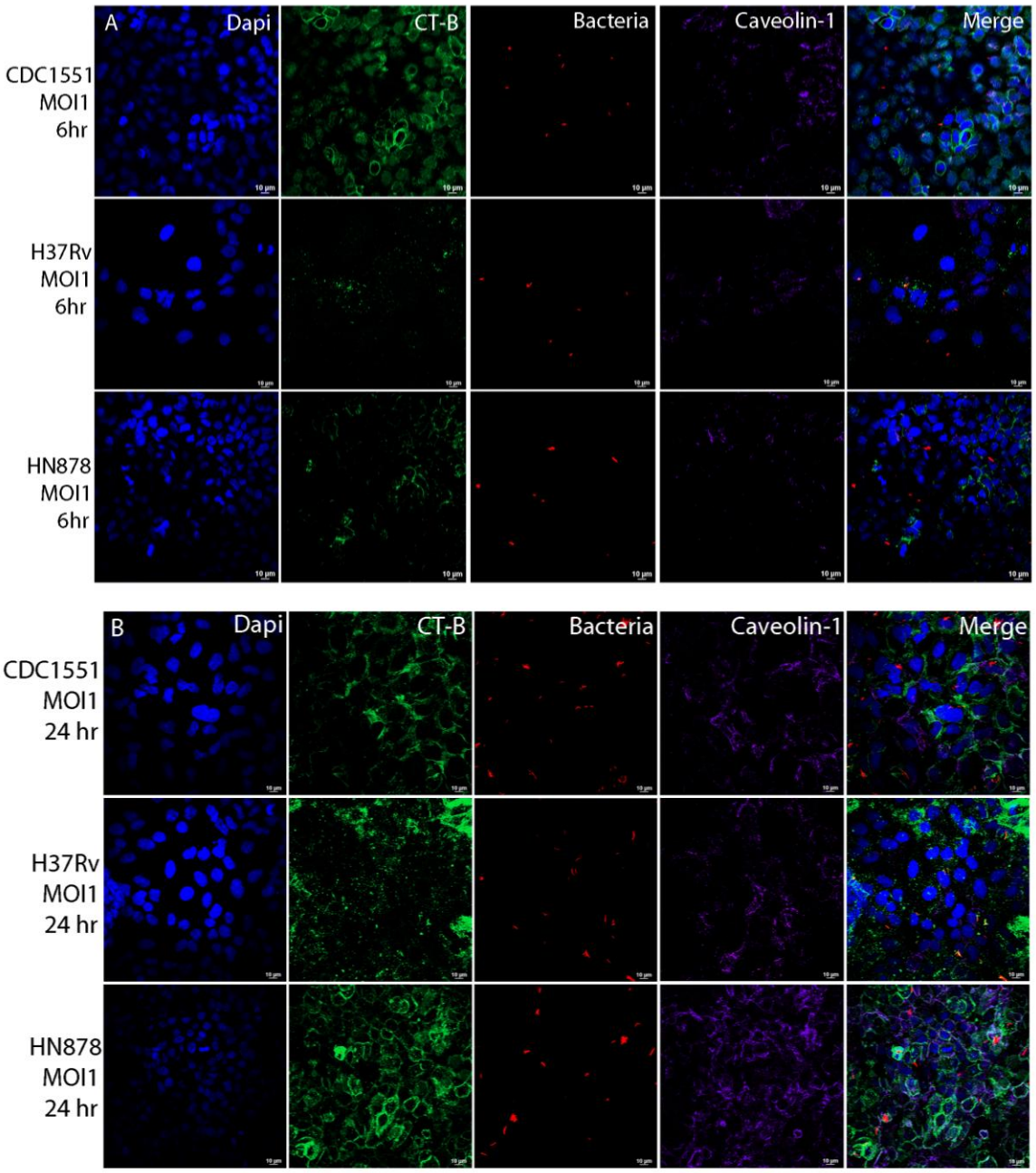

Supplemental Figure 1. Infection with *Mtb* strain H37Rv, HN878 and CDC1551 (MOI=1) induce dose--dependent LR aggregation at 6 hr and 24 hr post infection (hpi). A549 cells were infected with H37Rv, HN878 and CDC1551 (MOI = 1) and incubated at 37°C, 5% CO_2 for 6 hr (A) or 24 hr (B) as described. An increase in CT-B/caveolin-1 puncta is observed at 24hpi (Quantification in Fig 2). Images were obtained at 63x magnification with a Nikon A1R confocal system equipped with a Nikon Eclipse TiE confocal microscope. Infections were performed in triplicate and experiments repeated three times. Fifteen fields were imaged per coverslip for each experiment. Images are representative of overall findings from three experiments.

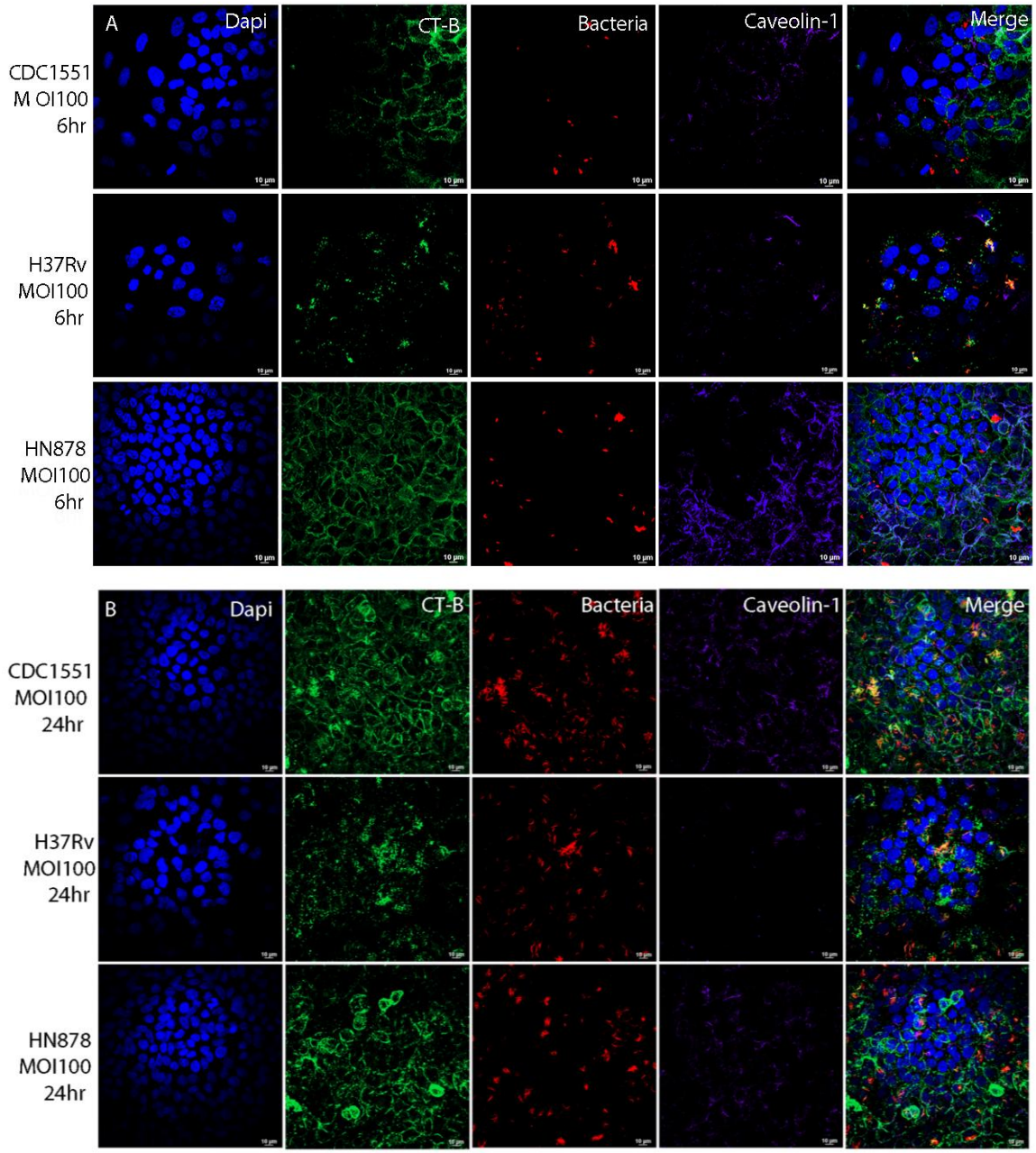

Supplemental Figure 2. Infection with *Mtb* strain H37Rv, HN878 and CDC1551 (MOI=100) induce dose--dependent LR aggregation at 6 hr and 24 hours post infection (hpi). A549 cells were infected with H37Rv, HN878 and CDC1551 (MOI = 100) and incubated at 37°C, 5% CO_2 for 6 hr (A) or 24 hr (B) as described. An increase in CT-B/caveolin-1 puncta is observed at 24hpi (Quantification in Fig 2). Images were obtained at 63x magnification with a Nikon A1R confocal system with a Nikon Eclipse TiE confocal microscopy. Infections were performed in triplicate and experiments repeated three times. Fifteen fields were imaged per coverslip for each experiment.. Images are representative of overall findings from three experiments.

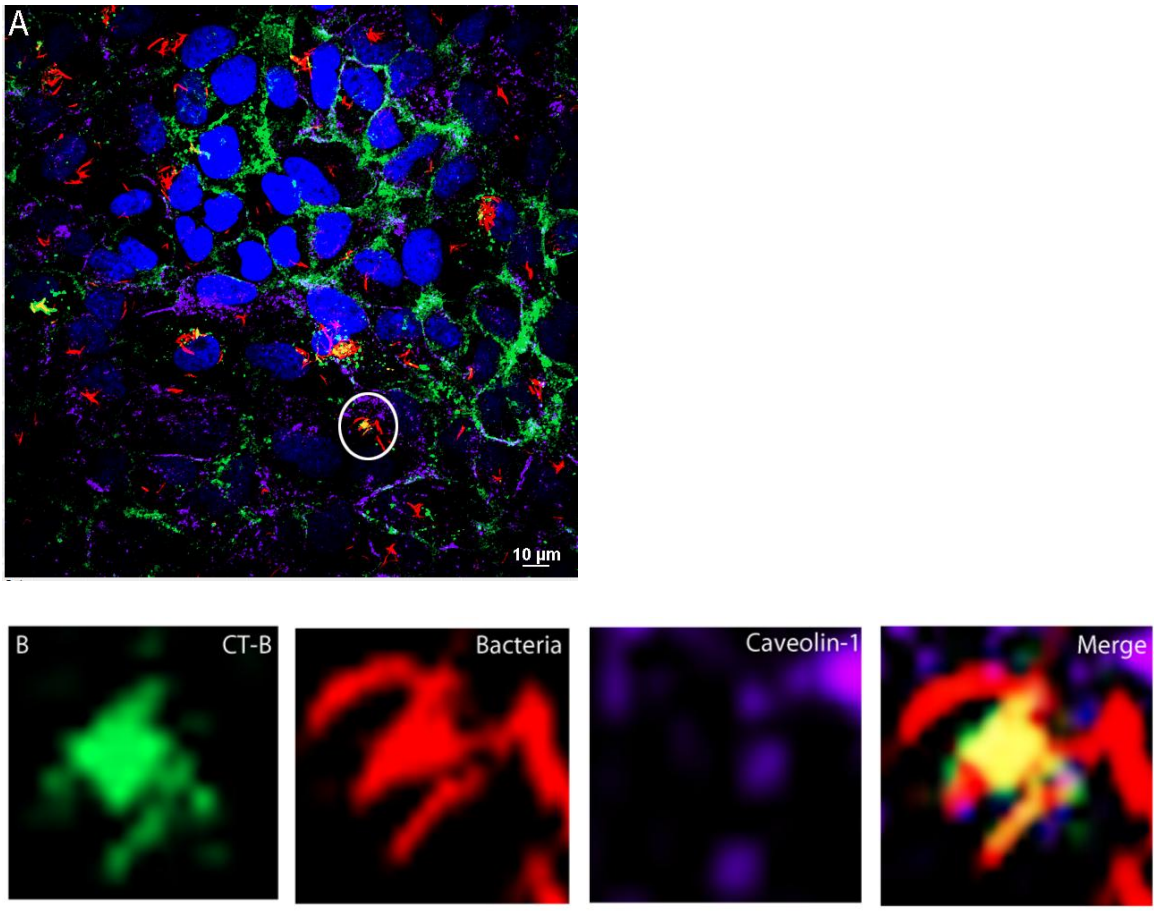

Supplemental Figure 3. A Magnified section from a confocal image of A549 cells infected with CDC1551 at 24 hpi demonstrates colocalization of LR markers. A549 Type II alveolar epithelial cells were infected with CDC1551 (MOI = 10) and prepared for confocal microscopy as described. Images were obtained at 63x magnification with a Nikon A1R confocal system with a Nikon Eclipse TiE confocal microscope (A). The circle indicates the area from which the magnified image was obtained. The encircled area has been cropped and magnified to illustrate the colocalization of CT-B, Caveolin-1 and bacteria for the purposes of quantification as described in the methods (B).

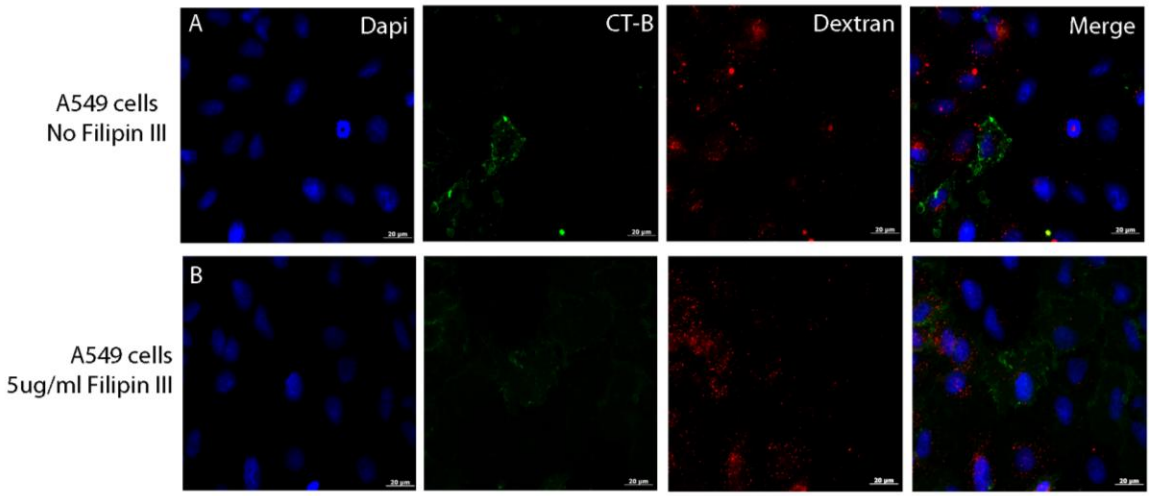

Supplemental Figure 4. Treatment of A549 type II alveolar epithelial cells with Filipin III does not impact endocytosis of dextran. Filipin- (A) or non-Filipin (B) treated A549 cells were incubated with 10,000 MW dextran-TR for 30 min and uptake assessed by confocal microscopy. Quantification using Image J indicated no significant difference in dextran endocytosed (data not shown). Dextran treatments were performed in duplicate and experiments repeated twice. Images are representative of overall findings.

CHAPTER 5

CONCLUSION

Mycobacterium tuberculosis (*Mtb*) is an ancient pathogen which has plagued both humans and animals for thousands of years. Researchers have attempted to characterize the host/pathogen interaction in an effort to develop a means to prevent infection or treat the resulting disease, tuberculosis. Until recently, these efforts have focused on addressing the immune response elicited when *Mtb* bacilli are internalized by alveolar macrophages (9, 63, 67, 242-243). While these phagocytic cells are assuredly important in the course of infection, the increase in incidence of tuberculosis worldwide suggests that we are missing important aspects of the host/pathogen relationship which could aid in our ability to combat the disease. Pneumocyte epithelial cells, which comprise the majority of cells in the lung alveolus, have been investigated in recent years for their role during *Mtb* infection (22, 58). However, there has been no previous research focused on the trafficking of *Mtb* bacilli in type II alveolar epithelial cells, which could provide greater insight into how this pathogen circumvents the host immune responses.

The trafficking of *Mtb* bacilli in macrophages has been well characterized. Previous work has demonstrated that this pathogen can inhibit fusion of late endosomes and lysosomes with the bacteria-containing compartment in a process referred to as Phagosomal Maturation Arrest (9, 45-46, 132, 242). The question that arises from these

studies is, does this process occur in the alveolar epithelial cells or do the bacteria have alternative mechanisms for survival in this cell type? In this report, it has been shown that approximately 50% of *Mtb* bacilli-containing compartments colocalized with the early endosomal marker Rab5 and the late endosomal marker Rab7 at 12 hours post infection (hpi) (Chapter 3). Further by 72 hpi approximately 80% of the bacilli-containing compartments colocalized with Rab7 alone. Therefore, unlike macrophages which demonstrate accumulation of early and not late endosomal markers on the *Mtb*-containing phagosome, bacilli appear to traffic to late endosomes in type II alveolar epithelial cells.

It has also been demonstrated in this report that *Mtb* bacilli survive and replicate the type II epithelial cells. Therefore, lysosomal markers were evaluated microscopically to determine if inhibition of lysosomal fusion occurred. Colocalization of cathepsin-L and Lysosomal Associated Membrane Protein-2 (LAMP-2), two lysosomal associated proteins, was shown to be inhibited during infection with *Mtb*, which supports findings of bacilli survival in the epithelial cell. Collectively these findings suggest that while *Mtb* bacilli can survive in alveolar epithelial cells by inhibiting lysosomal fusion, similar to PMA in macrophages, the process by which this occurs is unique to this cell type.

One possible explanation for the differences in *Mtb* trafficking in the type II epithelial cell compared to macrophages, may be the involvement of the autophagy pathway. Autophagy has been shown to play an important role in the trafficking, and in some instances, elimination of intracellular pathogens such as *Salmonella* and *Listeria* (26, 29, 97, 174) . However, other pathogens, such as *Shigella flexneri* and *Coxiella burnetti*, have been shown to utilize and manipulate this pathway to promote survival in host cells (23, 82, 153). In this report double-membrane compartments were observed to

be surrounding *Mtb* bacilli by transmission electron microscopy (Chapter 3). Other studies in macrophages have suggested that exogenous pharmacological up-regulation of the pathway could aid in elimination of mycobacteria species but the role this pathway may play during standard infection has not been examined. In the studies presented here, we have shown that approximately 90% of all *Mtb*-containing compartments are associated with the autophagy protein Lc3 at 72 hpi. These findings demonstrate that the autophagy pathway is the major route by which this pathogen traffics through the alveolar epithelial cell. The timing of the involvement of the autophagy pathway has been further characterized through the association of ATG-16, an upstream initiating protein of the autophagy pathway. ATG-16 appears to associate with the plasma membrane of the host cell and attached bacilli as early as three and six hpi. These findings support other published work which suggests that autophagy induction can initiate from the plasma membrane (178). Further, we have shown that inhibition of the autophagy pathway decreases bacterial survival while promoting host cell survival. These data suggest that *Mtb* bacilli have adapted mechanisms to circumvent host cell clearance by the autophagy pathway and that this process may be unique to mycobacterial infection of nonphagocytic cells. Further, the initiation of involvement of the autophagy pathway appears to occur at the plasma membrane which indicates that interactions between *Mtb* bacilli and the surface of the host cell determine the subsequent path of trafficking and may play an important role in bacterial survival.

The interaction that occurs between *Mtb* bacilli and the surface of the alveolar epithelial cell has been further characterized in the studies presented here. Cholesterol-dense regions of the plasma membrane known as lipid rafts (LR) have been shown to

play an important role in internalization of other intracellular pathogens (1, 6, 264). Interestingly, studies by Amer et al. have linked the internalization of pathogens by LR to the autophagy pathway, which would link the observations of autophagy involvement in the trafficking of *Mtb* bacilli in alveolar epithelial cells (6). Thus, we have investigated the role LR play during *Mtb* infection and have shown that live *Mtb* bacilli are capable of inducing aggregation of LR on the surface of the host cell. Mycobacterial proteins and cell wall components do not induce the LR aggregation. Rather, aggregation results from a mycobacterial protein secreted during the infection of type II epithelial cells. Further, studies with the cholesterol-disrupting agent Filipin III have demonstrated that LR aggregates are important for bacterial entry and survival at 24 hpi. Other researchers have demonstrated that, in macrophages, cholesterol in the membrane of the mycobacteria-containing phagosome is important for virulence (73). It has been shown that the *Mtb* protein ESAT-6, a known virulence factor for this pathogen, preferentially binds to cholesterol in the phagosome wall to form pores and facilitate the release of bacterial proteins into the host cell cytoplasm (54, 104). We hypothesize that LR aggregation is important for *Mtb* entry and survival in alveolar epithelial cells due to the role cholesterol aggregates may play in the ability of the bacteria to manipulate the autophagosomal compartment.

In conclusion these studies have demonstrated that *Mtb* bacilli are capable of manipulating the alveolar epithelial cell to promote bacterial survival, similar to events that occur in macrophages. However, the mechanism by which this occurs appears to be unique to the cell type examined here. It would appear that nonphagocytic cells traffic *Mtb* bacilli quite differently than phagocytic cells. Importantly, *Mtb* bacilli appear to be

capable of manipulating the epithelial environment as efficiently as the macrophage. These efforts to characterize mycobacteria interactions with the alveolar epithelial cell demonstrate the genetic flexibility of this pathogen in surviving and multiplying within multiple cell types. The epithelial cell is likely an important cell for harboring bacilli and facilitating bacterial replication leading to infection and latent disease. Understanding the dynamic interaction of *Mtb* and the alveolar epithelial cell could provide great insight into means by which this pathogen has successfully infected humans for thousands of years.

REFERENCES

1. **Abraham, S. N., M. J. Duncan, G. Li, and D. Zaas.** 2005. Bacterial penetration of the mucosal barrier by targeting lipid rafts. J Investig Med **53:**318-21.

2. **Abramoff, M. D., Magelhaes, P.J., Ram, S.J. .** 2004. Image Processing with ImageJ. Biophotonics International **11:**36-42

3. **Alcorn, J. L., J. M. Stark, C. L. Chiappetta, G. Jenkins, and G. N. Colasurdo.** 2005. Effects of RSV infection on pulmonary surfactant protein SP-A in cultured human type II cells: contrasting consequences on SP-A mRNA and protein. Am J Physiol Lung Cell Mol Physiol **289:**L1113-22.

4. **Alonso, S., K. Pethe, D. G. Russell, and G. E. Purdy.** 2007. Lysosomal killing of Mycobacterium mediated by ubiquitin-derived peptides is enhanced by autophagy. Proc Natl Acad Sci U S A **104:**6031-6.

5. **Ameni, G., M. Vordermeier, R. Firdessa, A. Aseffa, G. Hewinson, S. V. Gordon, and S. Berg.** 2011. Mycobacterium tuberculosis infection in grazing cattle in central Ethiopia. Vet J **188:**359-61.

6. **Amer, A. O., B. G. Byrne, and M. S. Swanson.** 2005. Macrophages rapidly transfer pathogens from lipid raft vacuoles to autophagosomes. Autophagy **1:**53-8.

7. **Antinori, S., L. Galimberti, G. L. Tadini, A. L. Ridolfo, C. Parravicini, R. Esposito, and M. Moroni.** 1995. Tuberculosis cutis miliaris disseminata due to multidrug-resistant Mycobacterium tuberculosis in AIDS patients. Eur J Clin Microbiol Infect Dis **14:**911-4.

8. **Aoki, K., S. Matsumoto, Y. Hirayama, T. Wada, Y. Ozeki, M. Niki, P. Domenech, K. Umemori, S. Yamamoto, A. Mineda, M. Matsumoto, and K. Kobayashi.** 2004. Extracellular mycobacterial DNA-binding protein 1 participates in mycobacterium-lung epithelial cell interaction through hyaluronic acid. J Biol Chem **279:**39798-806.

9. **Armstrong, J. A., and P. D. Hart.** 1971. Response of cultured macrophages to Mycobacterium tuberculosis, with observations on fusion of lysosomes with phagosomes. J Exp Med **134:**713-40.

10. **Atkinson, J. J., T. L. Adair-Kirk, D. G. Kelley, D. Demello, and R. M. Senior.** 2008. Clara cell adhesion and migration to extracellular matrix. Respir Res **9:**1.

11. **Auriac, A., A. Willemetz, and F. Canonne-Hergaux.** 2010. Lipid raft-dependent endocytosis: a new route for hepcidin-mediated regulation of ferroportin in macrophages. Haematologica **95:**1269-77.

12. **Banu, S., N. Honore, B. Saint-Joanis, D. Philpott, M. C. Prevost, and S. T. Cole.** 2002. Are the PE-PGRS proteins of Mycobacterium tuberculosis variable surface antigens? Mol Microbiol **44:**9-19.

13. **Barczak, A. K., P. Domenech, H. I. Boshoff, M. B. Reed, C. Manca, G. Kaplan, and C. E. Barry, 3rd.** 2005. In vivo phenotypic dominance in mouse mixed infections with Mycobacterium tuberculosis clinical isolates. J Infect Dis **192:**600-6.

14. **Barman, S., L. Adhikary, A. K. Chakrabarti, C. Bernas, Y. Kawaoka, and D. P. Nayak.** 2004. Role of transmembrane domain and cytoplasmic tail amino acid sequences of influenza a virus neuraminidase in raft association and virus budding. J Virol **78:**5258-69.

15. **Barry, C. E., 3rd, H. I. Boshoff, V. Dartois, T. Dick, S. Ehrt, J. Flynn, D. Schnappinger, R. J. Wilkinson, and D. Young.** 2009. The spectrum of latent tuberculosis: rethinking the biology and intervention strategies. Nat Rev Microbiol **7:**845-55.

16. **Bauman, S. J., and M. J. Kuehn.** 2009. Pseudomonas aeruginosa vesicles associate with and are internalized by human lung epithelial cells. BMC Microbiol **9:**26.

17. **Beharka, A. A., C. D. Gaynor, B. K. Kang, D. R. Voelker, F. X. McCormack, and L. S. Schlesinger.** 2002. Pulmonary surfactant protein A up-regulates activity of the mannose receptor, a pattern recognition receptor expressed on human macrophages. J Immunol **169:**3565-73.

18. **Behr, M. A., M. A. Wilson, W. P. Gill, H. Salamon, G. K. Schoolnik, S. Rane, and P. M. Small.** 1999. Comparative genomics of BCG vaccines by whole-genome DNA microarray. Science **284:**1520-3.

19. **Behrends, C., M. E. Sowa, S. P. Gygi, and J. W. Harper.** 2010. Network organization of the human autophagy system. Nature **466:**68-76.

20. **Ben Amor, Y., B. Nemser, A. Singh, A. Sankin, and N. Schluger.** 2008. Underreported threat of multidrug-resistant tuberculosis in Africa. Emerg Infect Dis **14:**1345-52.

21. **Berlin, L.** 2008. Tuberculosis: resurgent disease, renewed liability. AJR Am J Roentgenol **190:**1438-44.

22. **Bermudez, L. E., and J. Goodman.** 1996. Mycobacterium tuberculosis invades and replicates within type II alveolar cells. Infect Immun **64:**1400-6.

23. **Beron, W., M. G. Gutierrez, M. Rabinovitch, and M. I. Colombo.** 2002. Coxiella burnetii localizes in a Rab7-labeled compartment with autophagic characteristics. Infect Immun **70:**5816-21.

24. **Birkness, K. A., M. Deslauriers, J. H. Bartlett, E. H. White, C. H. King, and F. D. Quinn.** 1999. An in vitro tissue culture bilayer model to examine early events in Mycobacterium tuberculosis infection. Infect Immun **67:**653-8.

25. **Birkness, K. A., W. E. Swords, P. H. Huang, E. H. White, C. S. Dezzutti, R. B. Lal, and F. D. Quinn.** 1999. Observed differences in virulence-associated phenotypes between a human clinical isolate and a veterinary isolate of Mycobacterium avium. Infect Immun **67:**4895-901.

26. **Birmingham, C. L., V. Canadien, E. Gouin, E. B. Troy, T. Yoshimori, P. Cossart, D. E. Higgins, and J. H. Brumell.** 2007. Listeria monocytogenes evades killing by autophagy during colonization of host cells. Autophagy **3:**442-51.

27. **Birmingham, C. L., V. Canadien, N. A. Kaniuk, B. E. Steinberg, D. E. Higgins, and J. H. Brumell.** 2008. Listeriolysin O allows Listeria monocytogenes replication in macrophage vacuoles. Nature **451:**350-4.

28. **Birmingham, C. L., D. E. Higgins, and J. H. Brumell.** 2008. Avoiding death by autophagy: interactions of Listeria monocytogenes with the macrophage autophagy system. Autophagy **4:**368-71.

29. **Birmingham, C. L., A. C. Smith, M. A. Bakowski, T. Yoshimori, and J. H. Brumell.** 2006. Autophagy controls Salmonella infection in response to damage to the Salmonella-containing vacuole. J Biol Chem **281:**11374-83.

30. **Bloom, B. R., J. Flynn, K. McDonough, Y. Kress, and J. Chan.** 1994. Experimental approaches to mechanisms of protection and pathogenesis in M. tuberculosis infection. Immunobiology **191:**526-36.

31. **Braunstein, M., S. S. Bardarov, and W. R. Jacobs, Jr.** 2002. Genetic methods for deciphering virulence determinants of Mycobacterium tuberculosis. Methods Enzymol **358:**67-99.

32. **Briken, V., S. A. Porcelli, G. S. Besra, and L. Kremer.** 2004. Mycobacterial lipoarabinomannan and related lipoglycans: from biogenesis to modulation of the immune response. Mol Microbiol **53:**391-403.

33. **Brinkman, G. L.** 1968. The mast cell in normal human bronchus and lung. J Ultrastruct Res **23:**115-23.

34. **Brodin, P., M. I. de Jonge, L. Majlessi, C. Leclerc, M. Nilges, S. T. Cole, and R. Brosch.** 2005. Functional analysis of early secreted antigenic target-6, the dominant T-cell antigen of Mycobacterium tuberculosis, reveals key residues involved in secretion, complex formation, virulence, and immunogenicity. J Biol Chem **280:**33953-9.

35. **Brosch, R., S. V. Gordon, M. Marmiesse, P. Brodin, C. Buchrieser, K. Eiglmeier, T. Garnier, C. Gutierrez, G. Hewinson, K. Kremer, L. M. Parsons, A. S. Pym, S. Samper, D. van Soolingen, and S. T. Cole.** 2002. A new evolutionary scenario for the Mycobacterium tuberculosis complex. Proc Natl Acad Sci U S A **99:**3684-9.

36. **Brown, D. A., and J. K. Rose.** 1992. Sorting of GPI-anchored proteins to glycolipid-enriched membrane subdomains during transport to the apical cell surface. Cell **68:**533-44.

37. **Brudey, K., J. R. Driscoll, L. Rigouts, W. M. Prodinger, A. Gori, S. A. Al-Hajoj, C. Allix, L. Aristimuno, J. Arora, V. Baumanis, L. Binder, P. Cafrune, A. Cataldi, S. Cheong, R. Diel, C. Ellermeier, J. T. Evans, M. Fauville-Dufaux, S. Ferdinand, D. Garcia de Viedma, C. Garzelli, L. Gazzola, H. M. Gomes, M. C. Guttierez, P. M. Hawkey, P. D. van Helden, G. V. Kadival, B. N. Kreiswirth, K. Kremer, M. Kubin, S. P. Kulkarni, B. Liens, T. Lillebaek, M. L. Ho, C. Martin, I. Mokrousov, O. Narvskaia, Y. F. Ngeow, L. Naumann, S. Niemann, I. Parwati, Z. Rahim, V. Rasolofo-Razanamparany, T. Rasolonavalona, M. L. Rossetti, S. Rusch-Gerdes, A. Sajduda, S. Samper, I. G. Shemyakin, U. B. Singh, A. Somoskovi, R. A. Skuce, D. van Soolingen, E. M. Streicher, P. N. Suffys, E. Tortoli, T. Tracevska, V. Vincent, T. C. Victor, R. M. Warren, S. F. Yap, K. Zaman, F. Portaels, N. Rastogi, and C. Sola.** 2006. Mycobacterium tuberculosis complex genetic diversity: mining the fourth international spoligotyping database (SpolDB4) for classification, population genetics and epidemiology. BMC Microbiol **6:**23.

38. **Brudey, K., I. Filliol, S. Ferdinand, V. Guernier, P. Duval, B. Maubert, C. Sola, and N. Rastogi.** 2006. Long-term population-based genotyping study of Mycobacterium tuberculosis complex isolates in the French departments of the Americas. J Clin Microbiol **44:**183-91.

39. **Brudey, K., I. Filliol, M. Theodore, C. Sola, and N. Rastogi.** 2006. [Molecular epidemiology of tuberculosis in Guadeloupe from 1994 to 2000]. Pathol Biol (Paris) **54:**14-21.

40. **Calmette, A., C. Guérin, A. Boquet, and L. Nègre.** 1927. La vaccination préventive contre la tuberculose par le "BCG,". Masson et cie, Paris,.

41. **Cavalli, V., F. Vilbois, M. Corti, M. J. Marcote, K. Tamura, M. Karin, S. Arkinstall, and J. Gruenberg.** 2001. The stress-induced MAP kinase p38 regulates endocytic trafficking via the GDI:Rab5 complex. Mol Cell **7:**421-32.

42. **Chelen, C. J., Y. Fang, G. J. Freeman, H. Secrist, J. D. Marshall, P. T. Hwang, L. R. Frankel, R. H. DeKruyff, and D. T. Umetsu.** 1995. Human alveolar macrophages present antigen ineffectively due to defective expression of B7 costimulatory cell surface molecules. J Clin Invest **95:**1415-21.

43. **Chen, L., W. Song, I. C. Davis, K. Shrestha, E. Schwiebert, W. M. Sullender, and S. Matalon.** 2009. Inhibition of Na+ transport in lung epithelial cells by respiratory syncytial virus infection. Am J Respir Cell Mol Biol **40:**588-600.

44. **Clemens, D. L., and M. A. Horwitz.** 1995. Characterization of the Mycobacterium tuberculosis phagosome and evidence that phagosomal maturation is inhibited. J Exp Med **181:**257-70.

45. **Clemens, D. L., B. Y. Lee, and M. A. Horwitz.** 2000. Deviant expression of Rab5 on phagosomes containing the intracellular pathogens Mycobacterium tuberculosis and Legionella pneumophila is associated with altered phagosomal fate. Infect Immun **68:**2671-84.

46. **Clemens, D. L., B. Y. Lee, and M. A. Horwitz.** 2000. Mycobacterium tuberculosis and Legionella pneumophila phagosomes exhibit arrested maturation despite acquisition of Rab7. Infect Immun **68:**5154-66.

47. **Cohen, A. W., R. Hnasko, W. Schubert, and M. P. Lisanti.** 2004. Role of caveolae and caveolins in health and disease. Physiol Rev **84:**1341-79.

48. **Cole, S. T., R. Brosch, J. Parkhill, T. Garnier, C. Churcher, D. Harris, S. V. Gordon, K. Eiglmeier, S. Gas, C. E. Barry, 3rd, F. Tekaia, K. Badcock, D. Basham, D. Brown, T. Chillingworth, R. Connor, R. Davies, K. Devlin, T. Feltwell, S. Gentles, N. Hamlin, S. Holroyd, T. Hornsby, K. Jagels, A. Krogh, J. McLean, S. Moule, L. Murphy, K. Oliver, J. Osborne, M. A. Quail, M. A. Rajandream, J. Rogers, S. Rutter, K. Seeger, J. Skelton, R. Squares, S. Squares, J. E. Sulston, K. Taylor, S. Whitehead, and B. G. Barrell.** 1998. Deciphering the biology of Mycobacterium tuberculosis from the complete genome sequence. Nature **393:**537-44.

49. **Constant, P., E. Perez, W. Malaga, M. A. Laneelle, O. Saurel, M. Daffe, and C. Guilhot.** 2002. Role of the pks15/1 gene in the biosynthesis of phenolglycolipids in the Mycobacterium tuberculosis complex. Evidence that all strains synthesize glycosylated p-hydroxybenzoic methyl esters and that strains devoid of phenolglycolipids harbor a frameshift mutation in the pks15/1 gene. J Biol Chem **277:**38148-58.

50. **Crapo, J. D., B. E. Barry, P. Gehr, M. Bachofen, and E. R. Weibel.** 1982. Cell number and cell characteristics of the normal human lung. Am Rev Respir Dis **126:**332-7.

51. **Danelishvili, L., J. McGarvey, Y. J. Li, and L. E. Bermudez.** 2003. Mycobacterium tuberculosis infection causes different levels of apoptosis and necrosis in human macrophages and alveolar epithelial cells. Cell Microbiol **5:**649-60.

52. **Dao, D. N., K. Sweeney, T. Hsu, S. S. Gurcha, I. P. Nascimento, D. Roshevsky, G. S. Besra, J. Chan, S. A. Porcelli, and W. R. Jacobs.** 2008. Mycolic acid modification by the mmaA4 gene of M. tuberculosis modulates IL-12 production. PLoS Pathog **4:**e1000081.

53. **de Chastellier, C., and L. Thilo.** 2006. Cholesterol depletion in Mycobacterium avium-infected macrophages overcomes the block in phagosome maturation and leads to the reversible sequestration of viable mycobacteria in phagolysosome-derived autophagic vacuoles. Cell Microbiol **8:**242-56.

54. **de Jonge, M. I., G. Pehau-Arnaudet, M. M. Fretz, F. Romain, D. Bottai, P. Brodin, N. Honore, G. Marchal, W. Jiskoot, P. England, S. T. Cole, and R. Brosch.** 2007. ESAT-6 from Mycobacterium tuberculosis dissociates from its putative chaperone CFP-10 under acidic conditions and exhibits membrane-lysing activity. J Bacteriol **189:**6028-34.

55. **Debbabi, H., S. Ghosh, A. B. Kamath, J. Alt, D. E. Demello, S. Dunsmore, and S. M. Behar.** 2005. Primary type II alveolar epithelial cells present microbial antigens to antigen-specific CD4+ T cells. Am J Physiol Lung Cell Mol Physiol **289:**L274-9.

56. **Deretic, V.** 2008. Autophagy, an immunologic magic bullet: Mycobacterium tuberculosis phagosome maturation block and how to bypass it. Future Microbiol **3:**517-24.

57. **Deretic, V., S. Singh, S. Master, J. Harris, E. Roberts, G. Kyei, A. Davis, S. de Haro, J. Naylor, H. H. Lee, and I. Vergne.** 2006. Mycobacterium tuberculosis inhibition of phagolysosome biogenesis and autophagy as a host defence mechanism. Cell Microbiol **8:**719-27.

58. **Dobos, K. M., E. A. Spotts, F. D. Quinn, and C. H. King.** 2000. Necrosis of lung epithelial cells during infection with Mycobacterium tuberculosis is preceded by cell permeation. Infect Immun **68:**6300-10.

59. **Drennan, M. B., D. Nicolle, V. J. Quesniaux, M. Jacobs, N. Allie, J. Mpagi, C. Fremond, H. Wagner, C. Kirschning, and B. Ryffel.** 2004. Toll-like receptor 2-deficient mice succumb to Mycobacterium tuberculosis infection. Am J Pathol **164:**49-57.

60. **Duncan, M. J., G. Li, J. S. Shin, J. L. Carson, and S. N. Abraham.** 2004. Bacterial penetration of bladder epithelium through lipid rafts. J Biol Chem **279:**18944-51.

61. **Dussurget, O.** 2008. New insights into determinants of Listeria monocytogenes virulence. Int Rev Cell Mol Biol **270:**1-38.

62. **Eltringham, I. J., and F. Drobniewski.** 1998. Multiple drug resistant tuberculosis: aetiology, diagnosis and outcome. Br Med Bull **54:**569-78.

63. **Ernst, J. D.** 1998. Macrophage receptors for Mycobacterium tuberculosis. Infect Immun **66:**1277-81.

64. **Eskelinen, E. L., Y. Tanaka, and P. Saftig.** 2003. At the acidic edge: emerging functions for lysosomal membrane proteins. Trends Cell Biol **13:**137-45.

65. **Espert, L., P. Codogno, and M. Biard-Piechaczyk.** 2007. Involvement of autophagy in viral infections: antiviral function and subversion by viruses. J Mol Med **85:**811-23.

66. **Ferguson, J. S., J. L. Martin, A. K. Azad, T. R. McCarthy, P. B. Kang, D. R. Voelker, E. C. Crouch, and L. S. Schlesinger.** 2006. Surfactant protein D increases fusion of Mycobacterium tuberculosis-containing phagosomes with lysosomes in human macrophages. Infect Immun **74:**7005-9.

67. **Fratti, R. A., J. M. Backer, J. Gruenberg, S. Corvera, and V. Deretic.** 2001. Role of phosphatidylinositol 3-kinase and Rab5 effectors in phagosomal biogenesis and mycobacterial phagosome maturation arrest. J Cell Biol **154:**631-44.

68. **French, C. T., E. M. Panina, S. H. Yeh, N. Griffith, D. G. Arambula, and J. F. Miller.** 2009. The Bordetella type III secretion system effector BteA contains a conserved N-terminal motif that guides bacterial virulence factors to lipid rafts. Cell Microbiol **11:**1735-49.

69. **Gagneux, S., M. V. Burgos, K. DeRiemer, A. Encisco, S. Munoz, P. C. Hopewell, P. M. Small, and A. S. Pym.** 2006. Impact of bacterial genetics on the transmission of isoniazid-resistant Mycobacterium tuberculosis. PLoS Pathog **2:**e61.

70. **Gagneux, S., K. DeRiemer, T. Van, M. Kato-Maeda, B. C. de Jong, S. Narayanan, M. Nicol, S. Niemann, K. Kremer, M. C. Gutierrez, M. Hilty, P. C. Hopewell, and P. M. Small.** 2006. Variable host-pathogen compatibility in Mycobacterium tuberculosis. Proc Natl Acad Sci U S A **103:**2869-73.

71. **Gajate, C., F. Gonzalez-Camacho, and F. Mollinedo.** 2009. Involvement of raft aggregates enriched in Fas/CD95 death-inducing signaling complex in the antileukemic action of edelfosine in Jurkat cells. PLoS One **4:**e5044.

72. **Garcia-Perez, B. E., J. C. Hernandez-Gonzalez, S. Garcia-Nieto, and J. Luna-Herrera.** 2008. Internalization of a non-pathogenic mycobacteria by macropinocytosis in human alveolar epithelial A549 cells. Microb Pathog **45:**1-6.

73. **Gatfield, J., and J. Pieters.** 2000. Essential role for cholesterol in entry of mycobacteria into macrophages. Science **288:**1647-50.

74. **Gekara, N. O., T. Jacobs, T. Chakraborty, and S. Weiss.** 2005. The cholesterol-dependent cytolysin listeriolysin O aggregates rafts via oligomerization. Cell Microbiol **7:**1345-56.

75. **Gideon, H. P., and J. L. Flynn.** 2011. Latent tuberculosis: what the host "sees"? Immunol Res **50:**202-12.

76. **Goerdt, S., and C. E. Orfanos.** 1999. Other functions, other genes: alternative activation of antigen-presenting cells. Immunity **10:**137-42.

77. **Goldsmith, C. S., L. H. Elliott, C. J. Peters, and S. R. Zaki.** 1995. Ultrastructural characteristics of Sin Nombre virus, causative agent of hantavirus pulmonary syndrome. Arch Virol **140:**2107-22.

78. **Goluszko, P., and B. Nowicki.** 2005. Membrane cholesterol: a crucial molecule affecting interactions of microbial pathogens with mammalian cells. Infect Immun **73:**7791-6.

79. **Guerin, I., and C. de Chastellier.** 2000. Pathogenic mycobacteria disrupt the macrophage actin filament network. Infect Immun **68:**2655-62.

80. **Gutierrez, M. G., S. S. Master, S. B. Singh, G. A. Taylor, M. I. Colombo, and V. Deretic.** 2004. Autophagy is a defense mechanism inhibiting BCG and Mycobacterium tuberculosis survival in infected macrophages. Cell **119:**753-66.

81. **Gutierrez, M. G., B. B. Mishra, L. Jordao, E. Elliott, E. Anes, and G. Griffiths.** 2008. NF-kappa B activation controls phagolysosome fusion-mediated killing of mycobacteria by macrophages. J Immunol **181:**2651-63.

82. **Gutierrez, M. G., C. L. Vazquez, D. B. Munafo, F. C. Zoppino, W. Beron, M. Rabinovitch, and M. I. Colombo.** 2005. Autophagy induction favours the generation and maturation of the Coxiella-replicative vacuoles. Cell Microbiol **7:**981-93.

83. **Hall-Stoodley, L., G. Watts, J. E. Crowther, A. Balagopal, J. B. Torrelles, J. Robison-Cox, R. F. Bargatze, A. G. Harmsen, E. C. Crouch, and L. S. Schlesinger.** 2006. Mycobacterium tuberculosis binding to human surfactant proteins A and D, fibronectin, and small airway epithelial cells under shear conditions. Infect Immun **74:**3587-96.

84. **Hamid, Q., J. Shannon, and J. Martin.** 2005. Physiologic basis of respiratory disease. BC Decker, Inc., Hamilton.

85. **Hansen, C. G., and B. J. Nichols.** 2010. Exploring the caves: cavins, caveolins and caveolae. Trends Cell Biol **20:**177-86.

86. **Hauck, F. R., B. H. Neese, A. S. Panchal, and W. El-Amin.** 2009. Identification and management of latent tuberculosis infection. Am Fam Physician **79:**879-86.

87. **Hawgood, S.** 1989. Pulmonary surfactant apoproteins: a review of protein and genomic structure. Am J Physiol **257:**L13-22.

88. **Hayakawa, E., F. Tokumasu, G. A. Nardone, A. J. Jin, V. A. Hackley, and J. A. Dvorak.** 2007. A Mycobacterium tuberculosis-derived lipid inhibits membrane fusion by modulating lipid membrane domains. Biophys J **93:**4018-30.

89. **Henning, L. N., A. K. Azad, K. V. Parsa, J. E. Crowther, S. Tridandapani, and L. S. Schlesinger.** 2008. Pulmonary surfactant protein A regulates TLR expression and activity in human macrophages. J Immunol **180:**7847-58.

90. **Hessey, S. J., J. Spencer, J. I. Wyatt, G. Sobala, B. J. Rathbone, A. T. Axon, and M. F. Dixon.** 1990. Bacterial adhesion and disease activity in Helicobacter associated chronic gastritis. Gut **31:**134-8.

91. **Holt, P. G.** 1993. Development of bronchus associated lymphoid tissue (BALT) in human lung disease: a normal host defence mechanism awaiting therapeutic exploitation? Thorax **48:**1097-8.

92. **Hurley, J. H., E. Boura, L. A. Carlson, and B. Rozycki.** 2010. Membrane budding. Cell **143:**875-87.

93. **Jackson, W. T., T. H. Giddings, Jr., M. P. Taylor, S. Mulinyawe, M. Rabinovitch, R. R. Kopito, and K. Kirkegaard.** 2005. Subversion of cellular autophagosomal machinery by RNA viruses. PLoS Biol **3:**e156.

94. **Jager, S., C. Bucci, I. Tanida, T. Ueno, E. Kominami, P. Saftig, and E. L. Eskelinen.** 2004. Role for Rab7 in maturation of late autophagic vacuoles. J Cell Sci **117:**4837-48.

95. **Janes, P. W., S. C. Ley, A. I. Magee, and P. S. Kabouridis.** 2000. The role of lipid rafts in T cell antigen receptor (TCR) signalling. Semin Immunol **12:**23-34.

96. **Jutras, I., L. Abrami, and A. Dautry-Varsat.** 2003. Entry of the lymphogranuloma venereum strain of Chlamydia trachomatis into host cells involves cholesterol-rich membrane domains. Infect Immun **71:**260-6.

97. **Kageyama, S., H. Omori, T. Saitoh, T. Sone, J. L. Guan, S. Akira, F. Imamoto, T. Noda, and T. Yoshimori.** 2011. The LC3 recruitment mechanism is separate from Atg9L1-dependent membrane formation in the autophagic response against Salmonella. Mol Biol Cell **22:**2290-300.

98. **Kaksonen, M., C. P. Toret, and D. G. Drubin.** 2006. Harnessing actin dynamics for clathrin-mediated endocytosis. Nat Rev Mol Cell Biol **7:**404-14.

99. **Kang, B. K., and L. S. Schlesinger.** 1998. Characterization of mannose receptor-dependent phagocytosis mediated by Mycobacterium tuberculosis lipoarabinomannan. Infect Immun **66:**2769-77.

100. **Kashino, S. S., P. Ovendale, A. Izzo, and A. Campos-Neto.** 2006. Unique model of dormant infection for tuberculosis vaccine development. Clin Vaccine Immunol **13:**1014-21.

101. **Kelley, V. A., and J. S. Schorey.** 2003. Mycobacterium's arrest of phagosome maturation in macrophages requires Rab5 activity and accessibility to iron. Mol Biol Cell **14:**3366-77.

102. **Kinchen, J. M., K. Doukoumetzidis, J. Almendinger, L. Stergiou, A. Tosello-Trampont, C. D. Sifri, M. O. Hengartner, and K. S. Ravichandran.** 2008. A pathway for phagosome maturation during engulfment of apoptotic cells. Nat Cell Biol **10:**556-66.

103. **Kinchen, J. M., and K. S. Ravichandran.** 2008. Phagosome maturation: going through the acid test. Nat Rev Mol Cell Biol **9:**781-95.

104. **Kinhikar, A. G., I. Verma, D. Chandra, K. K. Singh, K. Weldingh, P. Andersen, T. Hsu, W. R. Jacobs, Jr., and S. Laal.** 2010. Potential role for ESAT6 in dissemination of M. tuberculosis via human lung epithelial cells. Mol Microbiol **75:**92-106.

105. **Kirkegaard, K., M. P. Taylor, and W. T. Jackson.** 2004. Cellular autophagy: surrender, avoidance and subversion by microorganisms. Nat Rev Microbiol **2:**301-14.

106. **Kohama, H., M. Umemura, Y. Okamoto, A. Yahagi, H. Goga, T. Harakuni, G. Matsuzaki, and T. Arakawa.** 2008. Mucosal immunization with recombinant heparin-binding haemagglutinin adhesin suppresses extrapulmonary dissemination of Mycobacterium bovis bacillus Calmette-Guerin (BCG) in infected mice. Vaccine **26:**924-32.

107. **Korfhagen, T. R., M. D. Bruno, G. F. Ross, K. M. Huelsman, M. Ikegami, A. H. Jobe, S. E. Wert, B. R. Stripp, R. E. Morris, S. W. Glasser, C. J. Bachurski, H. S. Iwamoto, and J. A. Whitsett.** 1996. Altered surfactant function and structure in SP-A gene targeted mice. Proc Natl Acad Sci U S A **93:**9594-9.

108. **Kowalski, M. P., and G. B. Pier.** 2004. Localization of cystic fibrosis transmembrane conductance regulator to lipid rafts of epithelial cells is required for Pseudomonas aeruginosa-induced cellular activation. J Immunol **172:**418-25.

109. **Kubica, G. P.** 1973. Differential identification of mycobacteria. VII. Key features for identification of clinically significant mycobacteria. Am Rev Respir Dis **107:**9-21.

110. **Kumari, M., and R. K. Saxena.** 2011. Relative efficacy of uptake and presentation of Mycobacterium bovis BCG antigens by type I mouse lung epithelial cells and peritoneal macrophages. Infect Immun **79:**3159-67.

111. **Lafont, F., G. Tran Van Nhieu, K. Hanada, P. Sansonetti, and F. G. van der Goot.** 2002. Initial steps of Shigella infection depend on the cholesterol/sphingolipid raft-mediated CD44-IpaB interaction. EMBO J **21:**4449-57.

112. **Lafont, F., and F. G. van der Goot.** 2005. Bacterial invasion via lipid rafts. Cell Microbiol **7:**613-20.

113. **Laisse, C. J., D. Gavier-Widen, G. Ramis, C. G. Bila, A. Machado, J. J. Quereda, E. O. Agren, and P. D. van Helden.** 2011. Characterization of tuberculous lesions in naturally infected African buffalo (Syncerus caffer). J Vet Diagn Invest **23:**1022-7.

114. **Lajoie, P., and I. R. Nabi.** 2007. Regulation of raft-dependent endocytosis. J Cell Mol Med **11:**644-53.

115. **Lambrecht, B. N., J. B. Prins, and H. C. Hoogsteden.** 2001. Lung dendritic cells and host immunity to infection. Eur Respir J **18:**692-704.

116. **Laurenzo, D., and S. A. Mousa.** 2011. Mechanisms of drug resistance in Mycobacterium tuberculosis and current status of rapid molecular diagnostic testing. Acta Trop **119:**5-10.

117. **Lawn, S. D., and A. I. Zumla.** 2011. Tuberculosis. Lancet **378:**57-72.

118. **Lazzarini, L. C., R. C. Huard, N. L. Boechat, H. M. Gomes, M. C. Oelemann, N. Kurepina, E. Shashkina, F. C. Mello, A. L. Gibson, M. J. Virginio, A. G. Marsico, W. R. Butler, B. N. Kreiswirth, P. N. Suffys, E. S. J. R. Lapa, and J. L. Ho.** 2007. Discovery of a novel Mycobacterium tuberculosis lineage that is a major cause of tuberculosis in Rio de Janeiro, Brazil. J Clin Microbiol **45:**3891-902.

119. **Lazzarini, L. C., S. M. Spindola, H. Bang, A. L. Gibson, S. Weisenberg, W. da Silva Carvalho, C. J. Augusto, R. C. Huard, A. L. Kritski, and J. L. Ho.** 2008. RDRio Mycobacterium tuberculosis infection is associated with a higher frequency of cavitary pulmonary disease. J Clin Microbiol **46:**2175-83.

120. **Le Lay, S., Q. Li, N. Proschogo, M. Rodriguez, K. Gunaratnam, S. Cartland, C. Rentero, W. Jessup, T. Mitchell, and K. Gaus.** 2009. Caveolin-1-dependent and -independent membrane domains. J Lipid Res **50:**1609-20.

121. **Lencer, W. I., T. R. Hirst, and R. K. Holmes.** 1999. Membrane traffic and the cellular uptake of cholera toxin. Biochim Biophys Acta **1450:**177-90.

122. **Levine, B.** 2005. Eating oneself and uninvited guests: autophagy-related pathways in cellular defense. Cell **120:**159-62.

123. **Levine, B., and D. J. Klionsky.** 2004. Development by self-digestion: molecular mechanisms and biological functions of autophagy. Dev Cell **6:**463-77.

124. **Lewis, K. N., R. Liao, K. M. Guinn, M. J. Hickey, S. Smith, M. A. Behr, and D. R. Sherman.** 2003. Deletion of RD1 from Mycobacterium tuberculosis mimics bacille Calmette-Guerin attenuation. J Infect Dis **187:**117-23.

125. **Lim, J. S., H. E. Choy, S. C. Park, J. M. Han, I. S. Jang, and K. A. Cho.** 2010. Caveolae-mediated entry of Salmonella typhimurium into senescent nonphagocytotic host cells. Aging Cell **9:**243-51.

126. **Lin, P. L., S. Pawar, A. Myers, A. Pegu, C. Fuhrman, T. A. Reinhart, S. V. Capuano, E. Klein, and J. L. Flynn.** 2006. Early events in Mycobacterium tuberculosis infection in cynomolgus macaques. Infect Immun **74:**3790-803.

127. **Lin, P. L., M. Rodgers, L. Smith, M. Bigbee, A. Myers, C. Bigbee, I. Chiosea, S. V. Capuano, C. Fuhrman, E. Klein, and J. L. Flynn.** 2009. Quantitative comparison of active and latent tuberculosis in the cynomolgus macaque model. Infect Immun **77:**4631-42.

128. **Lingwood, D., and K. Simons.** 2010. Lipid rafts as a membrane-organizing principle. Science **327:**46-50.

129. **Lonnroth, K., K. G. Castro, J. M. Chakaya, L. S. Chauhan, K. Floyd, P. Glaziou, and M. C. Raviglione.** 2010. Tuberculosis control and elimination 2010-50: cure, care, and social development. Lancet **375:**1814-29.

130. **Mahairas, G. G., P. J. Sabo, M. J. Hickey, D. C. Singh, and C. K. Stover.** 1996. Molecular analysis of genetic differences between Mycobacterium bovis BCG and virulent M. bovis. J Bacteriol **178:**1274-82.

131. **Malik, Z. A., G. M. Denning, and D. J. Kusner.** 2000. Inhibition of Ca(2+) signaling by Mycobacterium tuberculosis is associated with reduced phagosome-lysosome fusion and increased survival within human macrophages. J Exp Med **191:**287-302.

132. **Malik, Z. A., S. S. Iyer, and D. J. Kusner.** 2001. Mycobacterium tuberculosis phagosomes exhibit altered calmodulin-dependent signal transduction: contribution to inhibition of phagosome-lysosome fusion and intracellular survival in human macrophages. J Immunol **166:**3392-401.

133. **Manabe, Y. C., A. M. Dannenberg, Jr., S. K. Tyagi, C. L. Hatem, M. Yoder, S. C. Woolwine, B. C. Zook, M. L. Pitt, and W. R. Bishai.** 2003. Different strains of Mycobacterium tuberculosis cause various spectrums of disease in the rabbit model of tuberculosis. Infect Immun **71:**6004-11.

134. **Manca, C., L. Tsenova, C. E. Barry, 3rd, A. Bergtold, S. Freeman, P. A. Haslett, J. M. Musser, V. H. Freedman, and G. Kaplan.** 1999. Mycobacterium tuberculosis CDC1551 induces a more vigorous host response in vivo and in vitro, but is not more virulent than other clinical isolates. J Immunol **162:**6740-6.

135. **McClean, S., and M. Callaghan.** 2009. Burkholderia cepacia complex: epithelial cell-pathogen confrontations and potential for therapeutic intervention. J Med Microbiol **58:**1-12.

136. **McDonough, K. A., and Y. Kress.** 1995. Cytotoxicity for lung epithelial cells is a virulence-associated phenotype of Mycobacterium tuberculosis. Infect Immun **63:**4802-11.

137. **McDonough, K. A., Y. Kress, and B. R. Bloom.** 1993. Pathogenesis of tuberculosis: interaction of Mycobacterium tuberculosis with macrophages. Infect Immun **61:**2763-73.

138. **Mehta, P. K., C. H. King, E. H. White, J. J. Murtagh, Jr., and F. D. Quinn.** 1996. Comparison of in vitro models for the study of Mycobacterium tuberculosis invasion and intracellular replication. Infect Immun **64:**2673-9.

139. **Menozzi, F. D., J. H. Rouse, M. Alavi, M. Laude-Sharp, J. Muller, R. Bischoff, M. J. Brennan, and C. Locht.** 1996. Identification of a heparin-binding hemagglutinin present in mycobacteria. J Exp Med **184:**993-1001.

140. **Meyer-Morse, N., J. R. Robbins, C. S. Rae, S. N. Mochegova, M. S. Swanson, Z. Zhao, H. W. Virgin, and D. Portnoy.** 2010. Listeriolysin O is necessary and sufficient to induce autophagy during Listeria monocytogenes infection. PLoS One **5:**e8610.

141. **Mikota, S. K., L. Peddie, J. Peddie, R. Isaza, F. Dunker, G. West, W. Lindsay, R. S. Larsen, M. D. Salman, D. Chatterjee, J. Payeur, D. Whipple, C. Thoen, D. S. Davis, C. Sedgwick, R. J. Montali, M. Ziccardi, and J. Maslow.** 2001. Epidemiology and diagnosis of Mycobacterium tuberculosis in captive Asian elephants (Elephas maximus). J Zoo Wildl Med **32:**1-16.

142. **Mitchell, J. S., W. S. Brown, D. G. Woodside, P. Vanderslice, and B. W. McIntyre.** 2009. Clustering T-cell GM1 lipid rafts increases cellular resistance to shear on fibronectin through changes in integrin affinity and cytoskeletal dynamics. Immunol Cell Biol **87:**324-36.

143. **Mollenhauer, H. H.** 1964. Plastic Embedding Mixtures for Use in Electron Microscopy. Stain Technol **39:**111-4.

144. **Moreau, K., B. Ravikumar, M. Renna, C. Puri, and D. C. Rubinsztein.** 2011. Autophagosome precursor maturation requires homotypic fusion. Cell **146:**303-17.

145. **Mostowy, S., V. Sancho-Shimizu, M. A. Hamon, R. Simeone, R. Brosch, T. Johansen, and P. Cossart.** 2011. p62 and NDP52 proteins target intracytosolic Shigella and Listeria to different autophagy pathways. J Biol Chem **286:**26987-95.

146. **Mueller-Ortiz, S. L., E. Sepulveda, M. R. Olsen, C. Jagannath, A. R. Wanger, and S. J. Norris.** 2002. Decreased infectivity despite unaltered C3 binding by a DeltahbhA mutant of Mycobacterium tuberculosis. Infect Immun **70:**6751-60.

147. **Munoz, S., B. Rivas-Santiago, and J. A. Enciso.** 2009. Mycobacterium tuberculosis entry into mast cells through cholesterol-rich membrane microdomains. Scand J Immunol **70:**256-63.

148. **Nakagawa, I., A. Amano, N. Mizushima, A. Yamamoto, H. Yamaguchi, T. Kamimoto, A. Nara, J. Funao, M. Nakata, K. Tsuda, S. Hamada, and T. Yoshimori.** 2004. Autophagy defends cells against invading group A Streptococcus. Science **306:**1037-40.

149. **Nedeltchev, G. G., T. R. Raghunand, M. S. Jassal, S. Lun, Q. J. Cheng, and W. R. Bishai.** 2009. Extrapulmonary dissemination of Mycobacterium bovis but not Mycobacterium tuberculosis in a bronchoscopic rabbit model of cavitary tuberculosis. Infect Immun **77:**598-603.

150. **Nguyen, D. H., and J. E. Hildreth.** 2000. Evidence for budding of human immunodeficiency virus type 1 selectively from glycolipid-enriched membrane lipid rafts. J Virol **74:**3264-72.

151. **Nichols, B.** 2003. Caveosomes and endocytosis of lipid rafts. J Cell Sci **116:**4707-14.

152. **Oeltmann, J. E., J. K. Varma, L. Ortega, Y. Liu, T. O'Rourke, M. Cano, T. Harrington, S. Toney, W. Jones, S. Karuchit, L. Diem, D. Rienthong, J. W. Tappero, K. Ijaz, and S. A. Maloney.** 2008. Multidrug-resistant tuberculosis outbreak among US-bound Hmong refugees, Thailand, 2005. Emerg Infect Dis **14:**1715-21.

153. **Ogawa, M., T. Yoshimori, T. Suzuki, H. Sagara, N. Mizushima, and C. Sasakawa.** 2005. Escape of intracellular Shigella from autophagy. Science **307:**727-31.

154. **Ordway, D., M. Henao-Tamayo, M. Harton, G. Palanisamy, J. Troudt, C. Shanley, R. J. Basaraba, and I. M. Orme.** 2007. The hypervirulent Mycobacterium tuberculosis strain HN878 induces a potent TH1 response followed by rapid down-regulation. J Immunol **179:**522-31.

155. **Orlandi, P. A., and P. H. Fishman.** 1998. Filipin-dependent inhibition of cholera toxin: evidence for toxin internalization and activation through caveolae-like domains. J Cell Biol **141:**905-15.

156. **Ortalo-Magne, A., M. A. Dupont, A. Lemassu, A. B. Andersen, P. Gounon, and M. Daffe.** 1995. Molecular composition of the outermost capsular material of the tubercle bacillus. Microbiology **141 (Pt 7):**1609-20.

157. **Parker, H., K. Horsfield, and G. Cumming.** 1971. Morphology of distal airways in the human lung. J Appl Physiol **31:**386-91.

158. **Parra, M., T. Pickett, G. Delogu, V. Dheenadhayalan, A. S. Debrie, C. Locht, and M. J. Brennan.** 2004. The mycobacterial heparin-binding hemagglutinin is a protective antigen in the mouse aerosol challenge model of tuberculosis. Infect Immun **72:**6799-805.

159. **Parton, R. G., and A. A. Richards.** 2003. Lipid rafts and caveolae as portals for endocytosis: new insights and common mechanisms. Traffic **4:**724-38.

160. **Patel, H. H., and P. A. Insel.** 2009. Lipid rafts and caveolae and their role in compartmentation of redox signaling. Antioxid Redox Signal **11:**1357-72.

161. **Pattingre, S., L. Espert, M. Biard-Piechaczyk, and P. Codogno.** 2008. Regulation of macroautophagy by mTOR and Beclin 1 complexes. Biochimie **90:**313-23.

162. **Pedersen, K. W., Y. van der Meer, N. Roos, and E. J. Snijder.** 1999. Open reading frame 1a-encoded subunits of the arterivirus replicase induce endoplasmic reticulum-derived double-membrane vesicles which carry the viral replication complex. J Virol **73:**2016-26.

163. **Penney, D. P.** 1988. The ultrastructure of epithelial cells of the distal lung. Int Rev Cytol **111:**231-69.

164. **Pethe, K., S. Alonso, F. Biet, G. Delogu, M. J. Brennan, C. Locht, and F. D. Menozzi.** 2001. The heparin-binding haemagglutinin of M. tuberculosis is required for extrapulmonary dissemination. Nature **412:**190-4.

165. **Petiot, A., E. Ogier-Denis, E. F. Blommaart, A. J. Meijer, and P. Codogno.** 2000. Distinct classes of phosphatidylinositol 3'-kinases are involved in signaling pathways that control macroautophagy in HT-29 cells. J Biol Chem **275:**992-8.

166. **Pike, L. J.** 2009. The challenge of lipid rafts. J Lipid Res **50 Suppl:**S323-8.

167. **Pike, L. J.** 2006. Rafts defined: a report on the Keystone Symposium on Lipid Rafts and Cell Function. J Lipid Res **47:**1597-8.

168. **Pohl, C., and S. Jentsch.** 2009. Midbody ring disposal by autophagy is a post-abscission event of cytokinesis. Nat Cell Biol **11:**65-70.

169. **Popik, W., T. M. Alce, and W. C. Au.** 2002. Human immunodeficiency virus type 1 uses lipid raft-colocalized CD4 and chemokine receptors for productive entry into CD4(+) T cells. J Virol **76:**4709-22.

170. **Pralle, A., P. Keller, E. L. Florin, K. Simons, and J. K. Horber.** 2000. Sphingolipid-cholesterol rafts diffuse as small entities in the plasma membrane of mammalian cells. J Cell Biol **148:**997-1008.

171. **Prentice, E., W. G. Jerome, T. Yoshimori, N. Mizushima, and M. R. Denison.** 2004. Coronavirus replication complex formation utilizes components of cellular autophagy. J Biol Chem **279:**10136-41.

172. **Purdy, G. E., and D. G. Russell.** 2007. Lysosomal ubiquitin and the demise of Mycobacterium tuberculosis. Cell Microbiol **9:**2768-74.

173. **Purdy, G. E., and D. G. Russell.** 2007. Ubiquitin trafficking to the lysosome: keeping the house tidy and getting rid of unwanted guests. Autophagy **3:**399-401.

174. **Py, B. F., M. M. Lipinski, and J. Yuan.** 2007. Autophagy limits Listeria monocytogenes intracellular growth in the early phase of primary infection. Autophagy **3:**117-25.

175. **Pym, A. S., P. Brodin, R. Brosch, M. Huerre, and S. T. Cole.** 2002. Loss of RD1 contributed to the attenuation of the live tuberculosis vaccines Mycobacterium bovis BCG and Mycobacterium microti. Mol Microbiol **46:**709-17.

176. **Querbes, W., B. A. O'Hara, G. Williams, and W. J. Atwood.** 2006. Invasion of host cells by JC virus identifies a novel role for caveolae in endosomal sorting of noncaveolar ligands. J Virol **80:**9402-13.

177. **Radeva, G., J. Perabo, and F. J. Sharom.** 2005. P-Glycoprotein is localized in intermediate-density membrane microdomains distinct from classical lipid rafts and caveolar domains. FEBS J **272:**4924-37.

178. **Ravikumar, B., K. Moreau, L. Jahreiss, C. Puri, and D. C. Rubinsztein.** 2010. Plasma membrane contributes to the formation of pre-autophagosomal structures. Nat Cell Biol **12:**747-57.

179. **Reaves, B. J., N. A. Bright, B. M. Mullock, and J. P. Luzio.** 1996. The effect of wortmannin on the localisation of lysosomal type I integral membrane glycoproteins suggests a role for phosphoinositide 3-kinase activity in regulating membrane traffic late in the endocytic pathway. J Cell Sci **109 (Pt 4):**749-62.

180. **Reed, M. B., P. Domenech, C. Manca, H. Su, A. K. Barczak, B. N. Kreiswirth, G. Kaplan, and C. E. Barry, 3rd.** 2004. A glycolipid of hypervirulent tuberculosis strains that inhibits the innate immune response. Nature **431:**84-7.

181. **Regueiro, V., D. Moranta, M. A. Campos, J. Margareto, J. Garmendia, and J. A. Bengoechea.** 2009. Klebsiella pneumoniae increases the levels of Toll-like receptors 2 and 4 in human airway epithelial cells. Infect Immun **77:**714-24.

182. **Rink, J., E. Ghigo, Y. Kalaidzidis, and M. Zerial.** 2005. Rab conversion as a mechanism of progression from early to late endosomes. Cell **122:**735-49.

183. **Rippon, H. J., J. M. Polak, M. Qin, and A. E. Bishop.** 2006. Derivation of distal lung epithelial progenitors from murine embryonic stem cells using a novel three-step differentiation protocol. Stem Cells **24:**1389-98.

184. **Roberts, E. A., J. Chua, G. B. Kyei, and V. Deretic.** 2006. Higher order Rab programming in phagolysosome biogenesis. J Cell Biol **174:**923-9.

185. **Rocha-Ramirez, L. M., I. Estrada-Garcia, L. M. Lopez-Marin, E. Segura-Salinas, P. Mendez-Aragon, D. Van Soolingen, R. Torres-Gonzalez, R. Chacon-Salinas, S. Estrada-Parra, C. Maldonado-Bernal, C. Lopez-Macias, and A. Isibasi.** 2008. Mycobacterium tuberculosis lipids regulate cytokines, TLR-2/4 and MHC class II expression in human macrophages. Tuberculosis (Edinb) **88:**212-20.

186. **Rogee, S., E. Grellier, C. Bernard, A. Loyens, J. C. Beauvillain, C. D'Halluin J, and M. Colin.** 2007. Intracellular trafficking of a fiber-modified adenovirus using lipid raft/caveolae endocytosis. Mol Ther **15:**1963-72.

187. **Romano, P. S., M. G. Gutierrez, W. Beron, M. Rabinovitch, and M. I. Colombo.** 2007. The autophagic pathway is actively modulated by phase II Coxiella burnetii to efficiently replicate in the host cell. Cell Microbiol **9:**891-909.

188. **Ronander, E., M. Brant, H. Janson, J. Sheldon, A. Forsgren, and K. Riesbeck.** 2008. Identification of a novel Haemophilus influenzae protein important for adhesion to epithelial cells. Microbes Infect **10:**87-96.

189. **Rothberg, K. G., J. E. Heuser, W. C. Donzell, Y. S. Ying, J. R. Glenney, and R. G. Anderson.** 1992. Caveolin, a protein component of caveolae membrane coats. Cell **68:**673-82.

190. **Sato, K., T. Akaki, T. Shimizu, C. Sano, K. Ogasawara, and H. Tomioka.** 2001. [Invasion and intracellular growth of Mycobacterium tuberculosis and Mycobacterium avium complex adapted to intramacrophagic environment within macrophages and type II alveolar epithelial cells]. Kekkaku **76:**53-7.

191. **Saunders, G.** 1983. Pulmonary mycobacterium tuberculosis infection in a circus elephant. J Am Vet Med Assoc **183:**1311-2.

192. **Schaefer, M., N. Reiling, C. Fessler, J. Stephani, I. Taniuchi, F. Hatam, A. O. Yildirim, H. Fehrenbach, K. Walter, J. Ruland, H. Wagner, S. Ehlers, and T. Sparwasser.** 2008. Decreased pathology and prolonged survival of human DC-SIGN transgenic mice during mycobacterial infection. J Immunol **180:**6836-45.

193. **Schafer, J. J., and J. E. Mangino.** 2008. Multidrug-resistant Acinetobacter baumannii osteomyelitis from Iraq. Emerg Infect Dis **14:**512-4.

194. **Schlegel, A., T. H. Giddings, Jr., M. S. Ladinsky, and K. Kirkegaard.** 1996. Cellular origin and ultrastructure of membranes induced during poliovirus infection. J Virol **70:**6576-88.

195. **Schlesinger, L. S.** 1993. Macrophage phagocytosis of virulent but not attenuated strains of Mycobacterium tuberculosis is mediated by mannose receptors in addition to complement receptors. J Immunol **150:**2920-30.

196. **Schmid, D., J. Dengjel, O. Schoor, S. Stevanovic, and C. Munz.** 2006. Autophagy in innate and adaptive immunity against intracellular pathogens. J Mol Med **84:**194-202.

197. **Seto, S., K. Tsujimura, and Y. Koide.** 2011. Rab GTPases regulating phagosome maturation are differentially recruited to mycobacterial phagosomes. Traffic **12:**407-20.

198. **Shah, N. K., A. P. Alker, R. Sem, A. I. Susanti, S. Muth, J. D. Maguire, S. Duong, F. Ariey, S. R. Meshnick, and C. Wongsrichanalai.** 2008. Molecular surveillance for multidrug-resistant Plasmodium falciparum, Cambodia. Emerg Infect Dis **14:**1637-40.

199. **Shahnazari, S., and J. H. Brumell.** 2011. Mechanisms and consequences of bacterial targeting by the autophagy pathway. Curr Opin Microbiol **14:**68-75.

200. **Sharma, P., R. Varma, R. C. Sarasij, Ira, K. Gousset, G. Krishnamoorthy, M. Rao, and S. Mayor.** 2004. Nanoscale organization of multiple GPI-anchored proteins in living cell membranes. Cell **116:**577-89.

201. **Shenoi, S., S. Heysell, A. Moll, and G. Friedland.** 2009. Multidrug-resistant and extensively drug-resistant tuberculosis: consequences for the global HIV community. Curr Opin Infect Dis **22:**11-7.

202. **Shin, D. M., C. S. Yang, J. Y. Lee, S. J. Lee, H. H. Choi, H. M. Lee, J. M. Yuk, C. V. Harding, and E. K. Jo.** 2008. Mycobacterium tuberculosis lipoprotein-induced association of TLR2 with protein kinase C zeta in lipid rafts contributes to reactive oxygen species-dependent inflammatory signalling in macrophages. Cell Microbiol **10:**1893-905.

203. **Shin, S. S., M. Yagui, L. Ascencios, G. Yale, C. Suarez, N. Quispe, C. Bonilla, J. Blaya, A. Taylor, C. Contreras, and P. Cegielski.** 2008. Scale-up of multidrug-resistant tuberculosis laboratory services, Peru. Emerg Infect Dis **14:**701-8.

204. **Shui, W., L. Sheu, J. Liu, B. Smart, C. J. Petzold, T. Y. Hsieh, A. Pitcher, J. D. Keasling, and C. R. Bertozzi.** 2008. Membrane proteomics of phagosomes suggests a connection to autophagy. Proc Natl Acad Sci U S A **105:**16952-7.

205. **Simeone, R., A. Bobard, J. Lippmann, W. Bitter, L. Majlessi, R. Brosch, and J. Enninga.** 2012. Phagosomal Rupture by Mycobacterium tuberculosis Results in Toxicity and Host Cell Death. PLoS Pathog **8:**e1002507.

206. **Simons, K., and R. Ehehalt.** 2002. Cholesterol, lipid rafts, and disease. J Clin Invest **110:**597-603.

207. **Sinsimer, D., G. Huet, C. Manca, L. Tsenova, M. S. Koo, N. Kurepina, B. Kana, B. Mathema, S. A. Marras, B. N. Kreiswirth, C. Guilhot, and G. Kaplan.** 2008. The phenolic glycolipid of Mycobacterium tuberculosis differentially modulates the early host cytokine response but does not in itself confer hypervirulence. Infect Immun **76:**3027-36.

208. **Sjolund, M., J. Bonnedahl, J. Hernandez, S. Bengtsson, G. Cederbrant, J. Pinhassi, G. Kahlmeter, and B. Olsen.** 2008. Dissemination of multidrug-resistant bacteria into the Arctic. Emerg Infect Dis **14:**70-2.

209. **Smith, I.** 2003. Mycobacterium tuberculosis pathogenesis and molecular determinants of virulence. Clin Microbiol Rev **16:**463-96.

210. **Smith, J., J. Manoranjan, M. Pan, A. Bohsali, J. Xu, J. Liu, K. L. McDonald, A. Szyk, N. LaRonde-LeBlanc, and L. Y. Gao.** 2008. Evidence for pore formation in host cell membranes by ESX-1-secreted ESAT-6 and its role in Mycobacterium marinum escape from the vacuole. Infect Immun **76:**5478-87.

211. **Smith, N. H., R. G. Hewinson, K. Kremer, R. Brosch, and S. V. Gordon.** 2009. Myths and misconceptions: the origin and evolution of Mycobacterium tuberculosis. Nat Rev Microbiol **7:**537-44.

212. **Soutar, C. A.** 1976. Distribution of plasma cells and other cells containing immunoglobulin in the respiratory tract of normal man and class of immunoglobulin contained therein. Thorax **31:**158-66.

213. **Srivastava, K., D. S. Chauhan, P. Gupta, H. B. Singh, V. D. Sharma, V. S. Yadav, Sreekumaran, S. S. Thakral, J. S. Dharamdheeran, P. Nigam, H. K. Prasad, and V. M. Katoch.** 2008. Isolation of Mycobacterium bovis & M. tuberculosis from cattle of some farms in north India--possible relevance in human health. Indian J Med Res **128:**26-31.

214. **Stahlman, M. T., M. P. Gray, M. W. Falconieri, J. A. Whitsett, and T. E. Weaver.** 2000. Lamellar body formation in normal and surfactant protein B-deficient fetal mice. Lab Invest **80:**395-403.

215. **Stamm, L. M., J. H. Morisaki, L. Y. Gao, R. L. Jeng, K. L. McDonald, R. Roth, S. Takeshita, J. Heuser, M. D. Welch, and E. J. Brown.** 2003. Mycobacterium marinum escapes from phagosomes and is propelled by actin-based motility. J Exp Med **198:**1361-8.

216. **Stamm, L. M., M. A. Pak, J. H. Morisaki, S. B. Snapper, K. Rottner, S. Lommel, and E. J. Brown.** 2005. Role of the WASP family proteins for Mycobacterium marinum actin tail formation. Proc Natl Acad Sci U S A **102:**14837-42.

217. **Starr, T., T. W. Ng, T. D. Wehrly, L. A. Knodler, and J. Celli.** 2008. Brucella intracellular replication requires trafficking through the late endosomal/lysosomal compartment. Traffic **9:**678-94.

218. **Stead, W. W.** 1997. The origin and erratic global spread of tuberculosis. How the past explains the present and is the key to the future. Clin Chest Med **18:**65-77.

219. **Steele, C., R. R. Rapaka, A. Metz, S. M. Pop, D. L. Williams, S. Gordon, J. K. Kolls, and G. D. Brown.** 2005. The beta-glucan receptor dectin-1 recognizes specific morphologies of Aspergillus fumigatus. PLoS Pathog **1:**e42.

220. **Stone, B. J., and Y. Abu Kwaik.** 1998. Expression of multiple pili by Legionella pneumophila: identification and characterization of a type IV pilin gene and its role in adherence to mammalian and protozoan cells. Infect Immun **66:**1768-75.

221. **Suhy, D. A., T. H. Giddings, Jr., and K. Kirkegaard.** 2000. Remodeling the endoplasmic reticulum by poliovirus infection and by individual viral proteins: an autophagy-like origin for virus-induced vesicles. J Virol **74:**8953-65.

222. **Sun, J., A. E. Deghmane, H. Soualhine, T. Hong, C. Bucci, A. Solodkin, and Z. Hmama.** 2007. Mycobacterium bovis BCG disrupts the interaction of Rab7 with RILP contributing to inhibition of phagosome maturation. J Leukoc Biol **82:**1437-45.

223. **Swords, W. E., D. L. Chance, L. A. Cohn, J. Shao, M. A. Apicella, and A. L. Smith.** 2002. Acylation of the lipooligosaccharide of Haemophilus influenzae and colonization: an htrB mutation diminishes the colonization of human airway epithelial cells. Infect Immun **70:**4661-8.

224. **Tahir, S. A., G. Yang, A. A. Goltsov, M. Watanabe, K. Tabata, J. Addai, M. A. Fattah el, D. Kadmon, and T. C. Thompson.** 2008. Tumor cell-secreted caveolin-1 has proangiogenic activities in prostate cancer. Cancer Res **68:**731-9.

225. **Taylor, J. B., L. A. Hogue, J. J. LiPuma, M. J. Walter, S. L. Brody, and C. L. Cannon.** 2010. Entry of Burkholderia organisms into respiratory epithelium: CFTR, microfilament and microtubule dependence. J Cyst Fibros **9:**36-43.

226. **Tenner, A. J., S. L. Robinson, J. Borchelt, and J. R. Wright.** 1989. Human pulmonary surfactant protein (SP-A), a protein structurally homologous to C1q, can enhance FcR- and CR1-mediated phagocytosis. J Biol Chem **264:**13923-8.

227. **Teruya, H., F. Higa, M. Akamine, C. Ishikawa, T. Okudaira, K. Tomimori, N. Mukaida, M. Tateyama, K. Heuner, J. Fujita, and N. Mori.** 2007. Mechanisms of Legionella pneumophila-induced interleukin-8 expression in human lung epithelial cells. BMC Microbiol **7:**102.

228. **Thomas, R., and T. Brooks.** 2006. Attachment of Yersinia pestis to human respiratory cell lines is inhibited by certain oligosaccharides. J Med Microbiol **55:**309-15.

229. **Thomas, R., and T. Brooks.** 2004. Common oligosaccharide moieties inhibit the adherence of typical and atypical respiratory pathogens. J Med Microbiol **53:**833-40.

230. **Thomas, R. J., and T. J. Brooks.** 2004. Oligosaccharide receptor mimics inhibit Legionella pneumophila attachment to human respiratory epithelial cells. Microb Pathog **36:**83-92.

231. **Thorne, N., S. Borrell, J. Evans, J. Magee, D. Garcia de Viedma, C. Bishop, J. Gonzalez-Martin, S. Gharbia, and C. Arnold.** 2011. IS6110-based global phylogeny of Mycobacterium tuberculosis. Infect Genet Evol **11:**132-8.

232. **Togayachi, A., Y. Kozono, Y. Ikehara, H. Ito, N. Suzuki, Y. Tsunoda, S. Abe, T. Sato, K. Nakamura, M. Suzuki, H. M. Goda, M. Ito, T. Kudo, S. Takahashi, and H. Narimatsu.** 2010. Lack of lacto/neolacto-glycolipids enhances the formation of glycolipid-enriched microdomains, facilitating B cell activation. Proc Natl Acad Sci U S A **107:**11900-5.

233. **Torrelles, J. B., R. Knaup, A. Kolareth, T. Slepushkina, T. M. Kaufman, P. Kang, P. J. Hill, P. J. Brennan, D. Chatterjee, J. T. Belisle, J. M. Musser, and L. S. Schlesinger.** 2008. Identification of Mycobacterium tuberculosis clinical isolates with altered phagocytosis by human macrophages due to a truncated lipoarabinomannan. J Biol Chem **283:**31417-28.

234. **Triantafilou, M., S. Morath, A. Mackie, T. Hartung, and K. Triantafilou.** 2004. Lateral diffusion of Toll-like receptors reveals that they are transiently confined within lipid rafts on the plasma membrane. J Cell Sci **117:**4007-14.

235. **Trunz, B. B., P. Fine, and C. Dye.** 2006. Effect of BCG vaccination on childhood tuberculous meningitis and miliary tuberculosis worldwide: a meta-analysis and assessment of cost-effectiveness. Lancet **367:**1173-80.

236. **Tsai, M. C., S. Chakravarty, G. Zhu, J. Xu, K. Tanaka, C. Koch, J. Tufariello, J. Flynn, and J. Chan.** 2006. Characterization of the tuberculous granuloma in murine and human lungs: cellular composition and relative tissue oxygen tension. Cell Microbiol **8:**218-32.

237. **Tsenova, L., E. Ellison, R. Harbacheuski, A. L. Moreira, N. Kurepina, M. B. Reed, B. Mathema, C. E. Barry, 3rd, and G. Kaplan.** 2005. Virulence of selected Mycobacterium tuberculosis clinical isolates in the rabbit model of meningitis is dependent on phenolic glycolipid produced by the bacilli. J Infect Dis **192:**98-106.

238. **Ullrich, O., H. Horiuchi, C. Bucci, and M. Zerial.** 1994. Membrane association of Rab5 mediated by GDP-dissociation inhibitor and accompanied by GDP/GTP exchange. Nature **368:**157-60.

239. **Valway, S. E., M. P. Sanchez, T. F. Shinnick, I. Orme, T. Agerton, D. Hoy, J. S. Jones, H. Westmoreland, and I. M. Onorato.** 1998. An outbreak involving extensive transmission of a virulent strain of Mycobacterium tuberculosis. N Engl J Med **338:**633-9.

240. **van der Wel, N., D. Hava, D. Houben, D. Fluitsma, M. van Zon, J. Pierson, M. Brenner, and P. J. Peters.** 2007. M. tuberculosis and M. leprae translocate from the phagolysosome to the cytosol in myeloid cells. Cell **129:**1287-98.

241. **Vergne, I., J. Chua, and V. Deretic.** 2003. Tuberculosis toxin blocking phagosome maturation inhibits a novel Ca2+/calmodulin-PI3K hVPS34 cascade. J Exp Med **198:**653-9.

242. **Vergne, I., J. Chua, H. H. Lee, M. Lucas, J. Belisle, and V. Deretic.** 2005. Mechanism of phagolysosome biogenesis block by viable Mycobacterium tuberculosis. Proc Natl Acad Sci U S A **102:**4033-8.

243. **Vergne, I., J. Chua, S. B. Singh, and V. Deretic.** 2004. Cell biology of mycobacterium tuberculosis phagosome. Annu Rev Cell Dev Biol **20:**367-94.

244. **Via, L. E., D. Deretic, R. J. Ulmer, N. S. Hibler, L. A. Huber, and V. Deretic.** 1997. Arrest of mycobacterial phagosome maturation is caused by a block in vesicle fusion between stages controlled by rab5 and rab7. J Biol Chem **272:**13326-31.

245. **Vieira, F. S., G. Correa, M. Einicker-Lamas, and R. Coutinho-Silva.** 2010. Host-cell lipid rafts: a safe door for micro-organisms? Biol Cell **102:**391-407.

246. **Vieira, O. V., C. Bucci, R. E. Harrison, W. S. Trimble, L. Lanzetti, J. Gruenberg, A. D. Schreiber, P. D. Stahl, and S. Grinstein.** 2003. Modulation of Rab5 and Rab7 recruitment to phagosomes by phosphatidylinositol 3-kinase. Mol Cell Biol **23:**2501-14.

247. **Wagner, D., F. J. Sangari, S. Kim, M. Petrofsky, and L. E. Bermudez.** 2002. Mycobacterium avium infection of macrophages results in progressive suppression of interleukin-12 production in vitro and in vivo. J Leukoc Biol **71:**80-8.

248. **Watson, R. O., and J. E. Galan.** 2008. Campylobacter jejuni survives within epithelial cells by avoiding delivery to lysosomes. PLoS Pathog **4:**e14.

249. **Welin, A., M. E. Winberg, H. Abdalla, E. Sarndahl, B. Rasmusson, O. Stendahl, and M. Lerm.** 2008. Incorporation of Mycobacterium tuberculosis lipoarabinomannan into macrophage membrane rafts is a prerequisite for the phagosomal maturation block. Infect Immun **76:**2882-7.

250. **Wheeler, D. S., M. A. Chase, A. P. Senft, S. E. Poynter, H. R. Wong, and K. Page.** 2009. Extracellular Hsp72, an endogenous DAMP, is released by virally infected airway epithelial cells and activates neutrophils via Toll-like receptor (TLR)-4. Respir Res **10:**31.

251. **WHO** 2010, posting date. Global tuberculosis control 2009: epidemiology, strategy, financing. Geneva: World Health Organization, 2009. [Online.]

252. **WHO.** 2010. Multidrug and extensively drug-resistant TB (M/XDR-TB): 2010 global report on surveillance and response. Geneva. World Health Organization.

253. **Wickremasinghe, M. I., L. H. Thomas, and J. S. Friedland.** 1999. Pulmonary epithelial cells are a source of IL-8 in the response to Mycobacterium tuberculosis: essential role of IL-1 from infected monocytes in a NF-kappa B-dependent network. J Immunol **163:**3936-47.

254. **Xu, Y., C. Jagannath, X. D. Liu, A. Sharafkhaneh, K. E. Kolodziejska, and N. T. Eissa.** 2007. Toll-like receptor 4 is a sensor for autophagy associated with innate immunity. Immunity **27:**135-44.

255. **Xu, Z. X., T. Ding, V. Haridas, F. Connolly, and J. U. Gutterman.** 2009. Avicin D, a plant triterpenoid, induces cell apoptosis by recruitment of Fas and downstream signaling molecules into lipid rafts. PLoS One **4:**e8532.

256. **Yam, K. C., I. D'Angelo, R. Kalscheuer, H. Zhu, J. X. Wang, V. Snieckus, L. H. Ly, P. J. Converse, W. R. Jacobs, Jr., N. Strynadka, and L. D. Eltis.** 2009. Studies of a ring-cleaving dioxygenase illuminate the role of cholesterol metabolism in the pathogenesis of Mycobacterium tuberculosis. PLoS Pathog **5:**e1000344.

257. **Yang, Z., and D. J. Klionsky.** 2010. Mammalian autophagy: core molecular machinery and signaling regulation. Curr Opin Cell Biol **22:**124-31.

258. **Young, D. B., H. P. Gideon, and R. J. Wilkinson.** 2009. Eliminating latent tuberculosis. Trends Microbiol **17:**183-8.

259. **Young, R. M., D. Holowka, and B. Baird.** 2003. A lipid raft environment enhances Lyn kinase activity by protecting the active site tyrosine from dephosphorylation. J Biol Chem **278:**20746-52.

260. **Yu, C., M. Alterman, and R. T. Dobrowsky.** 2005. Ceramide displaces cholesterol from lipid rafts and decreases the association of the cholesterol binding protein caveolin-1. J Lipid Res **46:**1678-91.

261. **Yu, X., N. Lu, and Z. Zhou.** 2008. Phagocytic receptor CED-1 initiates a signaling pathway for degrading engulfed apoptotic cells. PLoS Biol **6:**e61.

262. **Yuan, Y., D. D. Crane, R. M. Simpson, Y. Q. Zhu, M. J. Hickey, D. R. Sherman, and C. E. Barry, 3rd.** 1998. The 16-kDa alpha-crystallin (Acr) protein of Mycobacterium tuberculosis is required for growth in macrophages. Proc Natl Acad Sci U S A **95:**9578-83.

263. **Zaas, D. W., M. Duncan, J. Rae Wright, and S. N. Abraham.** 2005. The role of lipid rafts in the pathogenesis of bacterial infections. Biochim Biophys Acta **1746:**305-13.

264. **Zaas, D. W., M. J. Duncan, G. Li, J. R. Wright, and S. N. Abraham.** 2005. Pseudomonas invasion of type I pneumocytes is dependent on the expression and phosphorylation of caveolin-2. J Biol Chem **280:**4864-72.

265. **Zaas, D. W., Z. Swan, B. J. Brown, J. R. Wright, and S. N. Abraham.** 2009. The expanding roles of caveolin proteins in microbial pathogenesis. Commun Integr Biol **2:**535-7.

266. **Zaas, D. W., Z. D. Swan, B. J. Brown, G. Li, S. H. Randell, S. Degan, M. E. Sunday, J. R. Wright, and S. N. Abraham.** 2009. Counteracting signaling activities in lipid rafts associated with the invasion of lung epithelial cells by Pseudomonas aeruginosa. J Biol Chem **284:**9955-64.

267. **Zheng, Y. Z., C. Boscher, K. L. Inder, M. Fairbank, D. Loo, M. M. Hill, I. R. Nabi, and L. J. Foster.** 2011. Differential impact of caveolae and caveolin-1 scaffolds on the membrane raft proteome. Mol Cell Proteomics **10:**M110 007146.

268. **Zullo, A. J., and S. Lee.** 2012. Mycobacterial induction of autophagy varies by species and occurs independently of mTOR inhibition. J Biol Chem.